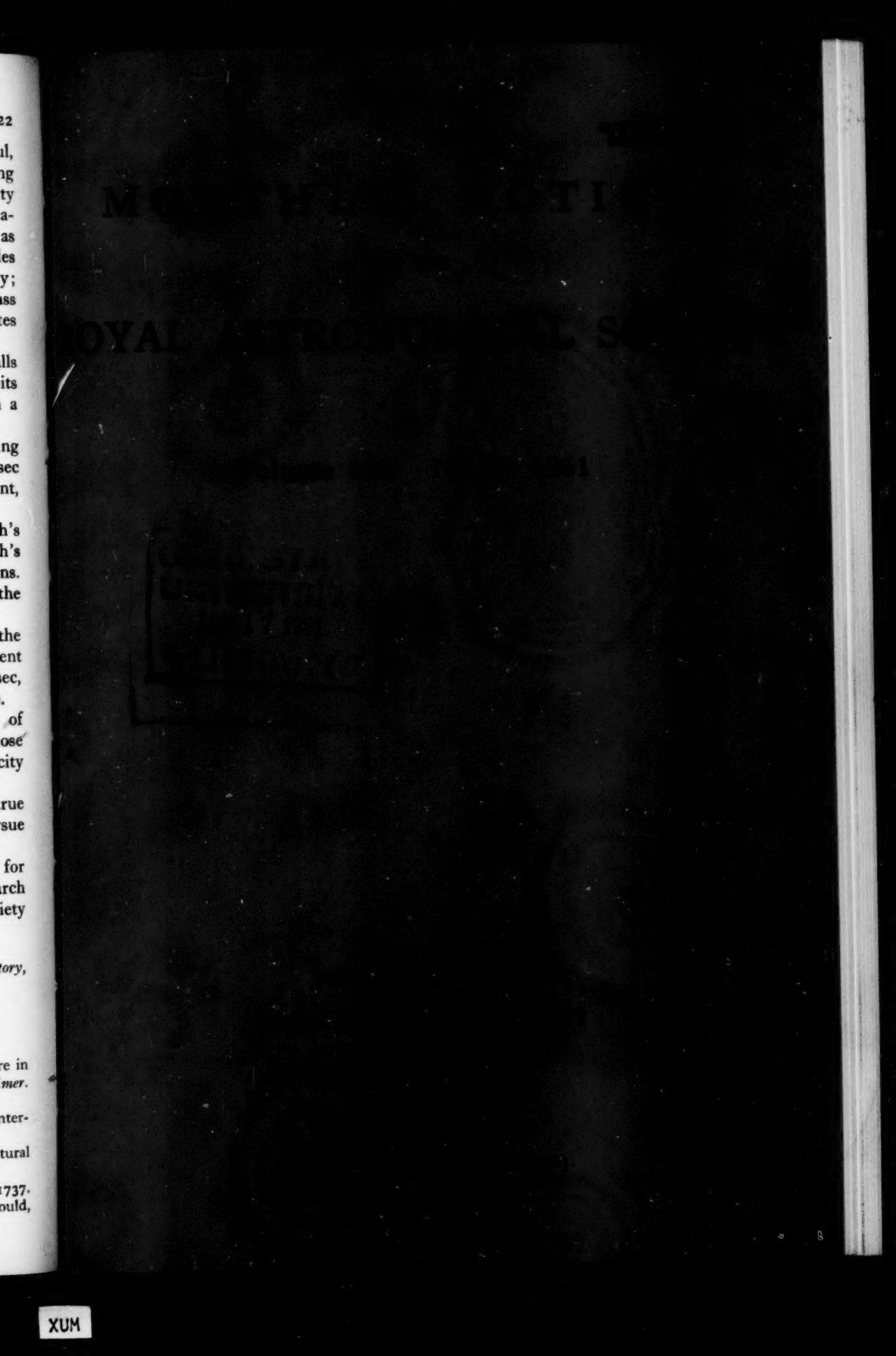

GEOPHYSICAL JOURNAL, VOLUME 4

The extra volume of the *Geophysical Journal* (Volume 4) to commemorate the seventieth birthday of Sir Harold Jeffreys, is now available.

The Geophysical Editors have organized the contributions of Sir Harold's distinguished colleagues and pupils, and hope that the papers in this special volume represent the most advanced work in the fields in which Sir Harold has long been interested.

Contributors include

S. Alterman	H. Bond M. Hasan
M. Bath	K. Hinkelmann
F. Birch	U. Hoffmeister
E. C. Bullard	J. E. Jackson
K. E. Bullen	J. A. Jacobs
P. Caloi	H. Jeffreys
A. H. Cook	M. Jobert
A. Day	D. G. King-Hele
F. F. Evison	L. Knopoff
P. Gaunaurd	R. L. Kovach
A. L. Hales	E. R. Lapwood

The complete volume, entirely bound in cloth buckram, is also available as a special publication.

Price £[illegible] ($[illegible] net)

Orders, with remittance, should be sent to the Assistant Secretary, Royal Astronomical Society, [illegible]

SPECIAL OFFER TO FELLOWS

Fellows of the Society may obtain this bound volume of the *Geophysical Journal* at a specially reduced price of £[illegible] 10s. 0d. ($[illegible] net). It is requested that Fellows wishing to purchase a copy send their orders with remittance, as soon as possible to

Assistant Secretary, Royal Astronomical Society, [illegible]

MONTHLY NOTICES
OF THE
ROYAL ASTRONOMICAL SOCIETY
Vol. 122 No. 2

VISCOUS DAMPING OF HYDROMAGNETIC WAVES IN THE CORONA

B. C. Landseer-Jones

(Received 1960 September 8)*

Summary

It is suggested that the heat lost by the corona is made good by energy given up in the viscous damping of hydromagnetic waves originating in the chromosphere. An estimate of the energy which the waves, generated by turbulent motion, would carry gives a value of 10^5 ergs cm^{-2} sec^{-1}. A frequency for the waves of 10^{-2} sec^{-1}, which seems to be the lowest possible, gives a fall in amplitude by $1/e$ in 10^{10} cm at a temperature of 10^6 °K. At higher frequencies, the distance for the same fall would be less.

The damping is found to be less the smaller the inclination of the wave-normal to the magnetic field. For a dipole type solar field, less energy would therefore be given to the corona over the poles than over the equator.

Introduction.—That turbulent motion in the photosphere would give rise to hydromagnetic waves, which would travel upwards into the chromosphere and corona and there give up their energy, was suggested first by Alfvén (**1**). This theory of coronal heating, in its original form, supposed that enough energy would be taken from the waves by Joule damping. It was therefore unable to withstand the criticism of Cowling (**2**), who showed that heating by electric currents in the waves must be far too small to maintain the temperature of the corona. It has been revived by the discovery by Piddington (**3**) that, under certain conditions, collisions between heavy ions moving with the wave and neutral particles can dissipate the energy of the wave much more quickly than Joule damping. In this case, the relative velocity of the colliding particles is not an electric current, bounded by limits to the strength of the magnetic field.

Piddington showed that hydromagnetic waves would reach the chromosphere and there be damped, in the neighbourhood of transition between neutral and ionized hydrogen, strongly enough for the heat lost from all higher levels to be made good. Although his process in this way explains the transfer of heat against the temperature gradient from the photosphere to as far as the chromosphere, it cannot be carried higher because of the lack of neutral particles in the corona. As a step towards explaining the high temperature of the corona, he has pointed out that protons in the undamped wave in the chromosphere could have speeds $\sim 10^7$ cm/sec and, in collision with neutral particles, these might be thrown upwards with an equivalent thermal energy to form a gas at 10^6 °K.

An objection to this idea of upholding the corona comes from the short mean free-path of protons at a temperature of 10^6 °K and a density of 10^9 cm^{-3}, which is about 10^7 cm, compared with the distance of at least 10^9 cm over which the temperature rises from the level where hydrogen becomes ionized to where 10^6 deg. is reached. The temperature would reach its maximum at the point where the upward-moving protons undergo their first collision.

*Received in original form 1960 May 6.

Some other way of transferring heat from the chromosphere to the corona seems needed. The dissipation of the energy of a wave by proton–electron collisions, as Joule damping, is known to be much too small. There remain proton–proton collisions, which lead to a loss of energy by the wave when the two particles are brought together by their thermal motion from different points in a non-uniform velocity field in the wave. This effect may be looked on as viscous damping. Although it is known to be negligible in the chromosphere, the coefficient of viscosity for collisions of this type increases as $T^{5/2}$. It is put forward in the present paper as a means by which hydromagnetic waves can heat the corona.

Hydromagnetic waves with viscous damping.—In a gas made up of equal numbers of protons and electrons, each with number-density n and partial pressure p, in which the particles gyrate much faster than they collide, the equation of motion of the protons may be written

$$m\frac{d}{dt}\boldsymbol{V}=\frac{e}{c}\boldsymbol{V}\wedge\boldsymbol{H}+e\boldsymbol{E}-\frac{1}{n}\nabla p+\boldsymbol{F}. \tag{1}$$

Here $\boldsymbol{V}$ is the velocity of the centre of gyration, $\boldsymbol{E}$ and $\boldsymbol{H}$ the electric and magnetic fields and $\boldsymbol{F}$ the forces of viscosity and friction, taken to be small compared with the other terms. There is a similar equation for the electrons. Neglecting $\boldsymbol{F}$ and supposing p to be given as a function of n, the operator $\nabla\wedge$ used on this equation and the relation $\nabla\wedge\boldsymbol{E}=-\frac{1}{c}\frac{\partial}{\partial t}\boldsymbol{H}$ give

$$\frac{\partial}{\partial t}\left(\frac{mc}{e}\nabla\wedge\boldsymbol{V}+\boldsymbol{H}\right)=\nabla\wedge\boldsymbol{V}\wedge\left(\frac{mc}{e}\nabla\wedge\boldsymbol{V}+\boldsymbol{H}\right).$$

Here the vorticity $mc/e\,\nabla\wedge\boldsymbol{V}$ would appear later as a Hall field, which is known to make the gas doubly-refracting for hydromagnetic waves. It is negligible compared with $\boldsymbol{H}$ for waves of frequency small compared with that of gyration of the ions. In this case

$$\frac{\partial}{\partial t}\boldsymbol{H}=\nabla\wedge\boldsymbol{V}\wedge\boldsymbol{H}. \tag{2}$$

If $\boldsymbol{A}$ is a vector such that

$$\nabla\wedge\boldsymbol{A}=\boldsymbol{H}$$

this equation is unchanged by a gradient transformation of $\boldsymbol{A}$, which may therefore be chosen so that equation (2) becomes

$$\frac{\partial}{\partial t}\boldsymbol{A}=\boldsymbol{V}\wedge\boldsymbol{H}=\boldsymbol{V}\wedge(\nabla\wedge\boldsymbol{A}). \tag{3}$$

In general, $\nabla.\boldsymbol{A}\neq 0$, since the gradient vectors in equation (1) which vanish under the operation $\nabla\wedge$ are included in $(\partial/\partial t)\boldsymbol{A}$ and their divergence does not always vanish.

When the momentum-density of the electrons is neglected, the equation of conservation of momentum for the gas is

$$nm\frac{d}{dt}\boldsymbol{V}=\nabla.(\Sigma+\Pi)=-\frac{1}{4\pi}\boldsymbol{H}\wedge\nabla\wedge\boldsymbol{H}-2\nabla p+\nabla.P \tag{4}$$

in which Σ is the Maxwell tensor, the electric field being neglected in the second form on the right-hand side, and Π the pressure, made up of the isotropic pressures and the viscous tensors. Friction, or its equivalent resistivity, does not appear

explicitly in this equation. It falls out altogether when the momentum of the electrons is neglected.

Suppose now that the magnetic field has the form

$$\boldsymbol{H}=\boldsymbol{H}_0+\boldsymbol{H}_1 \quad \text{with} \quad H_1 \ll H_0$$

and H_0, to the first order, constant. A vector $\mathbf{B}$ can then be found so that

$$n-n_0=\nabla.\mathbf{B}, \quad \boldsymbol{V}=-\frac{1}{n_0}\frac{\partial}{\partial t}\mathbf{B}, \quad \boldsymbol{A}=\frac{1}{n_0}\boldsymbol{H}_0\wedge\mathbf{B}. \tag{5}$$

Put into equation (4), these give a first-order linear equation

$$m\frac{\partial^2}{\partial t^2}\mathbf{B}=\frac{1}{4\pi n_0}\boldsymbol{H}_0\wedge\{\nabla\wedge(\nabla\wedge\boldsymbol{H}_0\wedge\mathbf{B})\}+2\gamma kT\nabla\nabla.\mathbf{B}+\left[\mu\nabla.\nabla\frac{\partial}{\partial t}\mathbf{B}\right]. \tag{6}$$

Viscosity is here represented by a typical term only, put in brackets. Without terms of this type, the equation has solutions which are undamped waves moving, as Piddington (4) has shown, in a triply-refracting medium. This may be seen at once from the equation here as, if $\mathbf{B}$ is a plane wave of frequency ν, it is a set of three scalar equations homogeneous in the initial values of the components of $\mathbf{B}$, in each of which there is a coefficient ν^2, giving in general three values of ν^2 for a wave of given length and direction.

As will be seen later, the waves chiefly of interest here are those for which

$$H_0^2/4\pi n_0 \gg \gamma kT$$

so that their potential energy lies in the magnetic field. Damping of waves of this type has been considered by van de Hulst (5) but without taking into account the effect of the magnetic field on the viscous stresses. This effect is not small and cannot be neglected, except for his purpose of showing the order of magnitude of the viscous term.

Taking a rectangular system of co-ordinates, with $\boldsymbol{H}_0$ along the z-axis, $\mathbf{B}$ may be taken to have a single component $B(x, z, t)$ along the x-axis. A complete expression for the stress tensor in a magnetic field has been given by Chapman and Cowling (6), and the components which are at present relevant are

$$P_{xx}=-\frac{2\mu}{\left(1+\frac{16}{9}\omega^2\tau^2\right)}\left\{\frac{2}{3}\frac{\partial}{\partial x}V_x+\frac{1}{6}.\frac{\partial}{\partial x}V_x.\frac{16}{9}\omega^2\tau^2\right\},$$

$$P_{xz}=-\frac{2\mu}{\left(1+\frac{4}{9}\omega^2\tau^2\right)}\frac{\partial}{\partial z}V_x.$$

Here ω is the frequency of gyration of the particles and τ the time between their collisions. The coefficient of viscosity for inverse-square collisions is

$$\mu=\frac{5}{8}\left(\frac{kmT}{\pi}\right)^{1/2}\left(\frac{2kT}{e^2}\right)^2 \Big/ A_2(2)=\alpha T^{5/2}, \quad \alpha=1\times10^{-16}$$

this value of α, which varies very slowly with the density, holding for both the chromosphere and the corona. As μ is proportional to $m^{1/2}$, the viscosity of the electrons is negligible.

When the frequency of collision is small compared with that of gyration, P_{xx} and P_{xz} become

$$P_{xx}=-\frac{\mu}{3}\frac{\partial}{\partial x}V_x \qquad P_{xz}=0.$$

When these are compared with their forms for no magnetic field ($\omega = 0$), it may be seen that the magnetic field has suppressed the force due to a shear in V_x along the z-axis, which is remarkable because the free-path in this direction is unaffected. The effect is due to a tendency for ions in thermal motion along the field to be brought by electromagnetic forces to the local velocity of drift normal to the field.

Putting V_x in P_{xx} in terms of B, equation (6) has the one component

$$\frac{\partial^2}{\partial t^2}B = \frac{H_0^2}{4\pi m x_0}\left(\frac{\partial^2}{\partial x^2}B + \frac{\partial^2}{\partial x^2}B\right) + \frac{\mu}{3mn_0}\frac{\partial^2}{\partial x^2}\frac{\partial}{\partial t}B \qquad (7)$$

with solutions in the form of plane waves

$$B = B_0 . \exp . 2\pi i\left(\nu t - \frac{x}{\lambda_x} - \frac{z}{\lambda_z} + i\kappa x\right), \quad \frac{1}{\lambda_x^2} + \frac{1}{\lambda_z^2} = \frac{1}{\lambda^2} = \frac{4\pi\nu^2 mn_0}{H_0^2} = \frac{\nu^2}{u^2},$$

$$\kappa = \frac{8}{3}\frac{\mu\nu^2\pi^3}{uH_0^2} = \frac{2}{3}\frac{\pi^2\mu\nu^3}{mn_0u^3}, \quad \kappa \ll \frac{1}{\lambda}.$$

If the wave-normal makes an angle θ with the magnetic field, the damping factor may be written

$$\exp(-2\pi\kappa z \tan\theta \sin\theta)$$

so that a wave is damped most strongly when its normal lies along the x-axis and undamped when its normal lies along the z-axis. Equation (6) may also be put into cylindrical polar coordinates and solutions found as spherical waves radiating from the origin

$$B = B_0\left[\exp 2\pi i\left\{\frac{(\rho^2+z^2)^{1/2}}{\lambda} + \nu t + \frac{i\kappa\rho}{(\rho^2+z^2)^{1/2}}\right\}\right]\Big/(\rho^2+z^2)^{1/2}.$$

The damping factor, when θ is the angle between wave-normal and the polar axis, has the same form as above, so that the amplitude is unchanged along the magnetic field and falls along any line at an angle to it.

Transfer of energy from the chromosphere to the corona.—Measurements of the profiles of lines on spectrograms of the emission of the chromosphere have been made by Redman and Suemoto (**7**) and interpreted as showing line-of-sight velocities of the emitting atoms rising to 16 km/sec at 2600 km above the solar surface. By means of interferometric methods, Clube (**8**) has concluded that a turbulent velocity of 16 km/sec is to be found at levels below 3000 km. The level where hydrogen becomes ionized is between 6000 and 7000 km and, according to the theory of Piddington mentioned earlier, it is here that energy is taken up most rapidly from hydromagnetic waves. A mean speed of turbulent motion of 20 km/sec therefore seems quite likely at this level.

Taking the density there to be $3 \times 10^9\,\mathrm{cm^{-3}}$ and the speed of hydromagnetic waves $1 \times 10^7\,\mathrm{cm\,sec^{-1}}$, the energy carried upwards by waves arising from this turbulence would be

$$3 \times 10^9 \frac{1{\cdot}7 \times 10^{-24}}{2}(2 \times 10^6)^2 . 1 \times 10^7 = 1 \times 10^5\,\mathrm{ergs\,cm^{-2}\,sec^{-1}}.$$

This is of the same order as estimates of the rate of loss of energy by the corona. At this level $T \sim 10^4$ °K, so that $\left(\frac{\gamma kT}{m}\right)^{1/2} \sim 10^6\,\mathrm{cm\,sec^{-1}}$.

Damping of the waves depends on their frequency. While there is no direct information about the period of turbulent motion in the chromosphere, an upper limit to the wavelengths formed there is set by the variation in density. If the

density n_0 in equation (7) is taken to vary exponentially along the z-axis with a scale-height ζ, solutions of this equation, neglecting viscosity, which asymptotically become plane standing waves, are Bessel's functions of the first and second kinds of order zero

$$B = B_{01}\,e^{\pm 2\pi i\nu t} J_0(s) \qquad \text{and} \qquad B_{02}\,e^{\pm 2\pi i\nu t} Y_0(s), \quad s = 4\pi\zeta/\lambda.$$

When $s < 1$, neither function is oscillatory and $Y_0(s) \to \infty$ as $s \to 0$. A wave-train can only be propagated if $s > 1$, that is $\lambda < 4\pi\zeta$. As in the chromosphere

$$\zeta = 1{\cdot}1 \times 10^8\,\text{cm},$$

waves could not be formed to travel upwards with length greater than $\sim 10^9$ cm, corresponding to a frequency of $10^{-2}\,\text{sec}^{-1}$. This gives the lowest value for the damping coefficient in the corona to be

$$\kappa_{\min} = 10^{-6}\,\nu^2 = 10^{-10}\,\text{cm}^{-1}.$$

As the speed of hydromagnetic waves is proportional to H_0, the upward flow of energy from the chromosphere will be greatest in regions where the magnetic field is unusually strong. For waves moving radially outwards, damping is more effective the greater the inclination of the magnetic field-lines to the vertical. If the steady field of the Sun is like that of a dipole, more energy should be absorbed by the corona over the equator than over the poles. A torsional oscillation during the sunspot cycle, by which the field-lines in the solar atmosphere are drawn out longitudinally to their greatest length at sunspot maxima, would at these times give the least difference between the polar and equatorial regions of the corona.

Acknowledgment.—The suggestions of a referee of the Society have greatly improved the argument in this paper.

50 *Hans Place,*
*London, S.W.*1:

1960 *September.*

References

(1) H. Alfvén, *M.N.*, **107**, 211, 1947.
(2) T. G. Cowling, The Solar System, I. *The Sun*, ed. G. B. Kuiper, Chicago Univ. Press, 1953, Chap. 8.
(3) J. H. Piddington, *M.N.*, **116**, 314, 1956.
(4) J. H. Piddington, *M.N.*, **115**, 671, 1955.
(5) H. C. van de Hulst, Problems of Cosmical Aerodynamics, I.U.A.T.M. and I.A.U. Symposium, Paris 1949, Dayton (Ohio), Chap. 6.
(6) S. Chapman and T. G. Cowling, *The Mathematical Theory of Non-Uniform Gases*, Cambridge Univ. Press 1952, p. 337.
(7) R. O. Redman and Z. Suemoto, *M.N.*, **114**, 524, 1954.
(8) S. V. M. Clube, *M.N.*, **118**, 18, 1958.

FIRST RESULTS OF RADIO STAR OBSERVATIONS USING THE METHOD OF APERTURE SYNTHESIS

P. F. Scott, M. Ryle and A. Hewish

(Received 1960 September 20)

Summary

Four surveys, centred on declinations of 52°, 50°, 42° and 05°, have been made at a wave-length of 1·7 m with a large interferometric radio telescope employing the new technique of aperture synthesis. Details of the observational method, calibration, data-reduction and analysis of the computed results are given. An assessment of the performance of the system shows that accurate measurements of the positions and flux densities of radio stars may be extended to limits well beyond those of any previous survey. Lists of sources are given for declinations between 52° and 50° and between 40° and 44°. Observations at 05° were made to study the distribution of radio stars outside the galactic plane; no evidence is found for a population of radio stars in the galactic halo.

---

1. *Introduction.*—The method of synthesizing a large radio telescope by combining observations made with movable elements in a number of different relative positions has already been described (Ryle and Hewish 1960). It was there shown how both pencil beam instruments and interferometers could be developed and how, in each case, one convenient system employed a long fixed aerial running East/West with a smaller aerial arranged to move on rails running North/South. With this arrangement it is only necessary to provide aerial rotation about the long axis to scan in declination while making use of the Earth's rotation to scan in right ascension.

A large interferometer operating at a frequency of 178 Mc/s which uses this method has been built for the study of radio stars. It was designed to obtain better positional accuracy for weaker sources so that a larger number might be available for optical examination and to obtain more reliable information on the apparent distribution of sources in space. The same radio telescope has already been used in an investigation of the surface brightness of radio stars (Leslie 1961) and for the measurement of the positions of 64 intense ones (Elsmore, Ryle and Leslie 1959).

The present paper is concerned with the use of the instrument with its full resolution. The envelope of the interference pattern then has half-widths of 25′ and 35′ in right ascension and declination respectively. The operation of the instrument and the methods of computation and data reduction are described in Section 2. The performance of the system is discussed in Section 3, and in Section 4 preliminary results of the observation of four areas of sky are summarized. The first two areas observed were centred on declinations of 50° and 52°; the later areas, observed with an improved recording system, were centred on 05° and 42°.

2. *The radio telescope.*

(*a*) *The aerial system.*—The aerial system consists of two elements, one of which is fixed and the other mounted on railway lines. Structural details have been discussed elsewhere (Ryle 1960). In the present observations the aerials are used together as a transit interferometer. Both elements are cylindrical reflectors having a parabolic section 65 ft in width and each is aligned on an East/West axis. The fixed element is 1450 ft in length and the movable one, 190 ft in length, traverses a distance of 1000 ft along rails in a North/South direction as shown in Fig. 1.

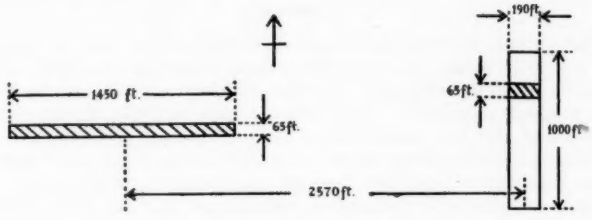

FIG. 1.—*Schematic diagram of the aerials.*

Both elements may be set to declinations between $-05°$ and $90°$. The reception pattern of each has a width of $4°{\cdot}6$ between half-power points in declination and this determines the area of the strip of sky under observation at a particular setting. In right ascension the reception pattern is related to the product of the reception patterns of the two aerials and to the frequency response of the output filter of the receiver as shown later. Its shape can be regulated either by the distribution of excitation along the fixed aerial or by means of the output filter response to give the narrowest reception pattern consistent with the lowest realizable side-lobe level. Side-lobes in right ascension at angles greater than $5°$ from the main beam are in any case removed by the lack of coherence between the signals arriving at the widely spaced aerials when using a receiver of bandwidth 4 Mc/s.

Initially, the desired reception pattern in right ascension was achieved by adjusting the excitation of the fixed aerial. Since the spatial frequency spectrum of the reception pattern is derived from the convolution of the aperture distribution of the two aerials it was only necessary to adjust the excitation in steps of length equal to that of the movable aerial. The adjustment was performed by the use of unsymmetrical transformers at the junctions of the branched feeder network. The aperture distribution adopted, the effective spectrum of the combined aerial system and the resulting reception pattern are shown in Fig. 2.

Later it was found more convenient to adopt a uniform excitation along the fixed aerial and to achieve the same reception pattern by using a suitable output filter. This method had the added advantage that the fixed aerial could also be used, independently, as an efficient total power system. In this mode of operation the spectrum of the aperture distribution is uniform, within a band determined by the length of the aerials, and its shape is adjusted to that required by a suitable output filter response. The processes of filtering and convolution are basically equivalent and in this case where the output of the receiver was already recorded in digital form it was convenient to carry out a direct convolution with a time function whose Fourier transform provides the required polar diagram.

The resulting reception pattern is then identical with that shown in Fig. 2. Noise components at frequencies higher than those introduced by the aerial are removed before convolution by a simple CR filter. The spectrum of the original signal, the convolving function and the CR filter are shown in Fig. 3.

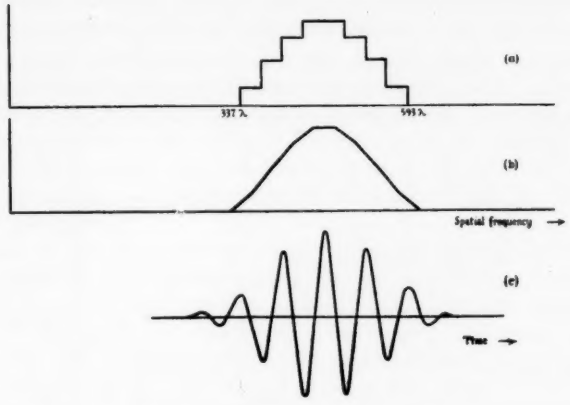

FIG. 2.—(*a*) *The aperture distribution of the fixed aerial.*
(*b*) *The spatial frequency spectrum of the aerial system.*
(*c*) *The reception pattern.*

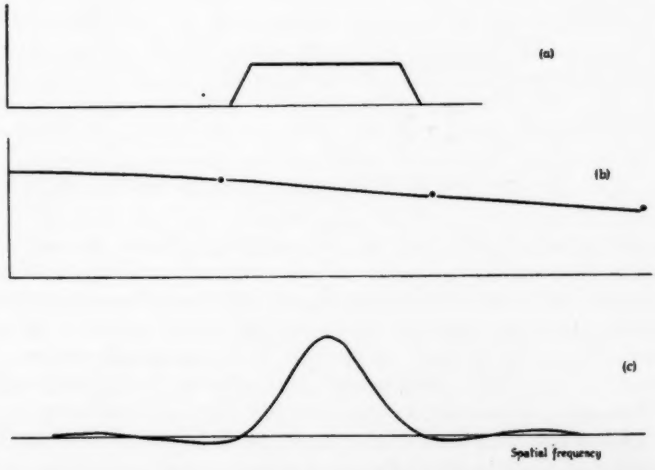

FIG. 3.—*The spectrum of the signal* (*a*), *the CR filter* (*b*) *and the convolving function* (*c*).

The resultant reception pattern in declination, after the synthesis is completed, is that of a 500 ft aperture. The required aperture distribution is here achieved by suitably weighting the observations made at the different positions of the movable aerial (Ryle and Hewish 1960).

(*b*) *The receiver and recorder.*—It is necessary, for synthesis, to record quantities of the form $E_aE_b\cos(\phi_a-\phi_b)$ where E_a, E_b, ϕ_a and ϕ_b represent the amplitudes and phases of the voltage induced in the two aerials. This form of correlation response can be obtained by the use of a phase-switching receiver (Ryle 1952). In the system used here two such receivers were connected to the aerials *via* a hybrid network as shown in Fig. 4 and arranged to provide outputs in antiphase. The difference in output of the two receivers then provides the required quantity and the use of the double system improves the signal/noise ratio by $\sqrt{2}$ (since the combined noise from the two preamplifiers is uncorrelated at the inputs of the two receivers). Furthermore, most types of interference are greatly reduced.

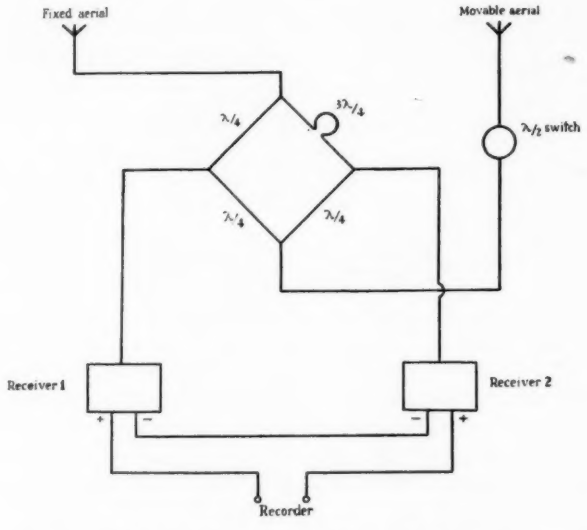

FIG. 4.—*Method of connecting two receivers to the aerials.*

Few sources of interference are received with appreciable intensity by both aerials, since the reception patterns do not overlap for a distance of about 20 miles. Intense and variable interfering signals containing frequency components near the switching frequency may however cause a small output even when the interference is incident on only one aerial. With the double receiver arrangement such signals appear in phase at the output and may be rejected with a ratio dependent on the gain equality of the receivers. It has been found in practice that ignition and lightning interference are attenuated by a factor of 20 compared with the output of a single phase-switching receiver which is itself very much less susceptible than a simple receiver.

Since large amounts of data must be recorded prior to computation, an automatic device has been developed for continuously digitizing the signal and recording it on punched tape. A normal type of pen recording is also used for immediate checking of performance. In the automatic recorder the signal is used to operate a self-balancing potentiometer on whose shaft is mounted an

optical digitizing disk with a cyclic permuting binary code of 8 digits. To minimize digitizing errors the sensitivity of the receiver is adjusted so that the noise level exceeds the digit interval by a factor of 3 or 4. In order to obtain synchronism between sampling points made at successive positions of the movable aerial the actual sampling rate is chosen to be a sub-multiple of 24 sidereal hours. The instant at which the record is sampled (about once every 8 seconds, depending on declination) is regulated by a gear train driven from a 50 c/s synchronous motor whose power supply is derived from a 100 kc/s sidereal crystal oscillator. An impulse from a control circuit disconnects the servo motor in the self-balancing potentiometer, thus storing the signal as a shaft position. Subsequent impulses cause the outputs of the photo-cells on the digitizer to be read and punched as two successive characters using a modified teleprint punch with standard five-hole tape. The servo drive is then reconnected and the shaft follows the signal until the next sampling time.

The minimum sampling rate which may be employed is determined by the envelope reception pattern (Bracewell 1956) and corresponds to approximately four samples of amplitude and phase of the quasi-periodic response in each beamwidth (to zero power). In this case the lobes of the interference pattern occurred at a frequency slightly greater than twice the minimum sampling rate. The output of the receiver was initially sampled four times in each cycle of the interference pattern. After further smoothing by the correlation process described in Section 2 (*a*) the sampling interval was increased, during computation, to give values of amplitude and phase once per cycle of the interference pattern.

(*c*) *Method of observation.*—With the declination of both aerials set to the required value the movable aerial is driven to the North end of the rails and observations are made for a period of $23\frac{1}{2}$ hours. For computation it is convenient if all tapes commence at exactly the same sidereal time and an interval must therefore be allowed for moving the aerial and for calibration, etc. before each day's observations. After completion of the first run the aerial is moved a distance of 42 ft and the observations are repeated for 24 positions of the movable aerial. The distance moved is somewhat less than the effective width of the aerial in order to eliminate the 'grating' side-lobe which would otherwise appear in the reception pattern at the extreme edge of the $4^{\circ}{\cdot}6$ strip (Ryle and Hewish 1960). It is necessary to maintain an equal path length to the two aerials so that a wide bandwidth may be used. This is achieved by a set of cables having electrical lengths equal to a whole number of wavelengths and arranged in a scale of two; these cables are altered with each aerial move to equalize the path difference to within 2·5 wavelengths.

At low declinations, where the effective North/South aperture is reduced, it would be possible to increase the distance between successive positions so long as the effective movement in the aperture plane did not exceed about 42 ft. Such a procedure would, however, reduce the signal/noise ratio slightly and so far has not been employed.

Throughout the observations separate records are kept of solar activity and ionospheric scintillations so that runs may be repeated if serious errors are likely to occur in any part of a particular record. Errors due to other sources of interference are either immediately evident on the pen record or are indicated by the data-checking procedure outlined below.

(*d*) *Calibration and checking.*—Before proceeding with the analysis of the data it is necessary to make a number of preliminary checks. It is particularly important to correct for any systematic variations in the sensitivity or phase of the system since these will introduce side-lobe responses into the synthesized reception pattern in declination. At each of the 24 positions of the movable aerial the phases and amplitudes of a number of intense sources are obtained from the recorded data. Knowing the accurate declination of these sources it is possible to predict the correct value of the phase for each aerial position and so to obtain a phase error for each source; provided the sources have a flux density greater than about 15×10^{-26} w.m^{-2} (c/s)$^{-1}$ they will not be affected appreciably by noise or confusion. A mean correction for both phase and amplitude can therefore be obtained for each run and used to correct the original data; corrections were seldom found to be necessary.

At the same time as this check is carried out the data are scanned in the computer for wrong values, caused for example by solar or terrestrial interference or by a fault in the digitizing system. This is done by convolving the data with a suitable function and comparing each number on the tape with the 'expected' value obtained by convolution. Errors detected in this way were reported whenever they exceeded five times the r.m.s. noise level. The necessary corrections were then fed into the computer together with the 24 data tapes. The required weighting factor for each position, which determines the reception pattern in declination, was also fed in at this stage.

(*e*) *The computation.*—It is necessary to carry out the computation in two steps since the data tapes must be fed into the computer serially whereas the calculation requires information, at a given sidereal time, from all the tapes simultaneously. During the first stage the data are sorted into a convenient layout in the store and during this process the convolution mentioned in Section 2 (*a*) is performed. Two convolving functions are used which yield the sine and cosine components, sampled once per cycle, of the quasi-periodic output from the receiver. These data, corrected for errors as described above, amount to about 100,000 numbers and are stored on magnetic tape in readiness for the main calculation.

At any given sampling time the data for the 24 aerial positions may be represented by the series C_{12}, S_{12} ..... C_{-12}, S_{-12}. The second stage of computation then gives 16 values of D_m

where $$D_m = \sum_{n=-12}^{n=+12} (C_n + iS_n) e^{imn\phi} \qquad \left(\phi = \frac{2\pi}{24}\right).$$

These values of D represent the output of the full synthesized interferometer, sampled at approximately the optimum interval in declination, within a range of 4°·6.

On completion of the calculation it is necessary to correct for the known primary reception pattern of the aerials which would otherwise cause the values of D at the edges of the declination strip to be systematically smaller than those at the centre. While 24 values of C_n and S_n are required only 16 values of D are computed since the overlapping of adjacent stations of the movable aerial implies that successive values of C_n and S_n are not entirely independent. The (complex) values of D are next transformed to $|D|$ and arg D and the printed output then gives the 16 values of $|D|$ across the sheet followed by a second line

giving corresponding values of arg D. $|D|$ is printed as an integer in the range 0–9999 and arg D as a fraction of a revolution in the range 0–99. The output is thus a two-dimensional map of the sky, sampled at discrete intervals, with declination running across the page and right ascension downwards. The sampling interval is approximately 20′ in declination and 7′·5 in right ascension, the precise value of the former depending on the declination of the centre of the strip. An example of the printed output is shown in Fig. 5.

Declination

40°	42°	44°		
1		1		
11 45 23 23 09 19 11 10	08 14 24 23 14 54 09 50		1440	$12^h\,02^m$
09 06 67 64 81 83 84 13	02 18 27 41 56 37 36 37			
98 43 08 15 04 12 26 04	04 19 36 26 18 38 67 32		1441	
07 08 59 58 32 85 87 21	03 21 27 38 53 41 41 44			
40 15 31 13 14 22 45 03	03 36 51 26 16 22 36 18		1442	
08 93 62 60 22 88 88 76	11 24 28 36 51 57 57 65			
10 31 78 33 17 21 51 10	02 46 67 18 14 20 31 21		1443	$12^h\,04^m$
60 73 60 55 20 88 86 73	66 28 30 39 68 70 67 67			
1				
51 44 20 50 17 14 30 13	05 49 61 04 26 16 12 08		1444	
64 70 60 58 22 98 87 66	63 27 30 45 81 75 64 45			
1				
72 47 29 48 16 02 07 19	05 37 40 17 34 51 83 04		1445	
69 65 59 58 17 17 78 58	66 26 28 90 89 79 80 47			
1		1 3		
87 66 05 24 19 03 02 19	04 24 23 37 38 66 35 82		1446	$12^h\,06^m$
67 53 56 57 11 80 44 54	73 23 25 88 91 82 81 85			
		3 6 1		
75 70 71 13 **22** 19 04 13	09 14 24 44 44 03 42 92		1447	
65 52 52 60 05 79 77 66	85 24 27 91 96 89 82 86			
		3 7 2		
68 68 46 10 17 25 12 13	09 15 26 44 38 47 35 23		1448	
68 58 47 40 05 80 90 83	89 20 24 92 97 82 82 85			
		2 5 1		
75 75 17 19 07 25 21 21	14 11 22 42 27 51 34 51		1449	$12^h\,08^m$
72 68 45 38 08 82 88 88	96 12 15 96 97 82 81 84			

Right ascension

FIG. 5.—*A part of the printed output. Numbers in the upper rows give values of $|D|$ and the lower rows the values of arg D; values of D over 99 are printed thus:* $\frac{7}{35} \equiv 735$. *$|D| = 71$ corresponds to a flux density of* 10^{-26} *w.m*$^{-2}$ *(c/s)*$^{-1}$.

During the progress of the main calculation a record is made of the probability distribution of $|D|$. This is computed in blocks of 20 successive samples in right ascension and the result is obtained on a second output channel. This information is required for statistical investigations of the distribution of radio stars (Scheuer 1957) and the application of the method will be discussed in another paper.

(*f*) *Analysis and interpretation of the results.*—The position of a given source in right ascension is determined precisely by the value of the phase (arg D) but it is necessary to interpolate, both in declination and right ascension, to find the accurate declination and flux density of a source. Since the reception pattern is known in both coordinates this interpolation is most conveniently carried out by a simple graphical process. In cases where the envelope reception pattern appears to have the wrong shape, it is probable that more than one source is present and values of the phase then give valuable information which may resolve the blend.

No attempt is made to reduce the collimation errors to zero for each series of observations. Instead, use is made of the accurate positions of 64 intense radio stars which have already been determined in an independent investigation (Elsmore, Ryle and Leslie 1959). Any declination strip will usually contain several of these sources and it is therefore possible to obtain both collimation errors and a flux density normalizing factor for each series of observations.

3. *Performance.*

(*a*) *The reception pattern.*—It is only necessary to consider the reception pattern along lines in right ascension and declination which intersect at the centre of the pattern. At other angles the response is given by the product of these patterns and side-lobes will be very small.

The observed reception pattern in right ascension, derived from a uniform excitation of the fixed aerial and the convolution method described in Section 2 (*a*), is shown in Fig. 6 (*a*); it is seen that the side-lobes are less than 0·5 per cent at angles greater than 1°.

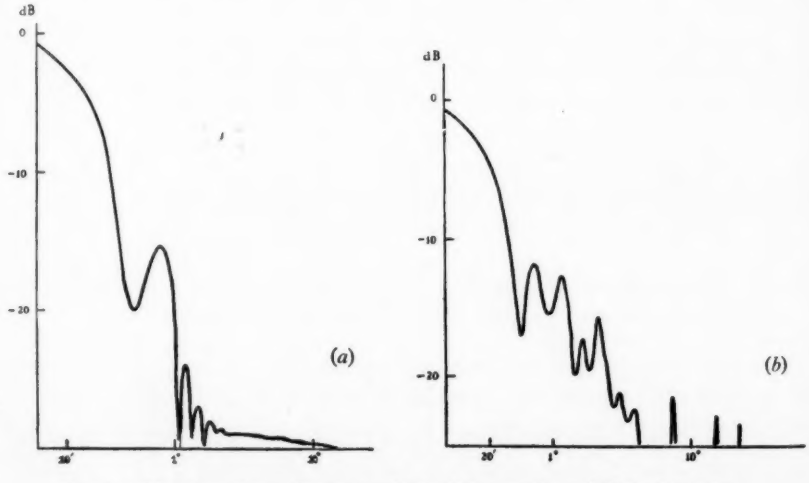

FIG. 6.—*The observed reception pattern (a) in right ascension and (b) in declination.*

In declination the reception pattern will be affected by errors which may occur in the phase or amplitude of the signal. While systematic errors can be removed as discussed in Section 2 (*d*) there will be random errors due, for example, to refraction in the ionosphere. Variations of amplitude are found to be of negligible importance compared with the phase variations which have an observed r.m.s. value of about 15°, corresponding to a figuring error of about $\lambda/25$ in the synthesized aperture. The latter introduce side-lobes with an r.m.s. level of about 6 per cent confined to the 4°·6 envelope; beyond this the response is less than 0·5 per cent. The observed reception pattern in declination is shown in Fig. 6 (*b*).

The cause of the random phase variations is not yet known. From existing knowledge of non-uniformity in the ionosphere it seems unlikely that they can be explained simply by ionospheric refraction and it is possible that they may be due in part to temperature variations in coaxial cables.

(*b*) *Sensitivity.*—The noise level for the initial observations at declinations of 50° and 52° was about three times higher than that of the later observations owing to errors introduced by the digitizer. For the surveys at declinations of 42° and 05° an improved digitizer was used and uniform excitation of the long aerial was adopted. To distinguish between true noise and the effect of weak unresolved sources, special records were made with one of the aerials replaced by a resistance at a temperature close to the effective sky temperature. Under these conditions there is no response from radio stars but the noise level due to the combined effects of preamplifier noise and the galactic background emission is the same; additional noise components due to weak terrestrial interference incident on one aerial are also included. The possible incidence of coherent interference in both aerials was investigated in a separate experiment and shown to be unimportant.

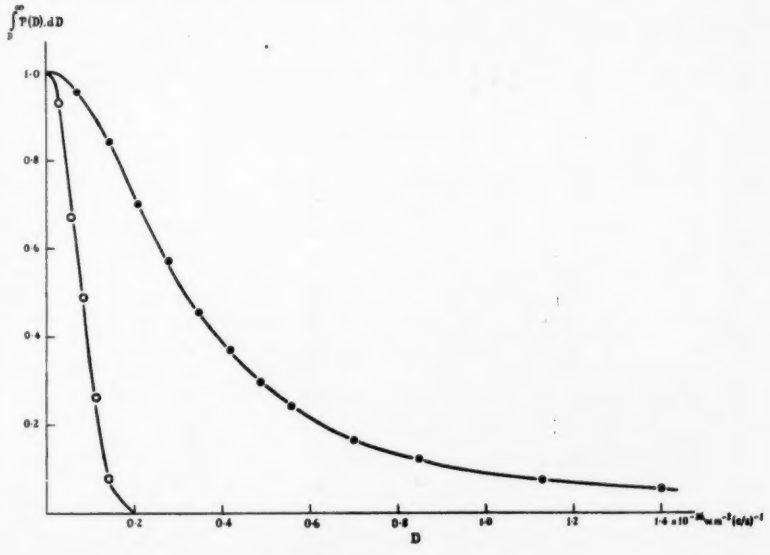

FIG. 7.—*The integrated probability distribution of* $|D|$ *for the 42° survey — · — · —, and that derived — o — o — from the noise measurement.*

The observed noise level was found to be $0{\cdot}08 \times 10^{-26}$ w.m^{-2} (c/s)$^{-1}$ as compared with an estimated theoretical value of $0{\cdot}045 \times 10^{-26}$ w.m^{-2} (c/s)$^{-1}$.

The integrated probability distribution of $|D|$ for the 42° survey is shown in Fig. 7 together with that derived from the independent noise measurement. It is evident from these curves that the noise on the records is likely to be unimportant, either in the measurement of individual sources, or in the statistical analysis of $|D|$.

4. *Observational results*

Four surveys have been made centred on declinations of 52°, 50°, 42° and 05°. The first two (52°, 50°) were carried out primarily to test the operation of the whole system. A declination strip 2°·5 wide was included in both surveys and a direct comparison of the results has been made. The noise and side-lobe level were both higher than in the later surveys which used an improved digitizer described in Section 2 (*b*).

The survey at 05° was made primarily to investigate the distribution of sources for different directions in the galaxy. The most recent survey at 42° represents the best series of observations for the study of individual sources and for application of the statistical method of analysis.

(*a*) *Comparison of surveys at declinations of* 52° and 50°.—The results obtained for the two surveys are entirely independent, both with respect to errors in flux density and position and to those arising from side-lobes. A comparison of results in the overlap region 2°·5 wide in declination thus provides an excellent overall test of the operation of the instrument.

In Table I a list is given of all sources in the overlap region having flux densities greater than 3×10^{-26} w.m^{-2} (c/s)$^{-1}$ and it is seen that there is extremely good agreement. Of the 67 sources listed, the majority show good positional agreement and have flux densities which agree to within 20 per cent. Two sources found on the 50° survey had flux densities of less than 2×10^{-26} w.m^{-2} (c/s)$^{-1}$ on the 52° survey; in one case the wrong right ascension lobe was chosen.

TABLE I

52° Survey R.A. h	m	s	Dec. °	′	Flux density 10^{-26} MKS	50° Survey R.A. h	m	s	Dec. °	′	Flux density 10^{-26} MKS
00	13	21·3	50	22·4	5·7	00	13	21·0	50	19·2	4·0
00	35	43·5	50	17·6	5·0	00	35	42·9	50	16·6	5·6
00	40	21·4	51	46·7	37	00	40	19·9	51	47·5	35
					<1·5	00	47	47·5	51	42·3	4·1
00	48	06·2	50	56·7	11·4	00	48	05·6	50	56·1	11·1
01	19	44·7	49	51·7	4·3	01	19	45·5	49	49·8	4·1
02	23	38·6	51	06·5	3·5	02	23	38·1	51	03·6	3·8
02	40	17·5	49	51·4	5·0	02	40	19·0	49	53·8	5·5
03	28	20·1	51	25·9	3·3	03	28	19·7	51	22·7	3·1
03	34	04·1	50	37·1	12·0	03	34	04·1	50	35·2	12·5
03	55	47·6	50	48·8	6·1	03	55	46·0	50	49·7	6·5
04	26	01·2	50	09·3	3·9	04	25	58·1	50	10·1	4·3
04	37	36·9	51	25·7	2·4	04	37	31·2	51	25·0	3·2
04	42	56·4	50	32·0	6·9	04	42	56·1	50	33·5	7·3
04	48	55·6	52	00·0	6·5	04	48	53·3	52	02·1	5·1
					<2·0	04	56	18·5	50	09·2	3·3
05	12	41·6	51	04·4	4·8	05	12	39·0	51	09·7	4·8

TABLE I—*continued*

52° Survey R.A. h	m	s	Dec. °	′	Flux density 10^{-26} MKS	50° Survey R.A. h	m	s	Dec. °	′	Flux density 10^{-26} MKS
05	15	40·2	50	49·8	9·0	05	15	38·1	50	52·6	8·9
05	22	11·0	51	37·4	6·2	05	22	08·5	51	39·1	5·9
05	38	44·6	49	48·7	53	05	38	42·9	49	51·0	64
06	15	58·7	51	03·2	2·9	06	15	57·0	51	08·8	2·7
06	25	54·0	50	28·6	4·3	06	25	53·9	50	32·2	4·9
06	28	49·9	50	23·3	3·1	06	28	50·2	50	27·4	2·5
06	35	45·2	51	08·5	3·2	06	35	44·8	51	08·4	2·1
06	50	15·2	50	16·1	4·1	06	50	18·6	50	24·8	2·0
07	00	30·1	50	33·0	3·1	07	00	31·6	50	35·7	2·5
07	03	47·9	50	04·5	4·9	07	03	46·5	50	09·3	4·3
07	24	17·4	50	39·3	3·0	07	24	16·6	50	42·2	2·9
07	28	37·9	51	17·6	3·1	07	28	35·7	51	20·0	2·6
07	29	48·7	51	58·2	4·2	07	29	45·5	52	01·9	2·7
07	36	30·1	51	30·0	4·6	07	36	27·9	51	39·0	4·6
08	29	44·6	51	09·6	6·9	08	29	40·4	51	17·3	5·8
08	35	33·8	51	09·6	3·5	08	35	31·0	51	16·0	2·1
08	35	58·7	50	29·6	3·4	08	35	55·2	50	35·9	2·5
08	39	39·4	51	04·1	3·2	08	39	34·4	51	11·4	2·4
09	00	25·4	50	24·1	3·1	09	00	21·7	50	30·1	3·2
10	31	20·8	50	29·5	6·0	10	31	17·4	50	31·3	5·9
10	39	08·9	50	30·9	5·6	10	39	07·7	50	29·3	5·5
11	30	34·7	50	27·3	3·2	11	30	31·3	50	29·1	4·1
11	36	13·0	50	36·2	3·2	11	36	11·4	50	35·7	2·6
11	43	07·8	50	04·4	9·4	11	43	05·9	50	02·3	8·9
11	50	52·0	49	52·3	5·1	11	50	49·8	49	50·8	5·5
11	51	12·5	51	35·7	3·1	11	51	11·5	51	34·2	3·4
12	20	29·6	50	49·1	3·7	12	20	27·0	50	47·4	3·6
12	49	29·0	50	52·4	4·3	12	49	28·5	50	52·1	4·5
13	17	44·5	52	06·2	2·9	13	17	41·7	52	06·3	3·5
13	29	37·1	50	26·1	4·1	13	29	39·0	50	25·1	4·9
13	43	29·2	50	03·1	7·4	13	43	29·2	50	00·9	11·5
14	41	24·4	50	51·7	4·6	14	41	21·1	50	49·9	3·3
14	46	59·5	50	30·5	2·8	14	46	59·7	50	25·5	3·2
14	52	24·7	50	12·7	4·2	14	52	24·8	50	15·0	4·7
16	52	40·5	52	05·2	3·5	16	52	43·6	52	03·2	3·7
17	00	10·2	50	49·5	3·2	17	00	13·2	50	54·3	3·2
17	23	06·0	51	00·5	11·2	17	23	11·8	51	02·4	10·8
17	29	51·6	50	05·7	3·8	17	29	56·7	50	11·4	4·1
18	17	50·5	50	28·5	7·4	18	17	56·8	50	28·1	7·6
19	40	21·4	50	28·1	8·5	19	40	26·7	50	29·5	7·3
20	07	49·4	50	08·6	5·3	20	07	54·4	50	12·1	3·8
20	30	12·5	51	45·6	5·9	20	30	17·8	51	45·3	5·7
20	37	07·1	51	07·1	12·5	20	37	10·4	51	09·0	12·1
20	40	36·3	50	17·2	6·7	20	40	42·2	50	21·1	7·1
20	55	44·6	50	47·1	4·3	20	55	49·5	50	48·1	4·5
21	22	43·0	50	49·4	3·5	21	22	46·9	50	45·4	3·7
21	22	53·7	51	54·2	4·2	21	23	00·6	51	57·1	4·5
21	50	15·4	49	45·3	4·2	Region not covered by survey					
23	45	34·8	51	05·6	3·3	23	45	36·2	51	03·9	3·0
23	46	08·8	50	26·4	3·3	23	46	55·0	50	17·9	3·0

A precise comparison of the positions yields an r.m.s. differential error of ~3′ in declination and ~4^s in right ascension. The declination errors appear to be random but there is a systematic error in right ascension which, when plotted against right ascension, approximates to a sinusoidal variation as shown in Fig. 8.

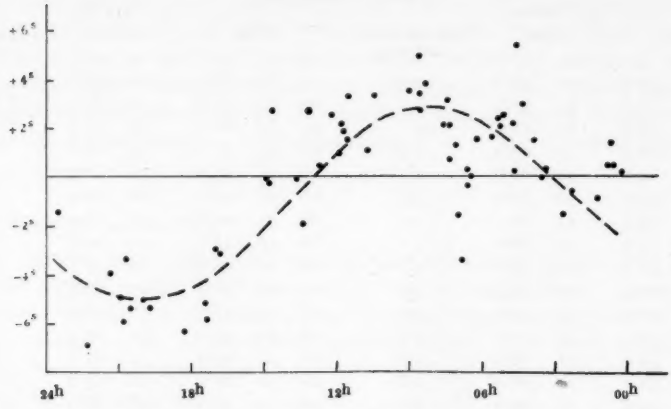

FIG. 8.—*A plot showing the systematic error in right ascension between the 50° and 52° surveys.*

The r.m.s. error of the individual surveys thus amounts to $\sim 1'$ in right ascension and $\sim 2'$ in declination. When the systematic error is more fully understood the error in right ascension should be reduced to $\sim 0'{\cdot}3$.

(*b*) *Survey at* 05°.—Previous observations have indicated that while most radio stars remote from the galactic plane are probably of extra-galactic origin there is a possibility that they can be accounted for by a class of objects in the galactic halo (Ryle 1958). This possibility may be eliminated by studying the isotropy of the distribution of sufficiently weak radio stars. A survey has therefore been made at a declination of 05° which includes longitudes towards the centre and anti-centre at galactic latitudes near 50° where the greatest anisotropy might be expected to occur.

Application of the statistical method enables deductions to be made about the number–intensity relationship of radio stars at a flux density considerably lower than that at which the sources can be reliably distinguished individually. The probability distribution of $|D|$ was computed for two areas towards the centre and anti-centre (right ascensions $22^h\,40^m - 02^h\,40^m$ and $10^h\,40^m - 14^h\,40^m$). The results are shown in Fig. 9. It is seen that any differences in these distributions are less than the statistical uncertainty and hence there is no evidence for a reduction in the density of radio sources in the longitude of the anti-centre. It will be shown in another paper (Hewish 1961) that this observation implies an isotropy which extends to at least 10,000 sources steradian.

(*c*) *The* 42° *survey*.—Positions and intensities were derived for sources having flux densities $> 2 \times 10^{-26}$ w.m^{-2} (c/s)$^{-1}$. 175 sources were found in an area of 0·3 steradians ($\alpha = 20^h\,40^m - 19^h\,15^m$, $\delta = 40° - 44°$); this number corresponds to an average of 1 source per 30 beam areas so that errors due to confusion should be small. A complete list of these sources is given in Table II. The quoted error for each source includes a confusion error derived from the probability distribution of $|D|$, a reading error and the residual collimation error; it does not include the systematic error in right ascension, discussed in Section 4 (*a*), for the 50° – 52° strip, which has an upper limit of $\pm 4^s$.

The radio sources M31 and NGC 1275 came within the region of the survey. A number of weak sources were found within the boundaries of M31 but, as discussed elsewhere (Baldwin and Costain 1960), there is no significant excess as compared with a neighbouring area of sky and hence no reason to associate them with the nebula. NGC 1275, a member of the Perseus cluster, has been resolved into two distinct components separated by 32′, together with a weak extended component which may be associated with the cluster as a whole. The new information about NGC 1275 will be discussed fully in another paper (Leslie and Elsmore 1961).

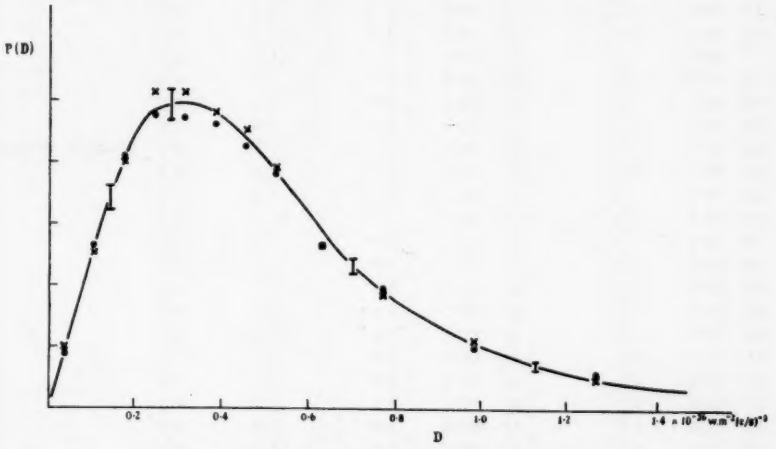

FIG. 9.—*The probability distribution of |D| for areas at galactic latitudes near 50° and longitudes towards the centre and the anti-centre.*
● R.A. $22^h\,40^m$ to $02^h\,40^m$
× R.A. $10^h\,40^m$ to $14^h\,40^m$

TABLE II

R.A.			Error	Dec.		Error	Flux density	Error	
h	m	s	±s	°	′	±′	10^{-26} MKS	±	
00	10	54·7	3·0	40	34·6	3·0	5·0	0·6	
00	19	09·6	2·0	43	10·7	3·0	3·5	0·6	
00	20	50·0	2·5	43	48·0	3·0	2·5	0·5	
00	28	06·7	2·5	40	53·2	3·0	2·5	0·5	
00	41	54·1	2·5	42	30·5	3·0	2·0	0·4	
00	45	25·6	2·0	40	06·0	3·0	3·2	0·5	Possibly complex
00	51	38·4	2·0	40	26·1	2·5	3·2	0·5	
00	53	58·1	2·5	43	58·0	3·0	2·4	0·5	
01	03	51·6	2·0	42	12·8	2·0	3·7	0·5	
01	09	22·7	2·0	41	37·0	2·5	3·6	0·5	
01	13	33·8	3·0	40	03·3	3·0	2·3	0·4	Possibly complex
01	20	32·0	2·5	40	34·8	4·0	2·8	0·5	Complex
01	44	55·3	2·5	43	09·3	3·0	2·5	0·5	
01	52	26·3	1·5	43	32·5	2·0	9·6	1·0	
01	53	17·3	2·0	41	48·9	2·5	3·1	0·5	
01	57	03·3	2·5	40	34·1	3·0	2·7	0·5	
02	16	00·6	2·0	42	24·4	2·5	3·9	0·6	

TABLE II—*continued*

R.A.			Error	Dec.		Error	Flux density	Error	
h	m	s	±s	°		±′	10^{-26} MKS	±	
02	20	08·3	1·5	42	49·6	2·0	16·6	1·5	
02	22	37·0	2·0	40	19·2	2·5	3·1	0·5	
02	32	45·6	1·8	41	11·1	2·0	4·5	0·5	
02	46	15·0	1·5	42	56·2	1·8	6·6	0·6	
02	54	33·9	2·5	40	40·4	3·0	2·0	0·4	
03	00	16·1	2·5	43	35·5	3·0	2·1	0·4	
03	02	30·1	2·5	43	55·5	3·0	2·8	0·5	
03	09	42·6	2·5	41	24·7	3·0	2·1	0·4	
03	11	23·6	1·5	43	06·0	1·8	8·5	0·8	
03	14	54·2	2·0	41	44·7	3·0	14·5	2·0	
03	16	28·6	1·5	41	21·0	1·5	41·0	4·0	
03	23	18·3	1·8	41	44·6	2·0	5·2	0·5	
03	27	07·1	1·8	40	53·4	2·0	5·5	0·6	
03	30	50·7	2·5	43	24·4	3·0	3·0	0·6	
03	44	37·8	3·0	40	39·1	3·0	2·8	0·5	Possibly complex
03	51	06·8	2·5	41	47·2	3·0	2·5	0·5	
03	54	19·6	2·5	41	42·4	3·0	2·4	0·5	
04	04	35·7	1·5	42	54·1	1·5	25·1	1·5	
04	16	49·1	2·5	43	37·2	3·0	2·8	0·5	
04	19	52·6	1·8	40	47·7	2·0	5·1	0·6	
04	22	37·8	2·5	41	21·2	3·0	2·8	0·5	
04	25	47·2	1·8	42	27·7	2·0	4·2	0·5	
04	29	08·0	1·5	41	33·7	1·5	14·9	1·0	
04	41	17·7	2·5	43	54·0	3·0	2·1	0·4	
04	46	04·4	2·5	42	13·0	3·0	2·1	0·4	
05	11	12·1	2·0	42	37·5	2·5	3·0	0·5	
05	25	15·5	1·8	41	40·5	2·0	4·0	0·6	
05	28	10·1	2·5	43	46·1	3·0	2·3	0·4	
06	02	43·0	2·0	41	37·9	3·0	4·1	0·6	Complex
06	11	24·0	2·0	42	53·1	2·5	3·0	0·5	
06	12	52·5	2·5	41	31·4	3·0	2·3	0·4	
06	13	32·5	2·5	40	41·4	3·0	2·5	0·5	
06	14	47·3	2·5	43	33·5	3·0	2·5	0·5	
06	21	36·5	2·0	40	01·3	2·0	6·6	0·7	
06	21	50·1	2·5	40	30·6	2·5	3·8	0·6	
06	27	13·3	2·5	42	31·4	3·0	2·0	0·4	
06	28	46·1	3·0	42	20·3	3·0	2·6	0·5	
06	42	51·8	2·5	40	49·7	2·5	2·8	0·5	
06	44	12·1	2·5	42	22·9	3·0	2·8	0·5	
06	47	22·4	2·5	41	33·5	3·0	2·6	0·5	
06	49	29·1	3·0	42	39·6	3·0	2·2	0·4	
06	52	37·4	3·0	42	42·2	4·0	2·2	0·4	
07	03	10·4	2·0	42	35·3	3·0	3·5	0·6	
07	09	02·6	2·5	40	55·3	3·0	2·2	0·4	
07	26	19·0	2·5	43	08·0	3·0	2·0	0·4	
07	31	51·7	1·8	43	49·2	2·0	5·0	0·7	
08	05	42·7	2·5	40	44·5	3·0	2·4	0·5	
08	06	39·5	1·5	42	36·8	1·8	9·6	1·0	
08	09	33·4	2·5	40	26·4	3·0	2·9	0·5	
08	20	05·1	1·8	43	07·6	2·0	5·4	0·7	
08	36	39·0	2·5	42	37·9	3·0	2·4	0·5	
08	36	56·0	2·0	40	13·0	2·5	3·3	0·6	
08	49	17·7	2·0	42	30·2	2·5	3·1	0·6	
08	56	47·5	3·0	40	34·6	4·0	2·3	0·5	
09	01	00·2	2·0	42	50·0	2·5	3·7	0·6	

TABLE II—*continued*

R.A.			Error	Dec.		Error	Flux density	Error	
h	m	s	±s	°	′	±′	10^{-26} MKS	±	
09	02	50·0	2·5	41	30·2	3·0	3·0	0·6	
09	03	50·2	4·0	42	55·4	5·0	2·7	0·5	Confused region
09	04	22·2	2·0	41	49·4	2·5	5·2	0·7	Confused region
09	06	19·5	1·5	43	05·0	2·0	19·5	1·5	Confused region
09	06	34·8	5·0	40	46·2	5·0	4·5	1·0	Confused region
09	06	46·6	5·0	41	19·7	5·0	4·0	0·8	Confused region
09	22	14·1	3·5	42	31·6	5·0	2·4	0·5	
09	22	52·2	3·5	42	17·3	5·0	2·0	0·5	
09	35	06·7	2·5	42	53·8	3·0	2·5	0·4	
09	36	14·0	2·0	40	30·2	2·0	3·4	0·5	
09	45	25·2	1·8	41	53·6	2·0	4·1	0·6	
09	45	53·0	2·5	40	47·6	3·0	2·3	0·4	
09	47	13·1	2·5	42	28·0	3·0	2·0	0·4	
10	07	27·4	1·5	41	49·9	1·8	6·0	0·8	
10	09	08·7	2·5	43	30·8	3·0	2·1	0·4	
10	13	00·8	2·0	40	59·6	2·5	3·8	0·6	
10	20	14·6	2·5	40	05·4	3·0	2·3	0·4	
10	22	33·0	2·0	43	15·2	2·5	4·5	0·7	
10	33	27·0	3·0	40	48·7	5·0	2·0	0·4	
10	34	20·4	2·5	40	27·7	3·5	3·1	0·5	
10	55	10·2	3·0	40	27·8	4·0	2·3	0·4	
10	56	10·0	1·5	43	17·8	1·5	11·2	1·4	
11	08	53·1	2·0	41	08·4	2·0	5·1	0·7	
11	09	53·4	2·0	43	43·1	2·0	6·3	0·8	
11	11	54·0	1·5	40	52·0	1·5	21·2	1·5	
11	28	07·4	2·5	43	42·2	4·0	3·2	0·6	
11	31	58·5	1·5	43	47·4	1·8	6·6	0·8	
11	32	06·2	3·0	40	56·6	3·5	2·8	0·5	
12	06	45·0	1·5	43	56·6	1·5	10·7	1·0	
12	20	08·8	2·5	40	50·9	3·5	2·0	0·4	
12	22	03·0	1·5	42	22·7	1·8	7·2	0·8	
12	31	55·0	2·5	43	10·7	3·0	2·5	0·5	
12	32	04·6	2·5	41	26·5	3·0	2·4	0·4	
12	49	44·7	2·5	43	18·6	3·0	2·3	0·4	
12	53	28·7	2·0	43	13·6	2·5	2·5	0·5	
12	58	14·6	1·5	40	23·0	1·8	8·6	1·0	
13	19	08·1	2·0	42	51·6	2·0	6·0	0·8	
13	19	41·7	4·0	43	27·7	5·0	2·4	0·5	
13	21	12·5	3·0	41	30·0	3·5	2·9	0·5	
13	24	54·1	2·5	43	08·1	3·0	2·1	0·4	
13	33	10·7	1·8	41	14·8	2·0	5·0	0·7	
13	40	27·3	3·0	43	51·5	3·0	2·2	0·4	
13	43	28·7	2·0	43	04·6	2·0	3·4	0·6	
13	50	26·5	3·0	43	14·9	3·5	2·6	0·5	
13	58	30·7	2·5	43	21·9	3·0	2·3	0·4	
14	10	21·5	2·0	43	51·3	2·5	2·7	0·5	
14	18	47·1	2·5	40	17·8	3·0	2·1	0·4	
14	18	50·3	2·5	43	51·8	3·0	2·7	0·5	
14	19	08·0	1·5	41	59·4	1·5	11·6	1·0	
14	35	03·8	2·5	42	57·1	3·0	2·5	0·5	
14	37	53·8	2·0	42	45·8	2·0	3·9	0·6	
14	44	35·0	2·0	41	44·5	2·5	2·3	0·4	
14	49	16·9	3·0	41	55·1	4·0	2·1	0·4	
14	55	51·0	2·5	42	11·3	3·0	2·3	0·4	
15	21	24·2	2·0	42	07·6	2·5	2·4	0·4	

TABLE II—*continued*

R.A.			Error	Dec.		Error	Flux density	Error	
h	m	s	±s	°	′	±′	10^{-26} MKS	±	
15	24	55·7	2·0	43	18·0	2·5	2·6	0·5	
15	55	02·0	1·5	43	07·7	1·8	7·3	0·8	
15	57	57·5	2·0	43	58·8	2·5	2·8	0·5	
16	10	10·4	2·5	40	47·2	3·0	2·3	0·4	
16	18	49·0	3·0	43	24·0	3·5	3·0	0·6	
16	19	45·7	3·0	43	56·6	4·0	2·0	0·4	
16	24	24·3	3·0	41	35·9	3·0	2·1	0·4	
16	37	15·5	3·0	42	38·8	4·0	2·3	0·4	
16	47	25·1	4·0	42	58·8	3·5	3·5	0·6	Complex
17	10	36·0	2·5	43	21·4	3·0	2·5	0·5	
17	14	31·3	4·0	43	42·4	5·0	2·9	0·5	Complex
17	23	43·4	1·8	40	36·9	2·0	5·4	0·7	
17	29	05·0	2·5	43	33·0	3·0	2·1	0·4	
17	29	14·0	2·5	40	56·6	3·0	2·0	0·4	
17	31	33·4	1·8	43	45·3	2·0	4·8	0·7	
17	37	24·0	2·0	42	48·6	2·5	4·9	0·7	
17	38	38·3	2·5	41	34·8	3·0	2·6	0·5	
17	49	09·4	3·0	43	53·4	3·5	2·3	0·4	
18	09	23·0	2·5	40	43·2	3·0	5·6	0·7	
18	11	48·0	1·8	43	01·4	2·0	4·1	0·6	
18	12	14·7	2·5	41	08·3	3·0	2·8	0·5	
18	14	17·2	2·5	42	56·2	2·5	2·5	0·5	
18	19	17·4	3·0	40	48·2	3·0	2·5	0·5	Complex
18	34	13·2	2·0	41	59·9	2·5	2·9	0·5	
18	39	12·7	2·5	40	36·1	2·5	3·0	0·6	
18	54	47·0	2·5	42	44·2	3·0	2·8	0·5	
19	10	41·7	3·0	40	14·0	3·5	3·5	0·6	
19	13	35·5	3·0	43	36·0	3·0	3·1	0·6	Possibly complex
20	42	54·1	3·0	40	20·7	4·0	2·0	0·4	
20	43	23·4	2·5	43	31·6	2·5	2·8	0·6	
20	47	09·8	2·0	42	58·3	2·0	6·1	0·7	
20	49	06·1	2·5	41	51·1	3·0	2·2	0·4	
20	56	15·6	2·5	42	40·2	3·0	2·5	0·5	
21	04	24·4	2·5	42	24·7	3·0	2·5	0·5	
21	19	26·1	2·0	43	32·9	2·0	3·8	0·6	
21	38	26·4	2·5	43	57·2	3·5	2·0	0·4	
21	56	55·4	2·5	43	30·4	3·0	2·3	0·5	
21	59	41·4	2·0	40	49·8	2·5	2·7	0·5	
22	09	01·3	2·5	42	52·9	3·0	2·2	0·4	
22	19	45·6	3·0	41	19·0	3·0	2·5	0·5	
22	21	12·3	1·8	43	19·4	2·0	3·2	0·6	
22	22	35·6	3·0	40	39·7	3·0	2·0	0·4	
22	24	35·2	2·5	41	27·6	3·0	2·5	0·5	
22	33	39·1	1·8	40	52·5	2·0	3·4	0·6	
22	37	58·1	2·0	43	16·4	2·5	2·0	0·4	
22	41	08·6	1·5	43	46·5	2·0	4·5	0·7	
22	49	46·7	2·0	43	47·0	2·5	2·8	0·5	
22	55	05·9	2·0	41	33·4	2·5	2·7	0·5	
23	02	36·2	2·0	40	11·4	2·5	2·8	0·5	
23	24	30·6	1·5	40	28·4	1·8	8·5	1·0	
23	30	58·0	2·5	43	26·6	3·0	2·3	0·4	
23	49	22·6	2·5	41	03·2	3·0	2·2	0·4	
23	51	23·8	3·0	40	01·7	2·5	3·1	0·6	
23	56	03·3	1·5	43	48·9	1·8	9·9	1·0	
23	58	46·1	2·0	41	35·5	2·0	3·9	0·6	

5. *Conclusion.*—The first surveys carried out at a wavelength of 1·7 m using the new principle of aperture synthesis have shown that the theoretical possibilities of the technique may be fully realized in practice.

A primary resolving power of $25' \times 35'$ has been achieved with a noise level of $0{\cdot}08 \times 10^{-26}$ w.m^{-2} (c/s)$^{-1}$. The side-lobes in right ascension are negligible beyond $\pm 1°$ from the centre of the beam; in declination the side-lobe level is ~5 per cent within $\pm 2\frac{1}{2}°$ and less than 0·5 per cent at greater angles. Radio stars may be reliably detected to a flux level of $2{\cdot}0 \times 10^{-26}$ w.m^{-2} (c/s)$^{-1}$, corresponding to one source/20 beam areas, with positional accuracies of $\pm 2'$ in declination and $\pm 1'$ in right ascension; at this limit the noise is still only 5 per cent so that statistical investigations may be used to study the distribution of radio stars at smaller flux densities.

Acknowledgments.—We are greatly indebted to Dr M. V. Wilkes of the University of Cambridge Mathematical Laboratory for providing the use of EDSAC II and other facilities, and to Dr D. J. Wheeler and Mrs R. Feinstein who were responsible both for the running and design of the programme. Our thanks are also due to Mr D. R. Marks, whose careful analysis of the computed results led to the final positions and flux densities of the radio stars. One of us (P.F.S.) is indebted to the D.S.I.R. for a maintenance allowance.

Mullard Radio Astronomy Observatory,
Cavendish Laboratory,
Cambridge:

1960 *September.*

References

Baldwin, J. E. and Costain, C. H., 1960, *M.N.*, **121**, 413.
Bracewell, R. N., 1956, *Aust. J. Phys.*, **9**, 297.
Elsmore, B., Ryle, M. and Leslie, P. R. R., 1959, *Mem. R.A.S.*, **68**, 61.
Hewish, A., 1961 (in preparation).
Leslie, P. R. R., 1961, *M.N.*, **122**, 51.
Leslie, P. R. R., and Elsmore, B., 1961, *Observatory* (in press).
Ryle, M., 1952, *Proc. Roy. Soc.* A, **221**, 351.
Ryle, M., 1958, *Proc. Roy. Soc.* A, **248**, 289.
Ryle, M., 1960, *J.I.E.E.*, **6**, 14.
Ryle, M. and Hewish, A., 1960, *M.N.*, **120**, 220.
Scheuer, P. A. G., 1957, *Proc. Camb. Phil. Soc.*, **53**, 764.

OBSERVATIONS OF THE ZODIACAL LIGHT FROM A VERY HIGH ALTITUDE STATION

I. The Average Zodiacal Light

D. E. Blackwell and M. F. Ingham

(Received 1960 October 6)

Summary

The paper presents measurements of the absolute surface brightness at three wavelengths, the polarization at two wavelengths and the position of the zodiacal light made from the high altitude station of Chacaltaya in the Bolivian Andes (height 17 100 ft, geomagnetic latitude 3° S). This site is particularly suited to such observations because the weather is good and the atmospheric extinction is close to that expected for a dust-free Rayleigh scattering atmosphere. The brightness and polarization measures extend to within 19° of the Sun. The colour is close to that of the Sun, but it is slightly more red; the polarization measures agree well with those recently obtained by Elsässer.

Introduction.—The zodiacal light has been the subject of many investigations during the last three centuries, although accurate measurement using modern techniques may be said to have begun only twenty years ago with the work of Elvey and Roach (**1**). It is now recognised, as a result of these investigations, that most of the zodiacal light originates in interplanetary space, and that it may be considered as the outermost part of the solar corona. Also, it has been supposed that much of this extra-terrestrial part, and perhaps all, is due to the scattering of sunlight by small solid particles, usually described as "dust", situated in interplanetary space at distances greater than 0·3 A.U. from the Sun—as was first suggested by Cassini in 1672 (**2**). This viewpoint was almost universally accepted until 1953, when Behr and Siedentopf (**3**) made the first accurate measurements of the degree of polarization of the zodiacal light, and on the basis of these measures put forward the hypothesis that approximately half of the surface brightness of the zodiacal light near elongation 35° is due to the scattering of sunlight by free electrons in interplanetary space, the electron density in the plane of the ecliptic at 1 A.U. from the Sun being about 600 electrons cm^{-3}. The remainder of the zodiacal light is supposed due to scattering by interplanetary dust particles.

It has seemed to the authors that there are good arguments against the existence of such a high concentration of free electrons in the plane of the ecliptic so far from the Sun (see, for example, Blackwell (**4**) and later papers in this series) and that the presence of these electrons should be confirmed by another and independent

method. This is the origin of the present investigation, which was made during an expedition planned for this purpose and sent from the Cambridge Observatories to the high altitude mountain site of Chacaltaya in Bolivia during 1958. As part of the programme of the expedition we took advantage of the exceptionally fine atmospheric conditions at Chacaltaya to re-evaluate the fundamental data concerning the brightness, polarization and position of the zodiacal light, and studies of possible variations of these quantities; these studies are described in two papers of this series. In a third paper we shall describe the spectrum of the zodiacal light that was obtained at Chacaltaya and discuss its bearing on the problem of the existence of interplanetary electrons, usually known as interplanetary gas. In a fourth paper we shall rediscuss the properties of the interplanetary dust.

Observing site.—The Chacaltaya observations described here have been made only on the inner zodiacal light within the range of elongation, $19° < \epsilon < 70°$. There are two reasons for this restriction; the first is that the problem of detecting free electrons in interplanetary space becomes rapidly easier as the elongation of the line of sight diminishes—for instance, at elongation 19° the line of sight approaches to within 0·33 A.U. ($\equiv 70R_{\odot}$) of the Sun—and indeed, the observing site was especially chosen so that observations could be made as close to the Sun as possible. The second reason is that at greater elongations there is a large and very uncertain correction for the night sky background, which requires special methods for its evaluation, and which in any case cannot be better investigated at Chacaltaya than at any other suitable mountain site.

The requirements for a site suitable for observations such as these are; (*a*) a situation in the tropics, from which the zodiacal light may be observed when its symmetry axis is nearly vertical at the horizon, (*b*) a very transparent atmosphere, so that photometric observations may be made with reasonable accuracy (i.e. with an error not greater than 5 per cent) to within a few degrees of the horizon, and (*c*) a good climate which enables observations to be made near to the horizon on successive nights with little interruption by cloud. The cosmic ray station of Chacaltaya, directed by Professor I. Escobar V, was found to fulfil these requirements well. The station is in the Bolivian Andes at a height of 17 100 ft, at latitude −16° 19′, longitude 68° 10′, and geomagnetic latitude −3°. It possesses a good west horizon at zenith distance 91° where the sky was usually of extreme clarity at sunset and during twilight and night, although the weather during the day was frequently poor. Our observing programme was scarcely interrupted by cloud.

As part of the purpose of the expedition was to obtain the absolute brightness of the zodiacal light and to seek a variation of brightness with time, the atmospheric extinction was measured whenever the zodiacal light was observed. The extinction measurements were made photoelectrically at the two effective wavelengths of 0·45 μ and 0·59 μ, using bright stars in the region of the zodiacal light and a distant standard lamp to keep a check on possible variations in the sensitivity of the photometer. A logarithmic plot of one set of observations at 0·45 μ, which is typical of all, is given in Fig. 1; here the brightness is related to the air mass calculated for a spherical earth, and the regularity of the observations show that the atmosphere is reasonably uniform within to a few degrees of the horizon. To illustrate the quality of the atmosphere at this site we give in Table I the atmospheric transmission measured on 23 evenings at zenith distance 75° over the western horizon (corresponding to an air mass of 2·35) for wavelengths 4500 A

and 5900 A. The zenith absorption at 5900 A is usually about $0^{m}.08$. The data are summarized in Table II, from which it will be seen that the extinction at both wavelengths is close to that expected theoretically for a dust-free Rayleigh scattering atmosphere (**5**).

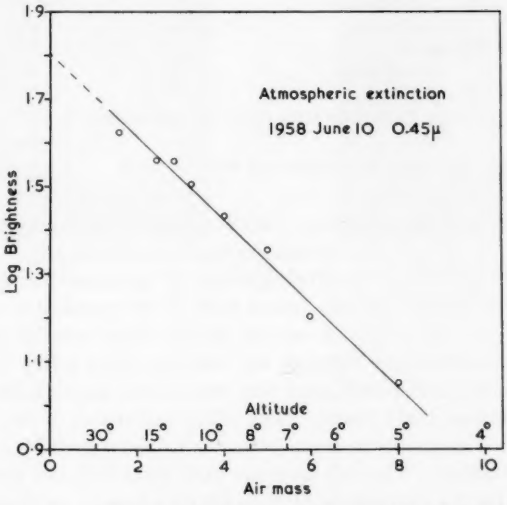

FIG. 1.—*Variation of the brightness of a star with path length.*

TABLE I

Atmospheric transmission (per cent) at zenith distance 75° at Chacaltaya (altitude 17 100 ft.)

Date	4500A	5900A	Date	4500A	5900A
June 4	60·0	72·0	July 2	60·0	72·0
5	58·0	69·6	3	61·0	73·0
9	55·8	66·8	4	58·9	70·7
10	59·0	72·0	5	51·0	61·1
12	54·5	65·3	7	52 0	62·0
13	52·9	66·9	8	50·3	60·6
15	60·0	69·8	9	49·2	59·0
16	57·5	65·4	11	60·0	72·0
17	60·0	73·2	14	56·7	68·0
18	60·0	72·0	15	56·3	66·5
19	55·9	69·8	16	57·0	68·4
			17	61·0	73·0

Apparatus.—The surface brightness and the degree of polarization of the zodiacal light were measured photographically using three cameras. A central camera, which was also used to measure the position of the axis of symmetry of the zodiacal light, was pointed directly at the ecliptic, and two others photographed areas of the sky near the horizon on each side of the ecliptic. All the cameras had simple lenses of 7 cm diameter and relative aperture $F/1{\cdot}7$, giving a plate scale of

TABLE II

Summary of atmospheric transmission data

	Percentage transmission	
	4500A	5900A
Transmission at $z=75°$ (average)	54·2	68·1
(maximum)	61·0	73·2
Zenith transmission (average)	86·1	91·5
corresponding absorption	(0^m·162)	(0^m·097)
(maximum)	88·9	93·1
corresponding absorption	(0^m·128)	(0^m·078)
Exponential absorption coefficient corresponding to maximum transmission	0·210	0·133
Theoretical absorption coefficient for Rayleigh scattering (5)	0·219	0·134

$1° \equiv 2{\cdot}14$ mm. The central camera used four lenses and photographic plates of size 12 in. × 12 in. on which the four images were simultaneously exposed, the field covered by each individual camera being about 56° in azimuth and 50° in altitude. The side cameras, containing two lenses each, photographed somewhat smaller fields. Two of the lenses of the central camera were used to photograph the zodiacal light simultaneously through the Chance filters OB10 (blue) and OY1 (orange) on Kodak IIaE plates, and also sometimes through the Chance filter OV1 (ultra-violet) on IIaO plates. The other two lenses of the central camera were used for the simultaneous measurement of polarization by a method which will be described later. The side cameras were used with the same filters as the central cameras for the measurement of brightness only. As the exposures were usually of about 10 minutes' duration, no guiding was necessary. After the photographs had been taken, calibration marks were impressed upon previously shielded parts of the plates using a step wedge and standard lamp, reduced in brightness with suitable neutral filters, and all the plates, from the central and side cameras, were processed together.

Measurement of the brightness of the average zodiacal light.—In this paper we take no account of possible variations of the zodiacal light, but merely average the data to give an observational model representing the "average" zodiacal light.

The surface brightness of the zodiacal light has been measured before on many occasions but, so far as we are aware, never under such good atmospheric conditions as exist at Chacaltaya. One of the difficulties in work of this kind is to distinguish between the zodiacal light and the background light of the night sky, and imperfect separation of these two is probably the chief source of uncertainty in the best of the modern data. A particular advantage of attempting this separation at a site such as Chacaltaya is that there the observed ratio of zodiacal light to night sky brightness is rather greater than usual because the atmospheric extinction is small and because observations can be made at small elongations where the zodiacal light is bright. We use the term "night sky" in a rather loose sense here; the zodiacal light could usually be seen when the Sun was depressed only 12° below the horizon and some of our observations of brightness (although none of the spectra) were made before the end of astronomical twilight.

A typical photograph taken with the central camera is shown in Plate 3; this photograph was taken through the OB10 filter using an exposure time of 10 minutes, the Sun being 19° below the horizon at the mid-point of the exposure. The

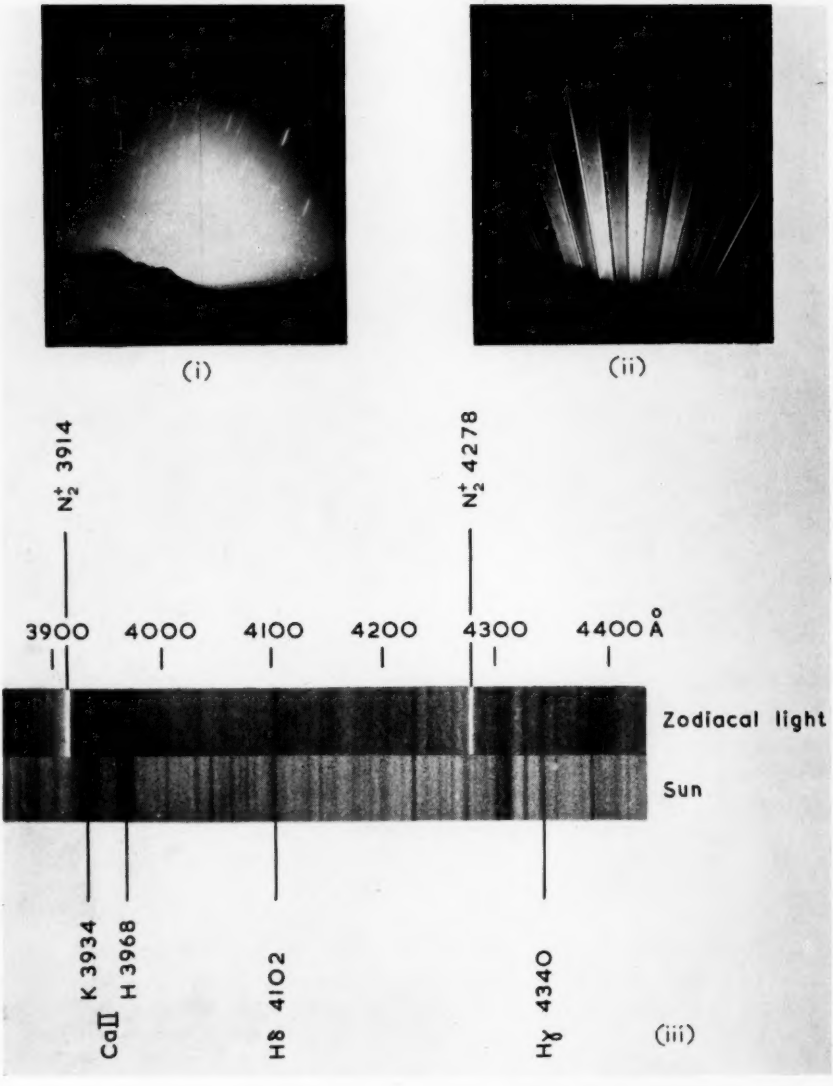

(i) Photograph of zodiacal light taken with single lens camera at Chacaltaya, 1958 August 2. Exposure 10 mins, Kodak IIaE plates used with Chance OY1 filter (effective wavelength 6200Å). Note the intersection of star trails with the depressed horizon. (ii) Photograph of zodiacal light taken through polaroid screens to determine the degree of polarization. The strong polarization is clearly shown. (iii) Spectra of the zodiacal light and the Sun.

quality of the atmosphere is demonstrated on the photograph by the presence of star trails which may be seen intersecting the depressed horizon at a distance of 80 miles.

We anticipate the detailed results here to give the response of the cameras to the zodiacal light as a function of wavelength. By this term we mean the product of the following factors; transmission of filters, transmission of camera lens, sensitivity of photographic emulsion, emission of zodiacal light, atmospheric transmission. The transmission of the camera lenses, which were made of white glass, was determined with a Carey spectrophotometer, and to make this easier an optical flat was polished on each side of a lens. The transmission of each filter was measured to an accuracy of 1 per cent of the incident light. The response curves for the three filters are shown in Fig. 2.

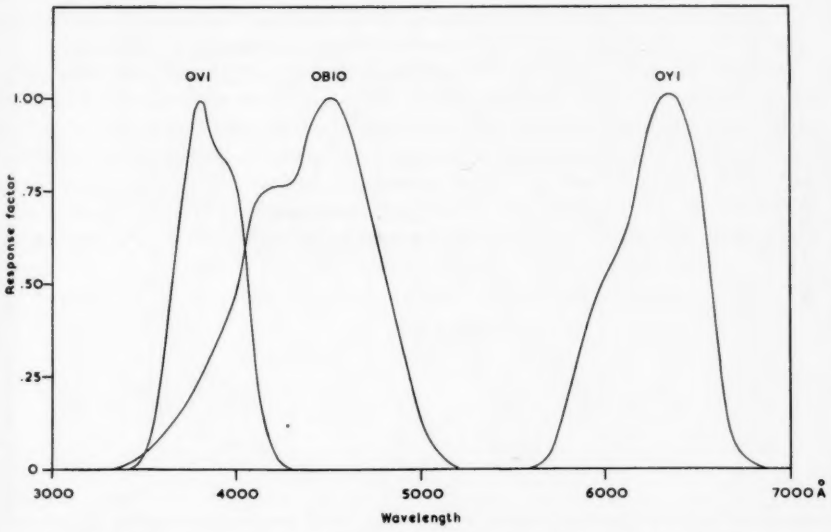

FIG. 2.—*Response curves for the three filters (the response is the product of filter transmission, transmission of camera lens, sensitivity of photographic emulsion, emission of zodiacal light, transmission of Earth's atmosphere).*

The effective wavelengths at which these three filters measure the emission of the zodiacal light depend upon the energy distribution in the spectrum of the standard lamp, and we simply refer here to a description of a method of determining these wavelengths (**6**). The three wavelengths are given in Table III.

TABLE III

Filter	*Effective wavelength*
OV1	3880A
OB10	4470
OY1	6200

The standard lamp was a 4v. 4 watt lamp selected for the optical quality of its envelope and run at the colour temperature of 2285 °K. It was calibrated by the

National Physical Laboratory, Teddington, over the range 4000 A to 7000 A with an error of not more than 1–2 per cent, and with rather more uncertainty at the shorter wavelengths.

Reduction of photographs.—To obtain the combined brightness of the zodiacal light and night sky background, the plates were scanned parallel to the horizon (i.e. approximately perpendicular to the ecliptic), using the Cambridge Observatories' recording microphotometer with a scanning spot of size 0·5 mm × 0·5 mm. The photographic densities so obtained were converted to brightness values using the calibration, and these energies were then multiplied by a camera vignetting factor which had been measured photoelectrically in the laboratory. A typical

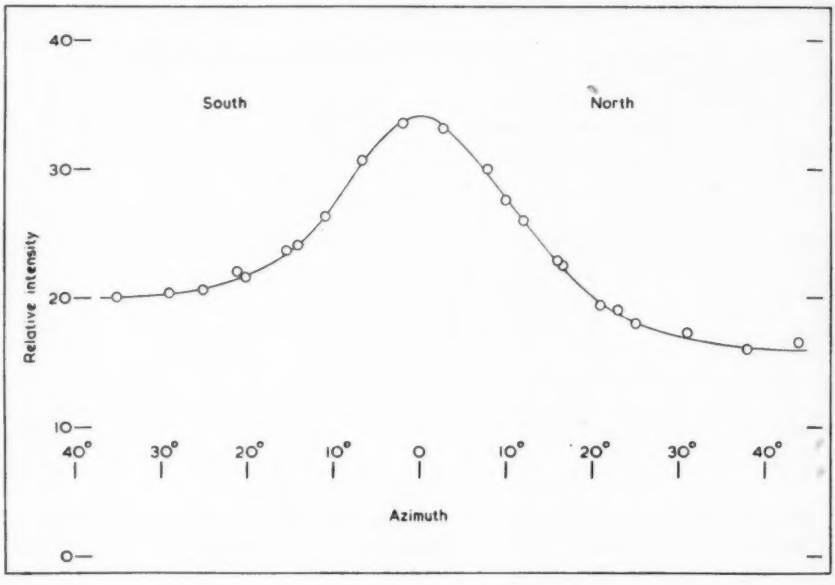

FIG. 3.—*Typical scan across the zodiacal light reduced to intensities.*

scan across the zodiacal light, at elongation 45°·5 and altitude 24°·3, which shows the brightness out to 40° on each side of the ecliptic is reproduced in Fig. 3. Such a scan results from combining microphotometer scans of the central photograph with scans of the two side photographs.

From scans such as these the ratio of the zodiacal light brightness on the ecliptic to the background brightness has been deduced using the methods and results of Roach (**7**). At these smaller elongations the error due to uncertainty in the brightness of the sky background is not great, being no more than 5 per cent. The observed zodiacal light brightness is now corrected for atmospheric extinction taking the altitude of the line of scan from the photograph. However, the correction for extinction is not straightforward. Blackwell (**4**) has suggested that it is not sufficient to allow for extinction by a simple application of the usual exponential relation with an absorption coefficient determined from observations of stars. The reason for this is that the zodiacal light is an extended source, and

some of the light from the outer parts will be scattered by the Earth's atmosphere into any point of observation, producing a spurious component. The effect has been examined quantitatively by Fessenkov (**8**) taking an extinction law of the form

$$I_{obs} = I_{incident}\, p^{\sec z}$$

and putting p equal to 0·83, corresponding to an exponential coefficient of 0·184. Fesenkov estimates the amount of spurious light to be 5·8 per cent on the axis of the zodiacal light at zenith distance 75°. At Chacaltaya, because of the lower atmospheric pressure, the amount of spurious light on axis may be expected to be approximately half of this (3 per cent) and to be less still in the red region (2 per cent). We do not regard the correction as an important one in measurements of absolute brightness at smaller elongations along the ecliptic, and especially if the observations are made at a very high altitude station, although, as Fesenkov points out, it is an important correction to measurements away from the axis.

In relating our absolute measurements of brightness to the average brightness of the solar disk, we use the data of Johnson (**9**) for the solar energy distribution.

Results of measurements of brightness.—The results of these measurements are shown in Figs. 4 and 5 where the brightness of the zodiacal light along the ecliptic, corrected for extinction, is plotted as a function of elongation for the two principal wavelengths used; the unit of brightness is that of the integrated solar disk. These diagrams show the brightness data for 22 evenings between the dates 1958 June 5 and Aug. 2, each night being represented by at least four points, and more if

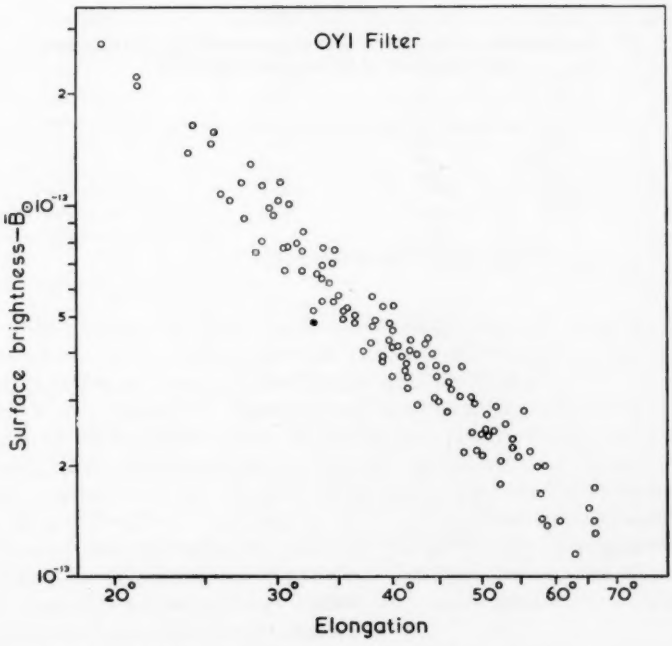

FIG. 4.—*Brightness of zodiacal light at wavelength* 6200A, OY1 *filter* (*unit; brightness of the integrated solar disk*).

more than one photograph is available. The spread of the results is rather great, being about 15 per cent at elongation near 35°, and we shall consider in Paper II of this series how far this spread can be interpreted as a real variation in brightness.

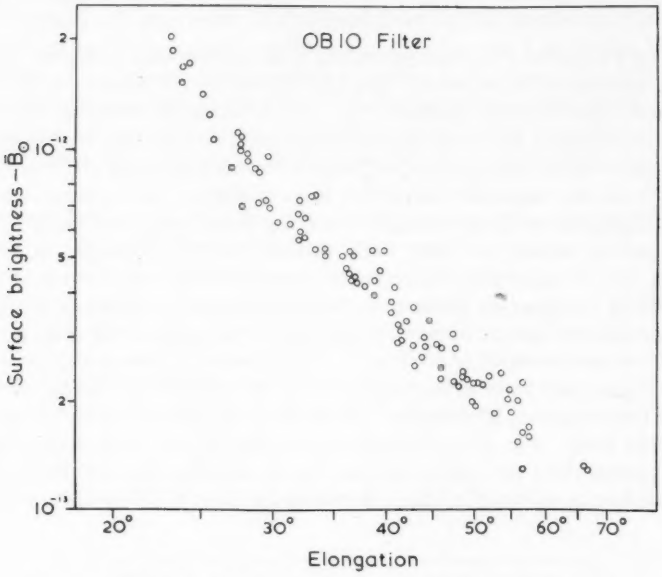

FIG. 5.—*Brightness of the zodiacal light at wavelength* 4470A, OB10 *filter (unit; brightness of the integrated solar disk).*

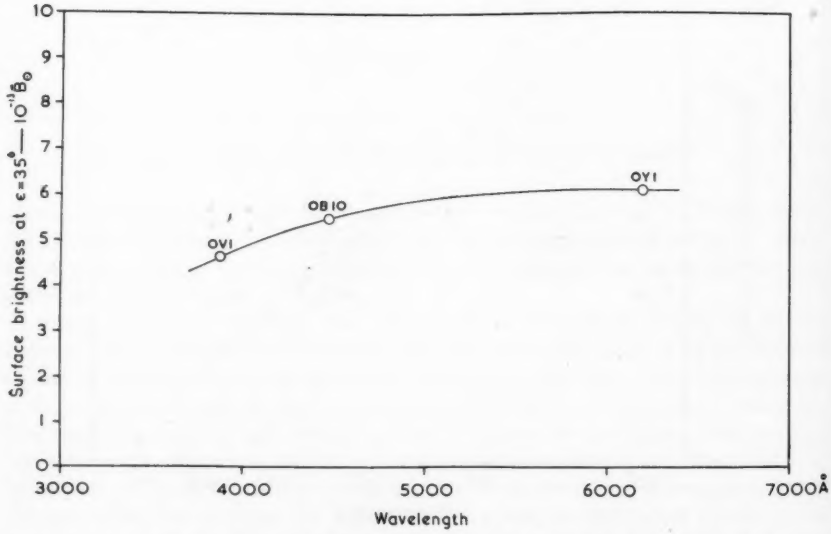

FIG. 6.—*Distribution of energy in the spectrum of the zodiacal light in comparison with that of the integrated solar disk.*

Fig. 6, obtained from the present observations, shows the distribution of energy in the spectrum of the zodiacal light at elongation 35°, corrected for extinction, in comparison with that for the average solar disk; this diagram also includes observations made on six evenings at wavelength 3880 A. The colour of the zodiacal light is closely similar to that of the Sun, as has been found by other observers who have determined its spectral type. For example, Behr and Siedentopf (**3**) found that it has the colour index of $0^m.46$ at elongation 40°, which may be compared with the value of $0^m.53$ for the Sun (**10**). However, the observations of Behr and Siedentopf were made over a comparatively restricted range of wavelengths. Elvey and Rudnick (**11**) deduce from their observations that the colour is very close to that of the Sun (although they do not quote an elongation), and a similar result has been given by Karimov (**12**).

The scan of Fig. 3 shows that the zodiacal light is highly symmetrical about a central axis, and our results show that the zodiacal light always has this remarkable symmetry when the Sun is not especially active; this result does not agree with that found by Behr and Siedentopf, who found marked asymmetries, but it is confirmed by the observations of Regener (**13**). We attribute these discrepancies partly to the necessarily greater inclination of the ecliptic to the vertical in the work of Behr and Siedentopf, and partly also to disturbance by weak aurorae in the higher latitudes.

TABLE IV

Observations of the brightness of the zodiacal light at elongation 40°
Unit—10^{-13} times mean brightness of solar disk

Observer	Latitude	Height (ft)	Date	Brightness
Behr and Siedentopf (**3**)	+46°	11700	1952	3·17
Barbier (**16**)	+44°	1900	1952/3	3·35
Roach *et al.* (**7**)	+36°	5415	1952/3	5·38
Regener (**9**)	+34°	9200	1953/4	5·52
*Blackwell (**17**)	−16°	9000	1955	2·90
Elsässer (**14**)	−29°	4550	1956	2·85
Divari and Asaad (**15**)	+24°	660	1957	3·26
Present work (at 6200 A) (average of all observations)	−16°	17100	1958	4·42

Mean brightness at elongation 40° is $3{\cdot}86 \times 10^{-13} B\odot$.

*One morning observation only.

Our measurements are most accurate at elongations in the neighbourhood of 40°, corresponding to an altitude near 20°, because here the correction for atmospheric extinction is not great and that for the night sky background is a minimum. In Table IV we compare our measurements of brightness at this elongation with the results of other investigators, including the results recently obtained by Elsässer (**14**) at the Boyden Station, S. Africa. As the colour of the zodiacal light is so close to that of the Sun we have not distinguished between observations made at different wavelengths. In reducing other observations we have adopted the Stebbins and Kron (**10**) value of −26·20 for the photographic magnitude of the Sun. There is considerable disagreement between the results of different observers even at this favourable elongation, the possible significance of which will be discussed in a later paper in this series.

The corona and the zodiacal light.—The relation between the brightness of the zodiacal light and that of the solar corona has been investigated several times.

It is now believed that most of the zodiacal light can be regarded as the outer part of the solar corona, and this viewpoint is supported by Fig. 7, in which the brightness of the solar corona and the present measures of the brightness of the zodiacal light at wavelength 6200 A are plotted against elongation; the corona measures are those of Blackwell (**6**) made from an open aircraft at a height of 30 000 ft during the eclipse of 1954 June 30. The present zodiacal light measures are useful for showing this relation, not only because they approach to within 19° of the Sun, but also because they were made at the same wavelength as those of the solar corona. There remains now a gap of only 5° between the farthest part of the corona that has been observed at a total eclipse and the innermost part of the zodiacal light.

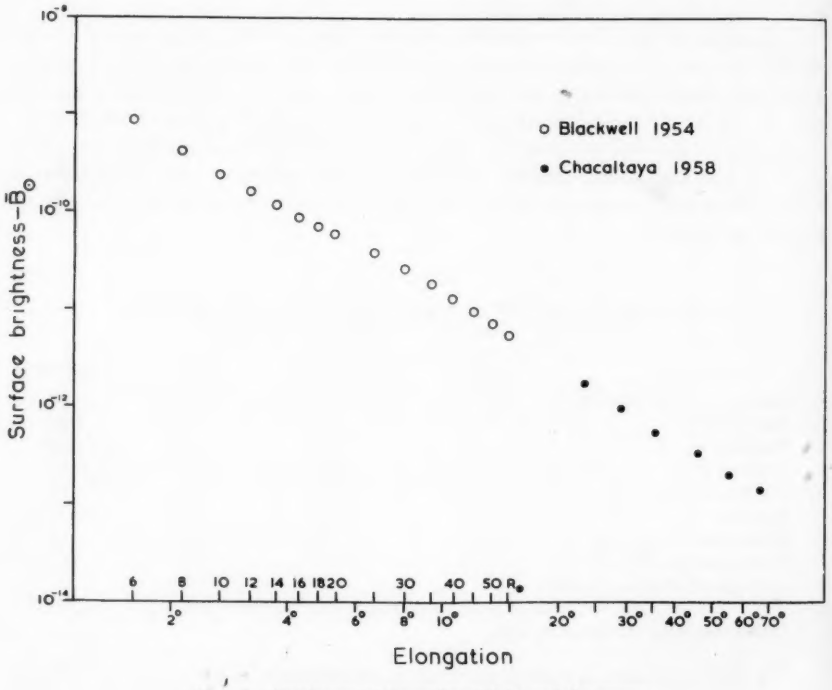

FIG. 7.—*Brightness of the zodiacal light and the corona.*

Measurement of the polarization of the zodiacal light.—The measurement of polarization is extremely difficult, partly because of the low surface brightness of the zodiacal light but chiefly because of the rather uncertain correction for the sky background, which increases with increasing elongation. The photoelectric measurements of Behr and Siedentopf (**3**) are outstanding among the early work; these measurements were made in the range of elongation $35° < \epsilon < 90°$ and showed a maximum polarization of about 23 per cent near elongation 35°. The range $20° < \epsilon < 30°$ was studied photographically by Blackwell (**17**) in 1955 using an open aircraft flying over the Pacific Ocean at a height of 9000 ft and at a position where the zodiacal light was vertical at the horizon. Elsässer (**14**) has recently made new photoelectric measurements at the Boyden Station in the range

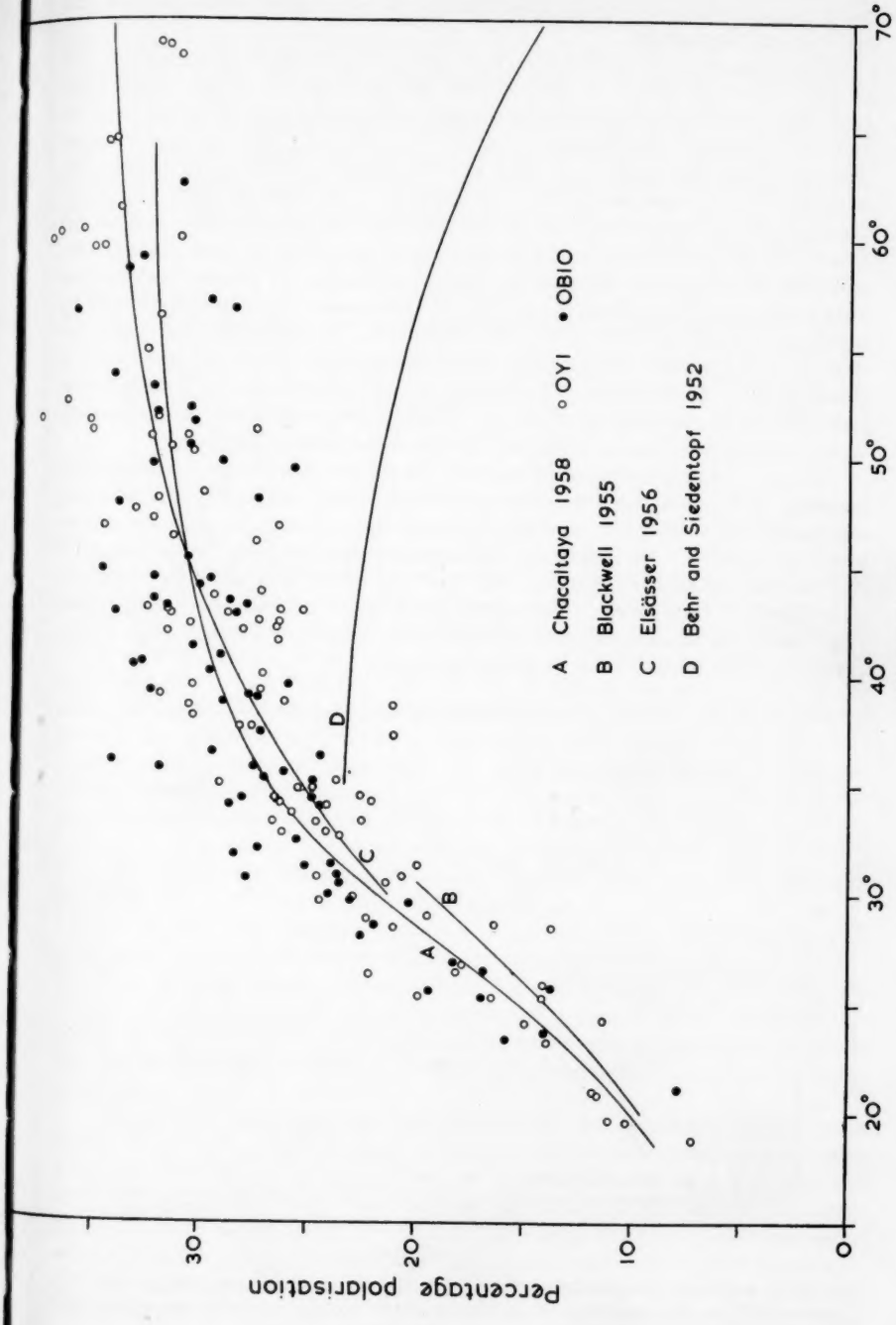

FIG. 8.—*Polarization of the zodiacal light at wavelengths 6200A and 4470A and comparison with data of other observers.*

$30° < \epsilon < 90°$, obtaining much larger values of polarization than those found by Behr and Siedentopf.

The measurements at Chacaltaya were made photographically using a grid of polaroid strips placed in contact with the photographic plate. The strips of the grid were arranged to be approximately radial to the expected position of the Sun at the time of a photograph (i.e. about 25° below the horizon), and were cut with their axes alternately in a radial and tangential direction so that each strip measured the appropriate polarized component of the zodiacal light. A typical photograph taken with this arrangement which shows the strong observed polarization is reproduced in Plate 3—the actual polarization is two or three times greater still than this, the factor depending upon the correction for the sky background. Laboratory tests showed that the polarization measures are not unduly affected by the large angular aperture of the objective lens. A correction was made for deviations of the strips from a radial direction when the Sun is not at a standard distance below the horizon. The method is quite sensitive and can easily detect polarizations of one or two per cent. Photographs were taken simultaneously with the same two filters as were used for the direct photography.

All of the measurements of polarization for the two wavelengths, corrected for night sky background, are shown in an unsmoothed state in Fig. 8 each night being represented by at least four or five points, and more when more than one photograph is available. No significant difference between the polarization values for the two wavelengths is apparent. In this diagram we plot also other available observations. The present results are in good agreement with those of Blackwell (**17**) and in excellent agreement with the recent results of Elsässer (**14**), but in poor agreement with those of Behr and Siedentopf (**3**).

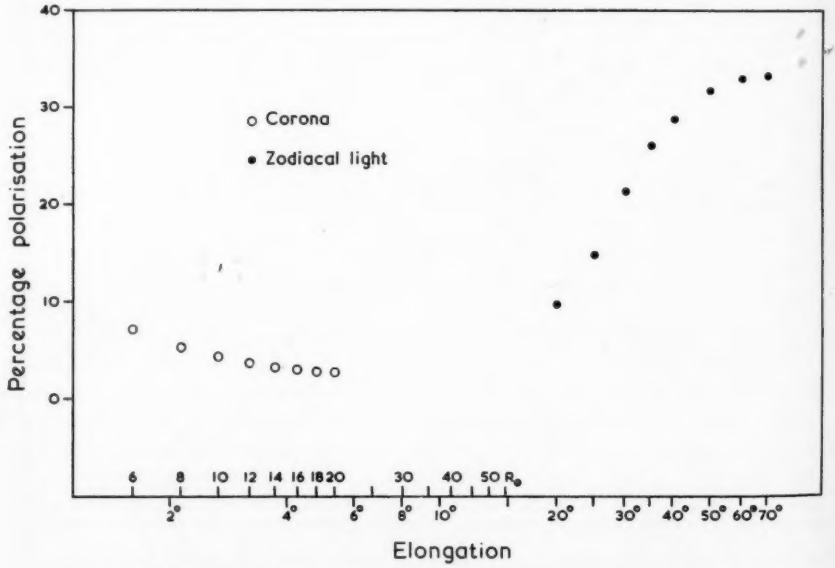

FIG. 9 —*Polarization of the zodiacal light and the solar corona. The corona data are those of Blackwell* (**6**) *from the* 1954 *eclipse; the zodiacal light data are an average of the measurements of Blackwell* (**17**), *Elsässer* (**14**) *and those from the present expedition.*

In Fig. 9 we suggest a working polarization curve formed by combining the Chacaltaya values with those of Elsässer and of Blackwell, and we suggest that the error of this curve is unlikely to be greater than ± 2 per cent of polarization; this diagram also shows the relation between the polarization of the zodiacal light and that of the corona.

In Table V we list values of the polarization for an observational model of the outer corona and zodiacal light regions based on the data summarized here. This model differs greatly from previous models because of the introduction of the new data, but we believe that it is more reliable.

TABLE V

Polarization of the outer corona (equatorial regions) and the zodiacal light

Elongation	Polarization	Elongation	Polarization
4°	3·0 per cent	30°	21·3 per cent
5°	2·8	35°	26·0
10°	4·0	40°	28·7
20°	9·7	50°	31·7
25°	14·8	60°	32·9
		70°	33·2

The position of the zodiacal light axis.—Accurate measurements of the position of the axis are very difficult to make. An accuracy of at least ± 0°·5 is required if the measurements are to be useful, and to obtain this accuracy we believe that the following conditions of observation are essential. The most important condition is that the axis should be nearly vertical at the horizon at the time of observation; if it is inclined to the horizon there is a systematic displacement which depends upon atmospheric extinction and is very difficult to estimate. Scarcely less important is the condition that the observations are made in a region of low geomagnetic latitude where displacements due to aurorae are at a minimum. Also, the observations should be made from a high altitude station so that the axis is displaced as little as possible from its true position by local variations in extinction, and preferably they should be made photographically or photoelectrically. Very few measurements have been made so far under these conditions.

The classical observations are those of Hoffmeister (**18**). These observations were made visually from a variety of stations, some of which were within the tropics, and the spread of the measurements is about ± 2°. The reductions were made very carefully, and this probably represents the extreme limit of precision that can be obtained visually. The results demonstrated that over a large range of longitude the axis deviates significantly from the ecliptic, the maximum deviation being about 2°.

Photographic measurements have been made by Donitch (**19, 20**) from Tamanrasset (in S. Algeria) using an *f*/4 guided camera and an exposure of 50 minutes. The observations were made at intervals between 1946 and 1949 and showed that the inclination of the axis to the ecliptic is about 2°, and the longitude of the ascending node is about 120° (in poor agreement with Hoffmeister who found values between 40° and 69°), although both of these quantities seemed variable.

These data appear to us to be quite convincing, but Fesenkov (**21**) has recently suggested that the axis coincides with the ecliptic. In a preliminary report on the

recent USSR expedition to Aswan, Egypt, he remarks that "the deviation of the axis of the zodiacal light from the ecliptic must be completely negligible, assuming it exists at all". This problem is not a trivial or pedantic one. It is very important to establish whether or not there really are systematic deviations, for any such are good evidence for an extra-terrestrial origin for the zodiacal light. Because of this we have used our photographs to obtain measures of the position of the

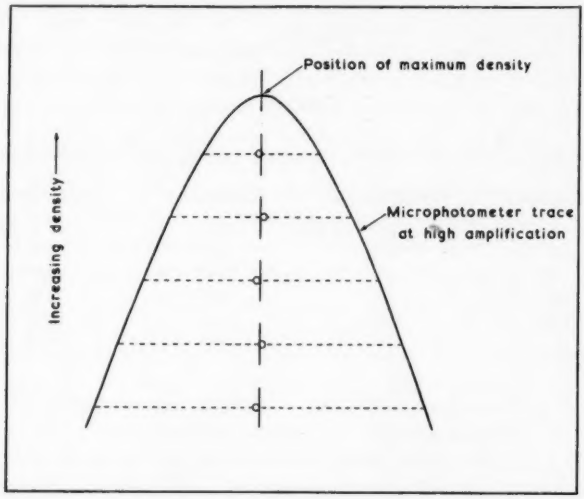

FIG. 10.—*Method of measuring microphotometer traces to find the position of the zodiacal light axis.*

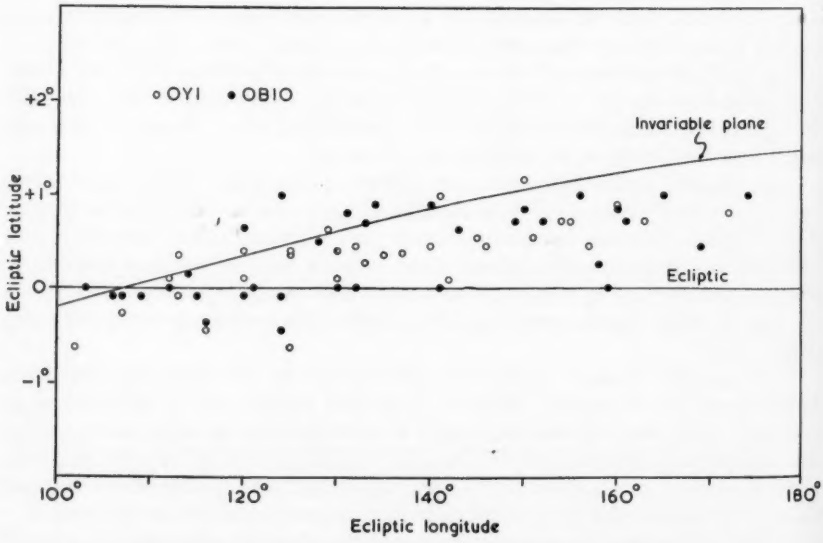

FIG. 11.—*Position of the zodiacal light axis in relation to the ecliptic.*

axis by making microphotometer scans across them parallel to the horizon and locating the position of maximum density, allowing for the presence of the brighter stars on the scans. The method used for measuring a typical trace is shown in Fig. 10, which is self-explanatory. The results of these measurements using only the photographs taken through the OB10 (blue) and OY1 (orange) filters, and between elongations 30° and 50°, are shown in Fig. 11 for all the dates of observation; here the deviation from the ecliptic is plotted against elongation. It will be seen that this method locates the position of the axis to within 0°·5 of ecliptic latitude and, further, there is no shift of the axis with wavelength. Although the range of longitude is not great, there seems to be a significant deviation of the axis from the ecliptic. According to our measures, the plane of the zodiacal cloud intersects the plane of the ecliptic at longitude 115°, and is inclined at an angle of about 1°·5. Both of these quantities are in reasonable agreement with the values quoted by Donitch. On Fig. 11 we also plot the position of the invariable plane of the solar system, and remark that it is close to the plane of the zodiacal cloud.

Acknowledgments.—We are very grateful to Professor I. Escobar V, Director of the Chacaltaya Cosmic Ray Laboratory, for putting the facilities of the Laboratory at our disposal. While at the Laboratory great help was given by him and all his staff. The expedition was financed by the Royal Society with a supplementary grant from the Department of Scientific and Industrial Research. All of the apparatus was made under the direction of Mr R. Overhill in the Observatories Workshops. We wish to express our gratitude to Professor R. O. Redman for his help and encouragement. Almost all of the computational work was carried out by Mrs G. Richards. The standard lamp was calibrated by the National Physical Laboratory.

The Observatories,
Madingley Road,
Cambridge:
1960 *October* 5.

References

(1) C. T. Elvey and F. E. Roach, *Ap. J.*, **85**, 213, 1937.
(2) J. D. Cassini, *Mem. Acad. Sci.*, Paris, **8**, 121, 1666–99.
(3) A. Behr and H. Siedentopf, *Zeits. f. Astrophys.*, **32**, 19, 1953.
(4) D. E. Blackwell, *Observatory*, **77**, 187, 1957.
(5) C. W. Allen, *Astrophysical Quantities*, p. 116, London, 1955.
(6) D. E. Blackwell, *M.N.*, **115**, 629, 1955.
(7) F. E. Roach, H. B. Petit, E. Tandberg-Hanssen, and D. N. Davis, *Ap. J.*, **119**, 253, 1954.
(8) V. G. Fesenkov, *Soviet A.J.*, **2**, 299, 1958.
(9) F. S. Johnson, *J. Meteorology*, **11**, 431, 1954.
(10) J. Stebbins and G. E. Kron, *Ap. J.*, **126**, 266, 1957.
(11) C. T. Elvey and P. Rudnick, *Ap. J.*, **86**, 342, 1937.
(12) M. G. Karimov, *A.J. U.S.S.R.*, **27**, 97, 1950.
(13) V. H. Regener, *Ap. J.*, **122**, 520, 1955.
(14) H. Elsässer, *Die Sterne*, **9–10**, 166, 1958.
(15) N. B. Divari and A. S. Asaad, *Soviet A.J.*, **3**, 832, 1960.
(16) D. Barbier, *Les Particles Solides dans les Astres*, Liège, p. 55.
(17) D. E. Blackwell, *M.N.*, **116**, 365, 1956.
(18) C. Hoffmeister, *A.N.*, **271**, 49, 1940.
(19) M. N. Donitch, *Bull. Astronomique*, **17**, 95, 1953.
(20) M. N. Donitch, *Bull. Astronomique*, **20**, 15, 1955.
(21) V. G. Fesenkov, *Soviet A.J.*, **2**, 276, 1958.

OBSERVATIONS OF THE ZODIACAL LIGHT FROM A VERY HIGH ALTITUDE STATION

II. Electron Densities in Interplanetary Space

D. E. Blackwell and M. F. Ingham

(Received 1960 October 6)

Summary

The evidence for and against the existence of an interplanetary gas is reviewed. Spectra of the zodiacal light obtained in 1958 at the high altitude station of Chacaltaya (height 17 100 ft) in Bolivia with a dispersion of 38 A/mm are described and used to investigate the concentration of free electrons in the plane of the ecliptic at 1 A.U. from the Sun. No electrons could be detected along a line of sight at elongation 32° and it is deduced that the electron density at 1 A.U. is not greater than 120 cm^{-3}.

Introduction.—In Paper I of this series we mentioned the hypothesis that the number density of free electrons in the plane of the ecliptic at the distance of 1 A.U. from the Sun is about 600 cm^{-3}. This hypothesis is now widely assumed to be correct, and in the first part of this paper we give a critical review of the evidence for and against it. In the second part we describe our observations of the zodiacal light spectrum made at Chacaltaya in 1958 and the conclusions about interplanetary electron densities that may be drawn from them.

The evidence for interplanetary electrons.—Some of the evidence has already been considered by Blackwell (**1**), Elsässer (**2**), Cole (**3**) and various contributors to a Geophysical Discussion held in London (**4**). The first suggestion that the electron density at 1 A.U. from the Sun may be as great as 600 cm^{-3} arose from the accretion theory of the solar corona put forward by Hoyle, Bondi and Lyttleton (**5**) in 1947.

(i) *The evidence from the zodiacal light.*—In 1953 Behr and Siedentopf (**6**) sought to obtain the electron density far from the Sun using zodiacal light data. They then made the first accurate measurements of the degree of polarization of the zodiacal light along the ecliptic and found a maximum value of about 23 per cent near elongation 35°. Until this time it had been universally supposed that the zodiacal light is due entirely to the scattering of sunlight by dust contained within the solar system, but Behr and Siedentopf suggested that its great polarization could not be accounted for by dust scattering alone and that therefore there must also be a contribution from electron scattering. The assumption that the light scattered by the dust is of zero polarization leads to electron densities of the order of 600 cm^{-3} at 1 A.U. from the Sun (**6**, **7**).

The recent measurements of the polarization of the zodiacal light by Elsässer (**8**) and the present authors (see Paper I) render the Behr and Siedentopf argument even more forceful. These observations give a maximum value of 33 per cent, which is correspondingly more difficult to explain by dust scattering alone than the value of 23 per cent derived by Behr and Siedentopf. Even so, the argument for the existence of an electron scattered component still depends

entirely upon an assumption that, plausible though it is, has never been tested.

We stress that acceptance of the Behr and Siedentopf hypothesis inevitably implies acceptance of the symmetry properties of the electron cloud. As already explained, the zodiacal light is symmetrical about a plane which is very close to the ecliptic. If the electron density in this cloud at 1 A.U. from the Sun is as great as 600 cm^{-3} the electron-scattered component of the zodiacal light contributes about one half of the total brightness near elongation 35°, and therefore it also must be nearly symmetrical about the ecliptic, implying that the electron cloud is symmetrical about the plane of the ecliptic. It may be that such a symmetry is unacceptable—and indeed this, as demonstrated later, forms an argument against the existence of such a cloud of electrons. The argument can also be inverted. If other kinds of observation require the existence of a cloud of electrons of this density—as observations of comets apparently do—then we deduce that such a cloud must contribute appreciably to the zodiacal light and must therefore be nearly symmetrical about the plane of the ecliptic. If the original observations do not show that the electron cloud has this symmetry, or if the cloud cannot reasonably be expected to show it, then the interpretation in terms of a cloud of electrons must be wrong.

The work of Beckers (**9**) on the zodiacal light spectrum has apparently confirmed the Behr and Siedentopf hypothesis. Beckers has compared the central intensities of the Fraunhofer lines in the zodiacal light spectrum with the intensities of the same lines in the solar spectrum, using for this purpose a spectrum of the zodiacal light obtained by Hoffmeister (**10**) in 1935. Then, supposing that the interplanetary dust scatters the solar spectrum almost unchanged, and that the interplanetary electrons scatter a quasi-continuous spectrum in which the Fraunhofer lines have been almost obliterated by the large random velocities of the electrons, a separation of the dust and electron scattered components may be made. According to Beckers the result is that 50 per cent or more of the zodiacal light is due to electron scattering. This work will be considered in more detail later in this paper, but here we remark only that we believe it to be incorrect because proper allowance has not been made for the night sky background to the zodiacal light.

There is evidence, although all of it necessarily indirect, that interplanetary dust may indeed scatter highly polarized light. Some of the evidence is provided by cometary studies, for some of the light of a comet is due to the scattering of solar radiation by dust in its head, and this part may be separated from the remainder by a suitable choice of spectral region. Measurements on Comet Arend-Roland (1956h) and other comets show a maximum polarization of about 25 per cent (**11**). Admittedly, this is insufficient to account for the polarization of the zodiacal light, especially as the zodiacal light measurements are effectively a weighted average over a large range of scattering angles, but it goes a considerable way towards doing so. In any case, good agreement would not be expected because the scattering processes and the nature of the scattering material may not be the same in a comet head as in the zodiacal light. Fesenkov (**12**) has computed the expected polarization assuming that the interplanetary dust is similar to atmospheric aerosols; this gives the value of 28·5 per cent at elongation 70°. He infers from this that the Behr and Siedentopf hypothesis is an unnecessary one, although it may be correct. A similar conclusion has been reached by Whipple and Gossner (**13**) and by Kloverstrom and Rense

(**14**), on the basis of laboratory measurements, while van de Hulst (**15**) has considered that much, at least, of the polarization may be attributed to dust scattering. Öpik (**16**) was one of the first to question the validity of the Behr and Siedentopf hypothesis.

If we except Beckers' result, which we believe to be wrong, Fesenkov's conclusion fairly assesses the direct observational evidence for an appreciable electron component in the zodiacal light. On the other hand, if the electron component is assumed to exist we have to explain its symmetry about a plane which is so close to the ecliptic. If we suppose that the electrons, with the interplanetary gas, are flowing into or out of the Sun it is difficult to see how, in the short time available, they can become symmetrical about such a plane. Even if we suppose them to be permanent, or semi-permanent, members of the solar system, then it is equally difficult to see why the very weak gravitational forces associated with the plane of the ecliptic should dominate the random electromagnetic forces which are surely present. These difficulties are most easily removed at their source by abandoning the assumption that there exists an electron cloud of sufficient density to contribute significantly to the zodiacal light. This does not exclude the temporary existence of relatively narrow low density corpuscular streams.

(ii) *The evidence from comets.*—This evidence is based chiefly upon observations of the apparent motions of condensations in comet tails of type I. It is commonly supposed that these condensations are moving in orbits under the action of a repulsive force which is μ times as great as the gravitational attraction of the Sun at this distance, so that analysis of their motion gives the value of $1-\mu$. There have been many determinations of this quantity, and we mention here those of Bobrovnikov (**17**) for Halley's comet (1910 II) and the list given by Wurm (**18**); according to Wurm the mean value of $1-\mu$ is about 100, occasionally it increases to several thousand (**17**). Biermann (**19**, **20**) has suggested that these repulsive forces originate in interaction between corpuscular radiation and the plasma forming the comet tail. He finds that the acceleration α of a cometary ion exposed to a corpuscular stream is given by

$$\alpha = \frac{e^2}{\sigma m_{\mathrm{m}}} . n_{\mathrm{e}} V_{\mathrm{e}},$$

where m_{m} is the mass of a molecule, n_{e} the electron density in the corpuscular stream, and σ is the electrical conductivity which may be computed from the cross-sections for collisions between electrons and molecules, and electrons and protons. Inserting the appropriate values, this relation gives the acceleration as equal to $0{\cdot}1\, n_{\mathrm{e}}\,\mathrm{cm\,sec^{-2}}$. At 1 A.U. from the Sun, the acceleration due to the gravitational attraction of the Sun is about $0{\cdot}6\,\mathrm{cm\,sec^{-2}}$ The mean acceleration in comet tails is therefore about $60\,\mathrm{cm\,sec^{-2}}$, which corresponds to a electron density in the corpuscular stream of about $600\,\mathrm{cm^{-3}}$. The agreement with the value given by Behr and Siedentopf from the zodiacal light work is remarkable.

We would criticize this use of cometary data partly on the grounds that it is by no means certain that we are observing mass motion in the tail; the apparent motions of condensations may only be due to a changing excitation. Even if it is demonstrated that these really are mass motions we doubt whether the observed repulsive forces may always be attributed to the action of the Sun. The varying repulsive forces observed for condensations in different parts of a comet suggest

the presence of other mechanisms; for Halley's comet the condensations of the tail showed values of $1-\mu$ between 20 and 150, the average value of $1-\mu$ derived from the curvature of tail I (the ion tail) was 10 to 20, straight jets near the nucleus gave values between 1 and 6, while the envelopes showed approximate balance of repulsive and attractive forces.

(iii) *The evidence from magnetic storms.*—Biermann (**19, 21**) has also suggested that the observed value of the magnetic activity on quiet days in high geographical latitudes may be accounted for by supposing that it is due to a steady corpuscular stream of density 10^3 electrons cm^{-3} at 1 A.U. However, we regard this as a great over-estimate, for it is based on the Unsöld and Chapman (**22**) value of $10^5\,cm^{-3}$ for the particle density in a great magnetic storm. This value is certainly too great, for it, in turn, is based on the work of Brück and Rutllant (**23**) who attempted to observe a displaced K absorption line arising from these particles. In his photoelectric work, Smyth (**24, 25**) was unable to find any increase in absorption, which suggests an upper limit of $3\times10^3\,cm^{-3}$ for the particle density (**1**). In any case, such a high value as $10^5\,cm^{-3}$ is not supported by the observations of Paper III.

(iv) *The evidence from the etching of meteorites.*—Whipple and Fireman (**26**) have placed an upper limit on the rate at which meteorites have been etched by corpuscular radiation in interplanetary space; this limit is $3\times10^{-7}\,cm\,year^{-1}$. Supposing that the etching is by protons travelling from the Sun at an average speed of $10^8\,cm\,sec^{-1}$ (i.e. with energy 5000 eV), Whipple (**27**) finds that the corresponding upper limit to the proton density is about $40\,cm^{-3}$.

(v) *The evidence from cosmic radiation.*—It has been shown by Brunberg and Dattner (**28**) that the diurnal variation of cosmic ray intensity observed at the surface of the Earth is due to an anisotropy of the primary radiation reaching the Earth. These authors suggest that this anisotropy is caused by the co-rotation of the cosmic ray particles and the solar magnetic field. It is now suggested by Block (**29**) that this, in turn, means that the interplanetary gas is also in co-rotation. Block infers from this that the interplanetary gas density cannot be greater than $0{\cdot}1\,cm^{-3}$ because a gas of density greater than this could not be kept in co-rotation by any reasonable solar magnetic field; this value of $0{\cdot}1\,cm^{-3}$ corresponds to an Alfvén field with a strength of 12 gauss at the Sun's poles, which is much too high to be acceptable. It seems to us that the weakness of this conclusion lies in the original inference that the cosmic radiation is in co-rotation with the Sun.

(vi) *The evidence from ionospheric measurements.*—In his pioneering work on radio whistlers Storey deduced that the electron density at a distance of 3 radii from the Earth is about $400\,cm^{-3}$ (**30**). This value however is rather uncertain because the method used by Storey gives the total number of electrons along the path of the whistler; consequently, the value at the apex of the path depends rather critically on the assumed distribution of densities in the lower regions. Whilst there have been refinements of the technique by other workers—for example Allcock (**31**) has combined data obtained over a range of geomagnetic latitudes—precise knowledge of the electron density in the ionosphere beyond about 2 radii depends upon observations of "nose" whistlers, which give directly the electron density at the apex of the path (**32**). Helliwell* finds from a study of this type of whistler that the electron density at 5 radii is of the order of $100\,cm^{-3}$.

* R. A. Helliwell, private communication.

This short review shows that the electron density in interplanetary space is still uncertain by several orders of magnitude, and especially there is a dichotomy between the astronomical and the ionospheric data. None of the astronomical methods so far described is free of criticism and an independent method of investigation is required. We now turn to our own astronomical observations.

The method of measuring electron density used at Chacaltaya.—The method is similar to that used several times already for separating the F (dust) and K (electron) components of the inner corona. In this application there is independent evidence that the electrons of the corona are at a high kinetic temperature so that the light which is scattered by them has a virtually continuous spectrum, but the interplanetary dust may be expected to scatter light which, over small wavelength regions, has a spectrum identical with that of the Sun. A comparison of the central intensities of the Fraunhofer lines in the spectra of the Sun and corona therefore gives directly the ratio of the two components of the scattered light. The application of this method to the zodiacal light is not so straightforward because we do not know the kinetic temperature of the electrons, if they exist, at the relevant distance of about 0·5 A.U. from the Sun. However, we shall show later that the method can be made almost independent of this knowledge.

Assuming now that there are free electrons at 0·5 A.U. from the Sun, we suggest that it is unlikely that they have a kinetic temperature of less than 2×10^4 degrees. This is the value derived by Chamberlain (**33**) from an application of kinetic theory to the interplanetary gas. Values suggested by other authors are greater than this. Assuming hydrostatic equilibrium, Pottasch (**34**) derives the temperature of $2{\cdot}3 \times 10^5$ degrees at 0·1 A.U., while his curve extrapolates to $1{\cdot}0 \times 10^5$ degrees at 0·5 A.U. Chapman (**35**) has calculated the temperature out to 1 A.U., using an empirical function for the variation of angular velocity of rotation with distance from the Sun and assuming that the temperature gradient beyond 0·26 A.U. is close to the adiabatic gradient. His value at 0·5 A.U. is $1{\cdot}2 \times 10^5$ degrees.

The temperature of 2×10^4 degrees, the lowest likely value for the kinetic temperature, implies that the spectrum of the sunlight scattered by the electrons cannot be regarded as completely featureless. As an illustration of the weakening effect that may be expected we consider a line which in the solar spectrum is observed to have a central intensity of 50 per cent and an apparent width, at half intensity, compounded of natural width and instrumental broadening, of 5 A. At the temperature of 2×10^4 degrees and wavelength of 4500 A the whole width of the Doppler broadened line at half intensity is 20 A, corresponding to an apparent width of about 25 A. The depth of the broadened line may be computed by equating its area to that of the unbroadened solar line; the result is that a broadening of this amount reduces the depth by the factor 9·1, the depth of the broadened line being 5·5 per cent.

We next consider the combination of such a broadened line, which is due to electron scattering, with an unbroadened line due to dust scattering. The results of computations of the central intensity are given in Table I for a line originally of central intensity 50 per cent, for the three kinetic temperatures of infinity, 10^6 and 2×10^4 degrees and for three different proportions of the K and F components. We deduce from this table that if the ratio $K/(K+F)$ is equal to 0·5—the approximate value that would be required by the Behr and

Siedentopf hypothesis—then the effect of taking the temperature to be 2×10^4 degrees instead of infinity is just discernible, while if $K/(K+F)$ is equal to 0·1 or less the effect is no longer discernible in ordinary photographic photometry.

TABLE I

Central intensity of composite Fraunhofer line

$K/(K+F)$	$T=\infty$	$T=10^6$	$T=2\times10^4$
0·5	0·25	0·26	0·28
0·1	0·45	0·45	0·46
0	0·50	0·50	0·50

Alternatively, we may say that if the electron density is great, i.e. $K/(K+F) > 0{\cdot}1$, the uncertainty in temperature introduces an uncertainty in the density determination of about 10 per cent, but if the density is so low that $K/(K+F) < 0{\cdot}1$ then the errors of photographic photometry are greater than the uncertainties of interpretation. If it is our intention only to detect the presence of electrons along the line of sight—and it will be shown later that the density is so low that only an upper limit can be placed upon it—then the uncertainties in interpretation due to ignorance of the temperature are of no account.

This is an outline only of the method; its difficulties and refinements will be explained later.

The observations.—The spectrum of the zodiacal light has already been photographed, chiefly by Fath (**36**), Slipher (**37**), Hoffmeister (**10**) and Karimov (**38**). All of these spectra have been obtained at rather small dispersion.

The spectrograph used in this study has already been described (**39**). It incorporates a Schmidt camera of aperture 8 in and focal length 6·3 in, the correcting plate of which was made by one of us (M.F.I.) at the Cambridge Observatories; this, with an 8 in × 6 in Bausch and Lomb grating of 600 lines mm^{-1}, gives a dispersion in the second order at 4300 A of 38 A/mm. Each point in the spectrum is derived from an area of sky of diameter 3·4 degrees.

Several spectra of the zodiacal light were obtained with projected slit widths between 0·13 mm and 0·063 mm, all with the spectrograph raised to an altitude of 7° above the horizon. The best spectrum for our purpose was photographed on 103a–O film, specially made by Eastman Kodak, using a projected slit width of 0·063 mm and an integrated exposure of 7 hours spaced over nights between the dates July 4 and July 11; it covered the range 3500–4500 A in the second order. As a consequence of the long exposure this spectrum is an average over a range of 15° in elongation centred on elongation 30°, the contribution of each element in the zodiacal light being weighted according to its intensity. An allowance is made for this in the reductions, but as the properties of the zodiacal light vary only slowly with elongation this procedure does not introduce a significant error. In all of the observations the greatest care was taken to avoid beginning the exposure each evening until the last traces of Rayleigh scattering by the Earth's atmosphere had disappeared; in practice, the time of disappearance is quite easily determined. The spectrograph was thermally insulated, and measurements of a comparison spectrum, put on partly at the beginning and partly at the end of the exposure a week later, show that there was inappreciable loss of definition through lack of stability.

A spectrum of the night sky was obtained subsequently with an exposure of 7 hours and the same slit width, and a solar spectrum was obtained during twilight with an exposure of 30 s. All of these photographs were calibrated using a standard lamp and a step wedge. The ratio of the zodiacal light brightness to the night sky brightness was obtained photographically in the manner described in Paper I, and an average over the period of observation, weighted according to elongation and atmospheric extinction, was used.

The reduction of the observations.—Although the method is straightforward in principle, there are many uncertainties of a practical nature in its application. The observed spectrum is a superposition of three spectra of quite different origins, namely those of the zodiacal light (appreciably weakened by atmospheric absorption), the night sky emission and the twilight emission. The night sky spectrum can be observed virtually alone and its contribution to the observed spectrum can be allowed for in the usual way by direct photometry. The twilight emission spectrum cannot be observed separately and it is best to work as far as possible in those regions of the spectrum where its effect seems least obtrusive. This means that the D lines of the solar spectrum, which are otherwise so suitable, cannot be used in this investigation. The Hα line is unsuitable because of the possibility of emission from the night sky and also because close to the horizon the night sky spectrum is very complex in this region. The H and K lines of Ca^+ must also be treated with caution because of the occasional presence of a weak emission component of unknown origin (**40**).

A photograph of the spectrum of the zodiacal light made with a slit width of 0·063 mm is reproduced in Paper I (Plate 3) together with a spectrum of the twilight sky. It is clear that the zodiacal light spectrum as observed against the night sky contains Fraunhofer lines, but it should not immediately be deduced from this, as has been done (41), that the zodiacal light spectrum itself contains Fraunhofer lines. The reason for this is that the night sky spectrum also shows these lines, particularly H and K of Ca^+, the 4227 A line of Ca and the Balmer series. These lines show strongly on a high resolution spectrogram, and a proper allowance must be made for their effect. That it is also important to allow for the emission lines of the night sky spectrum is demonstrated by the almost complete absence of the line at 4046 A in the composite spectrum, which is filled in by the night sky emission line at 4048 A. The presence of an emission line at the centre of the K line is clearly shown in the reproduction.

The spectra have been scanned with the Cambridge Observatories' microphotometer, and in Fig. 1 we show a microphotometer record of a zodiacal light spectrum (superimposed upon the night sky spectrum) made with a spectrograph entrance slit width of 1 mm corresponding to a projected slit width on the film of 0·063 mm. In selecting lines for measurement we have avoided those which are near to distinct night sky emission lines, and have preferred those which are in regions of low night sky emission, where the correction for this emission is smallest.

The records have been reduced by first correcting them for the presence of the night sky spectrum. In this we use the results of Paper I to obtain the average contribution of the night sky over a broad band of wavelengths, and then interpolate to obtain the contribution at each wavelength. The average ratio of the brightness of the night sky to the combined brightness of zodiacal light and night sky in the region of 4300 A was 0·38.

The level of the continuum was added to the solar spectra with the help of the Utrecht Atlas; this continuum was then transferred to the zodiacal light spectra, making clear allowances for the superposed twilight emission spectrum. If an undetected emission line is superposed on a Fraunhofer line,

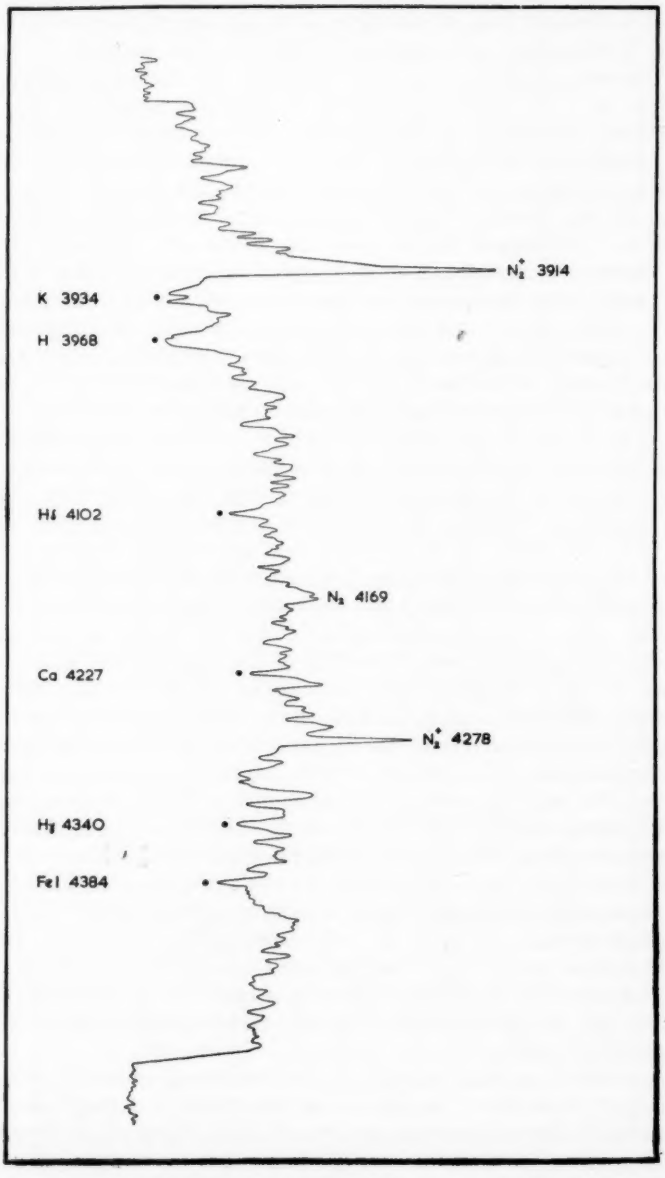

FIG. 1.—*Microphotometer record of the zodiacal light spectrum (superimposed on the night spectrum). Width of spectrograph entrance slit = 1 mm.*

the effect will be an apparent weakening of the Fraunhofer line which will simulate the presence of electron scattering. The line depths were then measured directly on each of the spectra with the results given in the third column of Table II. The results show approximate equality of the line depths in the zodiacal light spectrum and the solar spectrum.

TABLE II

Comparison of intensities of Fraunhofer lines in the zodiacal light spectrum and the solar spectrum

Line	$\left\lvert\int_{\lambda_0-\Delta\lambda}^{\lambda_0+\Delta\lambda} I_\lambda d\lambda\right\rvert_{\text{Zodiacal light}}$ / $\left\lvert\int_{\lambda_0-\Delta\lambda}^{\lambda_0+\Delta\lambda} I_\lambda d\lambda\right\rvert_{\text{Sun}}$	Line depth in z.l. spectrum / Line depth in solar spectrum
Ca 4227	0·96	
Fe 4384	0·94	0·94
Hγ 4341	0·93	1·10
Fe 4326	1·10	1·20
*Ca+H 3968	0·97	
G-band 4308	1·05	1·10
Hδ 4102	0·85	0·87
Average	0·97	1·04

* Corrected for presence of emission component.

A disadvantage of this method of reduction is that the result depends upon a single measurement of the microphotometer trace at the position of maximum absorption. To reduce the uncertainty of the measurement we have also evaluated the quantity

$$\frac{\left|\int_{\lambda_0-\Delta\lambda}^{\lambda_0+\Delta\lambda} I_\lambda d\lambda\right|_{\text{Zodiacal light}}}{\left|\int_{\lambda_0-\Delta\lambda}^{\lambda_0+\Delta\lambda} I_\lambda d\lambda\right|_{\text{Sun}}} = A$$

where λ_0 is the wavelength of maximum absorption and $\Delta\lambda$ is about 3 A. The equivalent width of a line, defined as

$$\int_0^\infty I_\lambda d\lambda$$

is unaltered by electron scattering, but if $\Delta\lambda$ is not too great a fraction of the Doppler width of the broadened line the quantity

$$\int_{\lambda_0-\Delta\lambda}^{\lambda_0+\Delta\lambda} I_\lambda d\lambda$$

is a good measure of the central intensity. For an electron temperature of 2×10^4 degrees, $\Delta\lambda$ may be as much as 3 A without introducing an appreciable uncertainty of interpretation, while the accuracy of measurement is considerably increased through the use of a greater length of microphotometer record. Results obtained by this method are given in column 2 of Table II. Combining the two methods of measurement, the mean result is

$$\frac{\left|\lim_{\Delta\lambda\to 0}\int_{\lambda_0-\Delta\lambda}^{\lambda_0+\Delta\lambda} I_\lambda d\lambda\right|_{\text{Zodiacal light}}}{\left|\lim_{\Delta\lambda\to 0}\int_{\lambda_0-\Delta\lambda}^{\lambda_0+\Delta\lambda} I_\lambda d\lambda\right|_{\text{Sun}}} = 1{\cdot}01 \pm 0{\cdot}10.$$

The uncertainty in this result is difficult to estimate; we simply suggest that it is very unlikely to be in error by more than 10 per cent. This estimate is a combination of the errors of photographic photometry with the uncertainty in the separation of observed zodiacal light intensity into a true zodiacal light intensity and a night sky component.

Interpretation in terms of the electron density in interplanetary space.—It is clear that these observations have not shown the presence of any free electrons along the line of sight. We now compute the electron density at 1 A.U. corresponding to $K/(K+F)=0{\cdot}1$, this being the least electron density detectable by these observations.

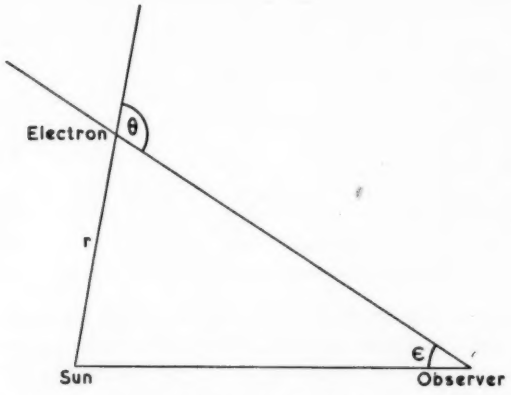

FIG. 2.—*Scattering of sunlight by interplanetary electrons.*

In the notation of Fig. 2, and defining surface brightness as the rate of flow of energy through unit area at the Earth's surface and contained within unit solid angle, we calculate the ratio, Φ, of the brightness of the electron cloud at elongation ϵ to that of the Sun to be given by

$$\Phi = \frac{3\sigma\Omega R}{16\pi \sin\epsilon} \int_{\epsilon}^{\pi} n_e(r)\{1+\cos^2\theta\}\, d\theta$$

neglecting the finite size of the Sun. Here, σ is the Thomson scattering coefficient, Ω is the solid angle subtended by the solar disk and $n_e(r)$ is the electron density at distance r from the Sun. The value of the electron density at a particular distance corresponding to a given value of Φ does not depend greatly upon the form of $n_e(r)$; as our final result is that n_e is small at distances of the order of 1 A.U., n_e varies at least as rapidly as $1/r^2$ and we take it to be proportional to $1/r^2$. In the computations we use the value for the brightness of the zodiacal light of Table IV (Paper I), i.e. the brightness at elongation 40° is $3{\cdot}86\times10^{-13}B_{\odot}$, and correct it to the appropriate wavelength using the data of Fig. 6 (Paper I). Putting $K/(K+F)<0{\cdot}1$, we find the final result

$$n_e \text{ (at 1 A.U.)} < 116\,\text{cm}^{-3}.$$

This upper limit for the electron density depends upon the assumption that the kinetic temperature is not less than 2×10^4 degrees. It seems to us that such an assumption is reasonable, but electrons in the concentrations required by the Behr and Siedentopf hypothesis could still be detected at much lower temperatures through the added presence of wings or line

broadening. In Fig. 3 we compare the observed profile of the Hγ line at 4341 A in the solar spectrum with that of the same line in the zodiacal light spectrum (corrected for background), and it is evident that there are no perceptible wings or a broadening of any kind. The difference in total width at half intensity between the two is less than 0·28 A, corresponding to a kinetic temperature of only 4 degrees. As this temperature is unreasonably low we conclude that in no circumstances are the present results compatible with the Behr and Siedentopf hypothesis, and that it is very unlikely that the electron density exceeds $120\,cm^{-3}$.

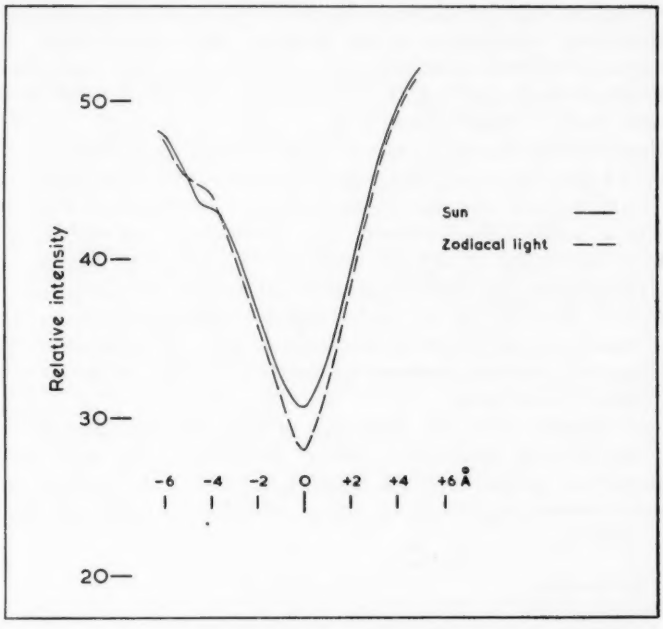

FIG. 3.—*Comparison of the observed profile of the* Hγ *line at* 4341A *in the zodiacal light spectrum with that of the same line in the solar spectrum.*

The narrow slit observations were made between July 4 and July 11 when the average enhancement in brightness of the zodiacal light over this period was about 8 per cent, but this change in brightness has not been detected as a change in Fraunhofer line intensity. Before changes of this kind can be detected spectroscopically it will be necessary to develop faster and more accurate methods of observation.

As already mentioned, our result is a direct contradiction of that obtained by Beckers (**9**). We attribute this chiefly to Beckers' neglect of the night sky background. The ratio of zodiacal light brightness to night sky background depends upon the quality of the sky and the conditions of observation, and none of these data seems to have been available to Beckers. Also, we regard it as essential to make observations of the solar spectrum and the night sky spectrum with the same spectrograph as was used for the zodiacal light observations, using also the same slit width.

There are two outstanding difficulties connected with our result. The first is that we must now attribute the whole of the polarization of the zodiacal light to scattering by dust particles in interplanetary space. Yet, as shown in Paper IV, this polarization is much greater than can be explained by laboratory experiments with likely scattering materials.

The second difficulty is related to the work of Biermann and Schlüter on the accelerations of condensations in comet tails, which has already been discussed. These two authors attribute the accelerations to the effect of a steady corpuscular stream of electron density about 600 cm^{-3} at 1 A.U. from the Sun. While we do not deny the occasional existence of such a corpuscular stream we suggest that the accelerations usually observed have a different origin.

An important consequence of our result is that the reliability of existing measurements of electron density in the outer corona is now very questionable. These measurements (**42**, **43**) are based upon observations of polarization and assume that the polarization of the *F* (dust) component is negligible in comparison with the total polarization. But the total polarization at elongation 5° is only 2·7 per cent, and if the polarization of the light scattered by dust at elongation 35° is 33 per cent, the polarization of the *F* component at 5° elongation may well be as much as 2·7 per cent. Our conclusion is that we have no reliable quantitative knowledge of electron densities beyond about 8 solar radii, and our only evidence for the existence of electrons beyond this distance is provided by the work of Hewish (**44**, **45**) and Vitkevitch (**46**) on the scattering of radio emission from the Crab nebula by the outer corona. However, such scattering observations only show the presence of electrons and do not enable a measurement of density to be made.

Acknowledgments.—We are especially grateful for assistance from Kodak Ltd. of Harrow, and Eastman Kodak of Rochester. The film used in the spectrograph was prepared by the latter Company. The correcting plate of the Schmidt camera was made by one of us (M.F.I.) under the direction of Dr E. H. Linfoot.

The Observatories,
Madingley Road,
Cambridge:
1960 *October* 5.

References

(1) D. E. Blackwell, *Observatory*, **77**, 187, 1957.
(2) H. Elsässer, *Mitteilungen des Astronomischen Instituts der Universität Tübingen*, Nr. 35.
(3) K. D. Cole, *Nature, Lond.*, **186**, 874, 1960.
(4) D. E. Blackwell, *Nature, Lond.*, **181**, 1238, 1958.
(5) H. Bondi, F. Hoyle and R. A. Lyttleton, *M.N.*, **107**, 184, 1947.
(6) A. Behr and H. Siedentopf, *Zeits. f. Astrophys.*, **32**, 19, 1953.
(7) D. E. Blackwell, *M.N.*, **116**, 365, 1956.
(8) H. Elsässer, *Die Sterne*, **9-10**, 166, 1958.
(9) J. M. Beckers, *Proc. Kon. Ned. Akad. Amsterdam*, Ser. B, **62**, No. 4, 1959.
(10) C. Hoffmeister, *Zeits. f. Astrophys.*, **19**, 116, 1939.
(11) D. E. Blackwell and R. V. Willstrop, *M.N.*, **117**, 590, 1957.
(12) V. G. Fesenkov, *Soviet A.J.*, **2**, 299, 1958.
(13) F. L. Whipple and J. L. Gossner, *Ap. J.*, **109**, 380, 1949.
(14) F. A. Kloverstrom and W. A. Rense, *Ap. J.*, **115**, 495, 1952.
(15) H. C. van de Hulst, *Les Particles Solides dans les Astres*, Liège, p. 89, 1955.
(16) E. J. Öpik, *Zeits. f. Astrophys.*, **35**, 43, 1954.

(17) N. T. Bobrovnikov, *Publ. Lick Obs.*, **17**, Pt. 2, 1931.
(18) K. Wurm, *Mitt. der Sternw. Hamburg-Bergedorf*, **8**, Nr. 51, 1943.
(19) L. Biermann, *Mem. Soc. Roy. des Sciences, Liège*, 4me ser. **13**, 291, 1953.
(20) L. Biermann, *Observatory*, **77**, 109, 195 .
(21) L. Biermann, *Zeits. f. Astrophys.*, **29**, 274, 1951.
(22) A. Unsöld and S. Chapman, *Observatory*, **69**, 219, 1949.
(23) H. A. Brück and F. Rutllant, *M.N.*, **106**, 130, 1946.
(24) M. J. Smyth, *M.N.*, **114**, 137, 1954.
(25) M. J. Smyth, *M.N.*, **114**, 503, 1954.
(26) F. L. Whipple and E. L. Fireman, *Nature, Lond.*, **183**, 1315, 1959.
(27) F. L. Whipple, *Journ. Geophys. Res.*, **64**, 1653, 1959.
(28) E. A. Brunberg and A. Dattner, *Tellus*, **6**, 73, 1954.
(29) L. Block, *Arkiv. f. Fysik*, **14**, 179, 1958.
(30) L. R. O. Storey, *Phil. Trans. Roy. Soc.*, **246**A, 113, 1953.
(31) G. McK. Allcock, *J. Atmos. Terr. Phys.*, **14**, 185, 1959.
(32) R. A. Helliwell, J. H. Crary, J. H. Pope and R. L. Smith, *J. Geophys. Res.*, **61**, 139, 1956.
(33) J. W. Chamberlain, *Ap. J.*, **131**, 47, 1960.
(34) S. R. Pottasch, *Ap. J.*, **131**, 68, 1960.
(35) S. Chapman, *Space Astrophysics*, ed. Liller, McGraw Hill, 1961.
(36) E. A. Fath, *Lick Obs. Bull.*, No. **165**, 1909.
(37) V. M. Slipher, *Journ. Roy. Astron. Soc. Canada*, **27**, 365, 1933.
(38) M. G. Karimov, *Astron. Journ. USSR*, **27**, 97, 1950.
(39) D. E. Blackwell, M. F. Ingham and H. N. Rundle, *Ap. J.*, **131**, 15, 1960.
(40) D. E. Blackwell, M. F. Ingham and H. N. Rundle, *Annales de Geophys*, **16**, 152, 1960.
(41) H. M. Johnson, *Observatory*, **78**, 125, 1958.
(42) D. E. Blackwell, *M.N.*, **116**, 321, 1956.
(43) R. Michard, *Annales d'Astrophys.*, **17**, 429, 1954.
(44) A. Hewish, *Proc. Roy. Soc.*, **228**A, 238, 1955.
(45) A. Hewish, *M.N.*, **118**, 534, 1958.
(46) V. V. Vitkevich, *Soviet A.J.*, **2**, 45, 1958.

OBSERVATIONS OF THE ZODIACAL LIGHT FROM A VERY HIGH ALTITUDE STATION

III. The Disturbed Zodiacal Light and Corpuscular Radiation

D. E. Blackwell and M. F. Ingham

(Received 1960 October 6)

Summary

Photometric observations of the zodiacal light made at Chacaltaya in the Bolivian Andes during 1958 show that there are changes in brightness which are correlated with geomagnetic activity. The changes in the zodiacal light and the surrounding sky during the intense magnetic storm of 1958 July 8–9 are described. The increase in sky brightness that was then observed is tentatively ascribed to scattering by free electrons in a corpuscular stream, the electron density in the stream being about 300 cm^{-3}. There was also a corresponding increase in zodiacal light brightness; the hypothesis that this may be attributed to fluorescence of the interplanetary dust on impact with the protons of this corpuscular stream is examined, but found to be inadequate.

Introduction.—Whilst at Chacaltaya the 1958 Cambridge Observatories expedition* made a special study of the variation with time of the brightness of the zodiacal light and the surrounding night sky. Previous studies of this problem by other observers had given conflicting data and we hoped that the exceptional atmospheric conditions at Chacaltaya would enable us to decide whether or not the zodiacal light itself varies in brightness or position. Whilst this was not the primary problem, we also wished to examine the possibility of detecting corpuscular radiation directly, during its passage between the Sun and Earth, through the scattering of sunlight by free electrons in the corpuscular stream. The time of the expedition was particularly favourable for studies of this kind, for the observations were made at the peak of the solar cycle during a period when the solar activity was exceptionally great.

Previous observations of changes in the brightness of the zodiacal light.—There have been many reports of variations in the brightness of the zodiacal light. We list some of these below, but at the same time we emphasize most strongly that studies of possible variations in the zodiacal light can be made only with great difficulty and any results should be treated with extreme caution. Worthwhile data can scarcely be obtained except from good photographic or photoelectric photometry carried out under excellent meteorological conditions in the tropics, and for this reason we reject almost all of the available visual observations, even

* The circumstances of the Cambridge Observatories expedition to Chacaltaya and the observations of the brightness, polarization and position of the zodiacal light made there are described in Paper I of this series.

though they have been made with the greatest care. The principal changes that have been reported are as follows.

(i) *Short period fluctations.*—Reports of changes occurring during one evening within a time interval of a few minutes are common. The best known study of this kind is that of Jones (**1**) made between 1853 April 2, and 1855 April 21, during a voyage on the Pacific Ocean chiefly between latitudes $+20°$ and $+40°$. Jones's observations were made visually whilst he was on board ship, and he recorded the brightness and position of the zodiacal light together with changes in its brightness which he called "pulsations". Hulburt (**2**) has drawn attention to the correlation that exists between these times of zodiacal light variability and the times of magnetic activity as observed at Greenwich. Jones himself was unaware of any such relationship, and it is difficult to escape the conclusion that the phenomena described by him did actually occur*. There are other reports in the literature—see, for example, Hulburt (**2**)—of changes in the zodiacal light during periods of auroral activity, but we postpone until later the question of whether the observer is deceived by the presence of aurorae into thinking that the zodiacal light has changed.

(ii) *Occasional enhancements of the zodiacal light during one whole night.*—Visual observations of this kind are not uncommon (**2**), and we refer here only to the unusually bright zodiacal light of 1896 March 4 (**3**), which occurred during a period of auroral activity. Apparent changes of brightness from night to night occur in most detailed lists of photometric observations—see, for example, Roach (**4**) and Huruhata (**5**)—although an opinion is rarely expressed about the reality of these apparent changes.

(iii) *An annual variation.*—An annual variation of brightness over a range of two to one has been observed photoelectrically by Elvey and Roach (**6**). Thom (**7**) has assembled many visual observations from a variety of sources and has found a similar variation.

(iv) *Long period variations.*—Huruhata (**5**) has made photoelectric observations over a period of four years, finding an irregular variation from year to year amounting at most to a factor of seven. Thom (**7**), using the previously mentioned visual data, also finds a variation and some correlation with solar activity. Table IV of Paper I, which lists absolute brightness values obtained by various observers during the period 1952-8, using non-visual techniques, apparently supports this idea that there is a variation from year to year.

All of this evidence is contradicted by Regener (**8**) who cannot find any significant variation during fourteen months continuous observation over the period 1953–4. It is perhaps significant, however, that his observations were made during a period of very low solar activity. A daily record of the appearance of the zodiacal light at the Harvard College Observatory (latitude 42°N) ever the period 1876–1890, has been analysed by Searle (**9**) who states that the variations which seem to have occurred cannot be established with certainty, and any support for a correlation between the variation and the occurrence of aurorae is certainly very feeble. Barbier (**10**) also, working photoelectrically at Haute-Provence (latitude

*He noted in his diary for 1854 January 30, "*There can be no doubt that there are pulsations in the zodiacal light.* I noticed them last evening; but, it being Sunday, made no particular record of them."

+44°), finds no evidence for a variation of zodiacal light brightness. He worked during the periods 1951–2 and 1952–3 when solar activity was low.

We conclude that it is not possible to deduce from the existing data whether or not the zodiacal light is of constant brightness.

The Chacaltaya observations.—The requirements for a site suitable for an investigation of possible variations of the zodiacal light are very stringent. Evidently the site must be near the geographical equator so that the varying inclination of the ecliptic to the horizon does not lead to systematic errors, and it must also be at a high altitude so that observations may be made close to the horizon, and have an excellent climate in which the extinction is low and varies little from night to night. In addition, it must be near the geomagnetic equator so that there is as little disturbance as possible from aurorae. Chacaltaya satisfies all of these requirements. In particular, it is at a low geomagnetic latitude (−3°) and so is especially suitable for the attempted observation of corpuscular radiation mentioned at the beginning of this paper.

The method of observing the zodiacal light and the results have already been described in Paper I. In this section we attempt to ascertain whether or not the observed variation in these data from day to day can be regarded as real.

Correlation between brightness measurements at λ4470A and λ6200A.—The measurements of brightness in these two spectral regions have been made almost completely independently, and we may therefore test the reliability of these measurements by examining the correlation between them. To do this we have,

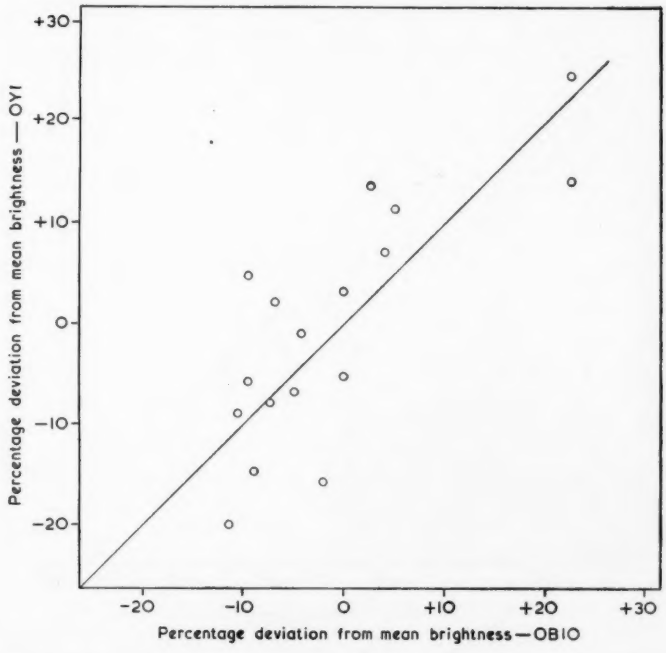

FIG. 1.—*Correlation between mean surface brightness of the zodiacal light at the two wavelengths* 4500A *and* 6200A.

for each photograph, averaged over all elongations the deviation from the mean brightness. In Fig. 1 we plot one set of measurements against the other and obtain a reasonably good correlation with a slope of unity, showing that the same relative change of brightness occurs in the two spectral regions.

Further, supposing that a perfect correlation may be expected to exist between the two quantities, the diagram shows that the probable error of such brightness measurements, averaged over one plate, is about 8 per cent.

Correlation between zodiacal light brightness and solar activity.—As it now seems likely that the observed variations of brightness are real, we attempt to correlate them with solar activity, as indicated by the magnetic index K_p. We have been particularly fortunate during the expedition to have observed the zodiacal light before, during and after the magnetic storm following an important solar flare. The flare occurred on July 7 at $00^h\,39^m$ U.T. and was recorded at Mitaka and Hawaii Observatories (**11**) as of importance 3^+. The intense magnetic storm which followed it on July 8–9 was one of the most important during the three year period 1957–9, the value of the planetary magnetic index K_p (**11**) remaining at 9 for 15 hours.

In Figs. 2 and 3 we reproduce the plot of surface brightness against elongation for the two colours, which has already been given in Paper I, and show the points appropriate to days when the magnetic index K_p was greater than 4 (i.e. exceptionally high) at the time of observation; evidently there is a fair correlation between magnetic index and brightness in the two colours.

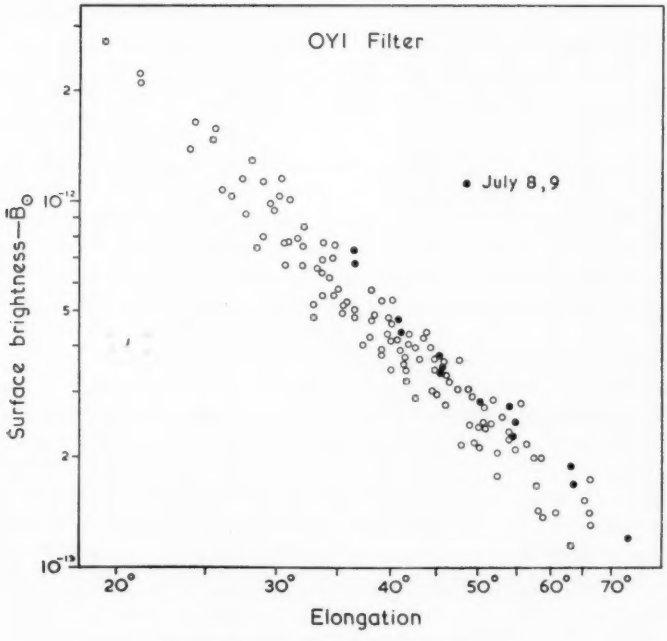

FIG. 2.—*Surface brightness of zodiacal light at wavelength* 6200A *showing values appropriate to active days.*

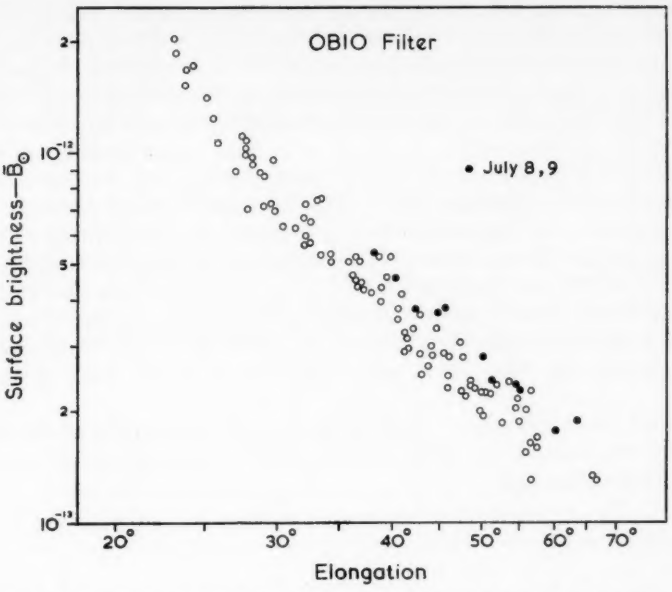

FIG. 3.—*Surface brightness of zodiacal light at wavelength 4500A showing values appropriate to active days.*

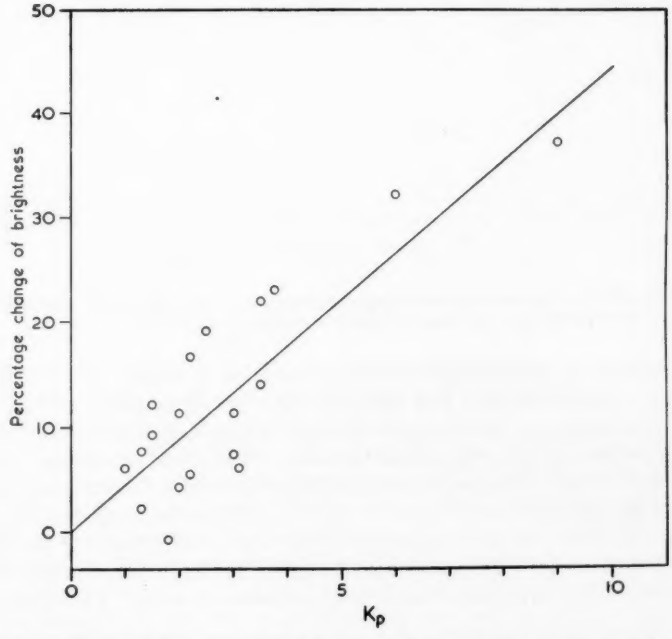

FIG. 4.—*Change of average brightness of zodiacal light as a function of magnetic index.*

To investigate this relation further we have formed for each day the deviation of brightness from the mean averaged over elongation and over the two colours. In Fig. 4 these deviations are plotted as a function of magnetic index for the time of observation, showing a remarkably good correlation, the total change in brightness when the magnetic index changes between 0 and 9 being about 40 per cent. The correlation is not substantially altered when a phase difference of up to one day is introduced. These results apparently justify the suspicion that has existed for more than a century, that the zodiacal light itself does change during a time of auroral activity. We emphasize that this observed change in zodiacal light brightness is quite distinct from a change in general sky brightness which may or may not be due to a localized aurora*. However, no rapid changes of the kind described by Jones were observed, either visually or photographically, and we are inclined to doubt whether these changes are associated with the zodiacal light itself, remembering that Jones often observed at rather high geomagnetic latitudes.

We have examined other published photometric data for the effect, but have found that the data are too scanty and the range of magnetic index too small to show a good correlation.

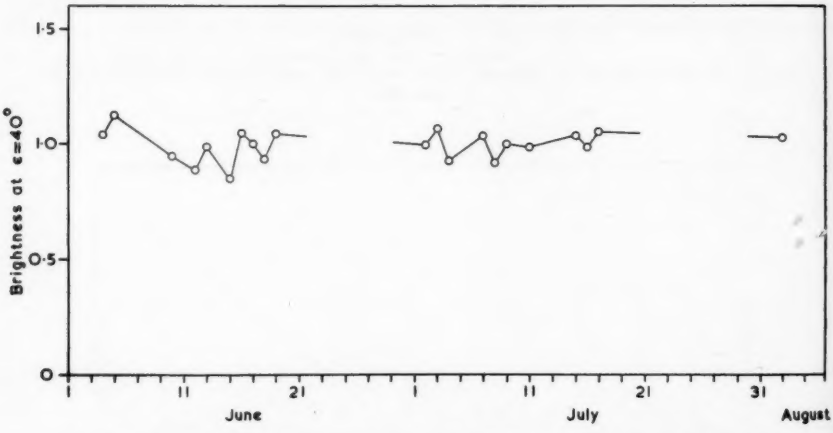

FIG. 5.—*Relation between brightness of zodiacal light at* $\epsilon = 40°$ *and date of observation; a correction has been made for magnetic activity using the data of Fig.* 4.

Examination of the data for an annual variation of brightness.—We are now able to use the graph of Fig. 4 to allow for the effect of magnetic activity on the zodiacal light brightness and to reduce the data to zero magnetic activity; the data may then be examined for an annual variation. Our observations are restricted to the period June 4–August 2, but this interval should be sufficient to show part of an annual variation, if it exists with an amplitude equal to that already reported. In Fig. 5 we plot against date the relative brightness of the zodiacal light at elongation 40° reduced to zero magnetic activity—this elongation being chosen because the brightness values are most accurate here. Each point on the

* The difficulty of distinguishing between a change in zodiacal light brightness and a change in sky brightness is further discussed on p. 150.

graph is a weighted mean of observations made in the blue and red regions. All of the photographs were taken at approximately the same time in the evening and reduced in the same way; a correction was made for extinction, using for this purpose observations of stars made with a photoelectric telescope. The graph shows no evidence for an annual variation of brightness such as has been observed by Elvey and Roach (**6**).

The position of the symmetry axis of the disturbed zodiacal light.—Six representative points on the symmetry axis for the dates July 8, 9 (when the magnetic index was greatest and the zodiacal light most disturbed) are shown plotted in Fig. 6, together with data from all other dates; the points for the two active days are averages for red and blue light. The scatter of all the points indicate the probable error of the data obtained on inactive days, and we conclude that the zodiacal light was not significantly displaced from it normal position on these two occasions.

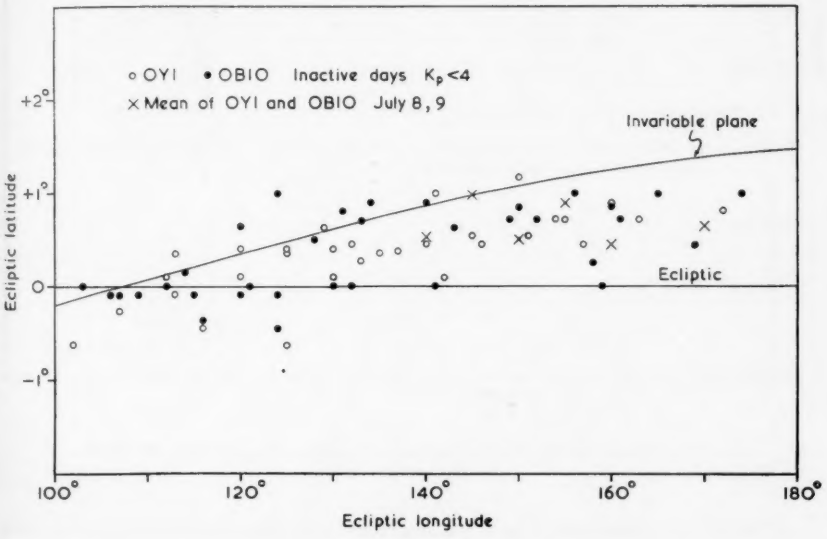

FIG. 6.—*Symmetry axis of quiet zodiacal light and points obtained on active days.*

Although we do not give isophotes for the zodiacal light, our scans show that there was not a significant change in the shape of these isophotes on the active days, i.e. the zodiacal light cone brightened as a whole.

The brightness of the night sky.—We quote here the night sky brightness at an altitude of 15° above the horizon, both on the ecliptic and at about 45° on each side of the ecliptic. The greatest change of brightness during the magnetic storm of July 8–9 was observed north of the ecliptic. To illustrate this we plot in Fig. 7 as a function of date the relative sky brightness measured in the red and blue regions, together with the planetary magnetic index K_p. There is evidently a close correlation between the brightness data for the two wavelength regions, and also a correlation between brightness and magnetic index; the increase

in brightness at the time of the storm on July 8–9 is particularly striking. The background sky brightness on the ecliptic, obtained by interpolation between the background at the sides of the zodiacal light, also changed, but it shows a much weaker correlation with magnetic index, the sharp rise on July 7 being scarcely discernible. The same is true of the brightness of the sky south of the ecliptic.

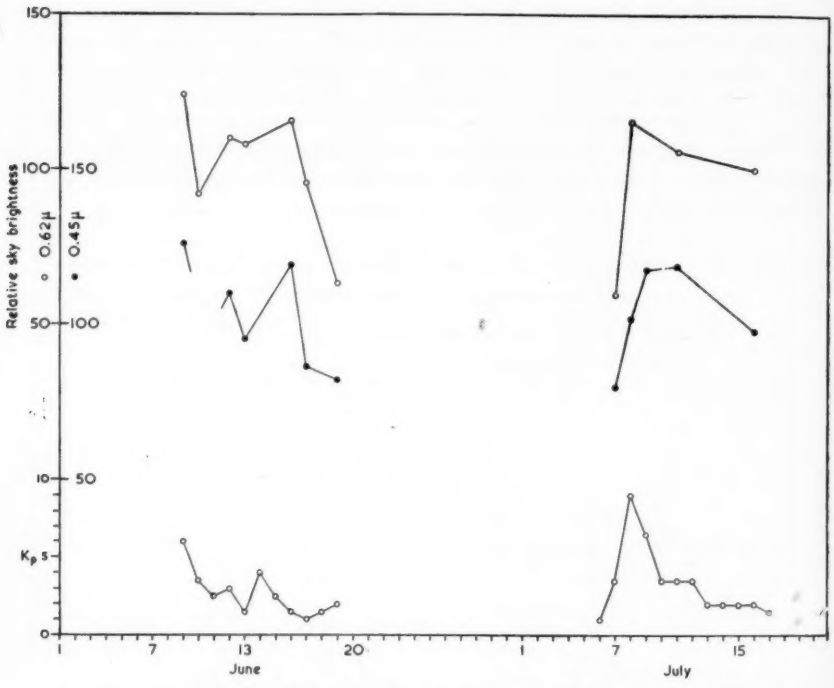

FIG. 7.—*Relation between sky brightness at* 4500A *and* 6200A *north of the ecliptic, and the magnetic index.*

The following diagram, Fig. 8, summarizes these observations of the effect of a solar flare on the zodiacal light and the neighbouring night sky. The diagram shows typical scans across the zodiacal light made under quiet conditions and soon after a solar flare; the level of the night sky background is also shown. The brightness of the zodiacal light itself increased but its position remained unchanged; these effects are superimposed on a changed night sky background. It is clear from this diagram that it is difficult to obtain the true brightness of the zodiacal light under disturbed conditions because of the uncertainty of the interpolation of the sky background between measures made north and south of the ecliptic. In our work we have made a linear interpolation. Because of this difficulty all observations of this nature should be treated with great caution. The most reliable data are those which refer to small elongations where the ratio of zodiacal light to the sky background is a maximum.

The colour of the increment of light from the northern night sky.—This is difficult to establish with precision. Using the data of Fig. 7 and allowing for extinction,

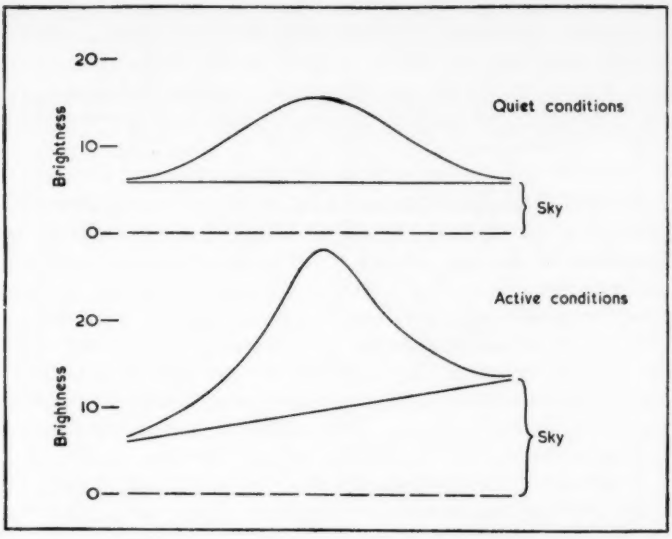

FIG. 8.—*Effect of a solar flare on the zodiacal light and night sky brightness. The diagram shows representative scans across the zodiacal light before, and soon after, a flare.*

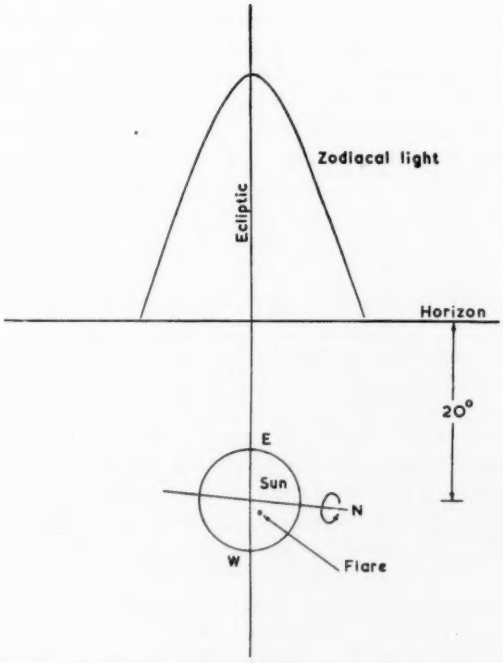

FIG. 9.—*Position of solar flare on July 7 in relation to the evening sky.*

we find that the extra light which comes from the northern night sky during enhanced magnetic activity has approximately the same colour as the solar disk. The actual ratio observed is

$$\frac{\text{Brightness of increment of night sky at } 0{\cdot}62\mu}{\text{Brightness of increment of night sky at } 0{\cdot}45\mu} \Big/ \frac{\text{Brightness of Sun at } 0{\cdot}62\mu}{\text{Brightness of Sun at } 0{\cdot}45\mu}$$
$$= 1{\cdot}15 \pm 0{\cdot}20.$$

The large probable error is a measure of the difficulty of this observation.

Interpretation of the observed effects of the solar flare.—We begin by describing the circumstances of the flare of July 7. The flare occurred at the following position on the solar disk $-$N24°, W09°. Examination of Fig. 9 shows that a jet of corpuscular radiation emitted from the region of this flare in a direction normal to the solar surface would be directed away from the Earth, and carried away further by the solar rotation. Nevertheless, the occurrence of an intense geomagnetic storm shows that the Earth must have passed through at least the outer parts of the stream during July 8–9. The corpuscular stream was also responsible for marked perturbations in the motion of the Satellite 1958δ1 (**12**). The increased brightness of the northern sky observed in the period June 9 onwards (see Fig. 7) is probably also due to the same active group, although no important flares were recorded during this period.

The observed increase in general sky brightness may be attributed either to an aurora or to the scattering of sunlight from the free electrons contained in a corpuscular stream. We incline to the second explanation for the following three reasons. First, the increase in sky brightness is observed chiefly in the part of the sky which is north of the ecliptic and this is compatible with scattering from a corpuscular stream emitted from an active region on the northern hemisphere of the Sun. Second, the colour of the additional sky light is close to that of the Sun, whereas aurorae often appear red or green. Third, aurorae occur only very rarely at the low geomagnetic latitude of 3°S. Alternatively, it might be argued that if the extra sky brightness is really due to scattering in interplanetary space, the increase should have started soon after the flare itself—whereas the brightness increased with the magnetic activity. This argument is not correct. According to Fig. 9, the corpuscular stream was initially directed away from the Earth, and the diagram of Fig. 10, which shows the corpuscular stream projected on to the plane of the ecliptic, shows that the effect need not be expected until at least one day after the flare.

Supposing that the effect is really due to scattering by corpuscular emission, we may calculate from the increase in brightness the order of magnitude of the electron density in such a temporary corpuscular stream, which should be distinguished from a more or less permanent interplanetary gas. If, on the other hand, the effect is not wholly due to electron scattering, the density obtained represents an upper limit. Taking the data already given, and assuming that we are looking through a total path length of about 0·5 A.U. in the corpuscular stream, the density would be about 300 electrons cm^{-3}, assuming that it is independent of distance from the Sun. Such a value is not incompatible with those already suggested on other grounds. For example, Biermann (**13**) has suggested that the disruption of comet tails is caused by solar corpuscular radiation, and he supposes a density between 10^3 and 10^5 atoms cm^{-3}. Chamberlain (**14**), using the observed intensity of Hα in aurorae, has proposed the value of 1 atom cm^{-3}. For a magnetic storm

showing a maximum value of the magnetic index K_p equal to 9, Ferraro (**15**) deduces the atom density in a cloud of corpuscules to be 40 cm^{-3}, although elsewhere he suggests (**16**) an upper limit of 100 cm^{-3}.

We suggest that these two effects which can contribute to an increase in the sky brightness after a flare, i.e. an aurora or scattering from temporary corpuscular radiation, may be distinguished by the change in the polarization of the sky light. If the extra light is auroral in origin, it would be unpolarized; whereas if it is due to electron scattering, it would be strongly polarized. Of course, such a separation is only practicable in tropical regions*, where aurorae are very infrequent.

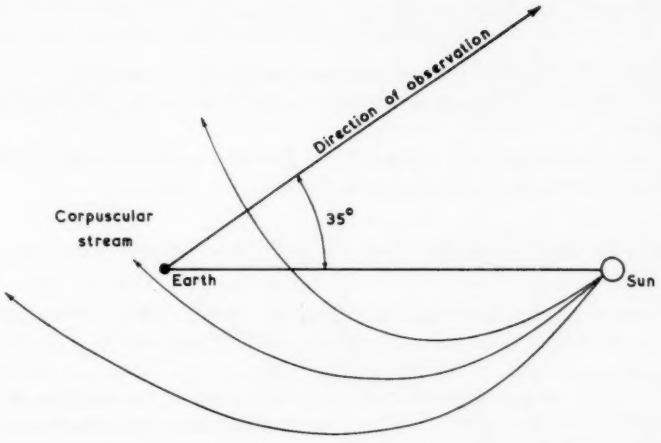

FIG. 10.—*Geometry of the emission of a corpuscular stream on July 7. Projection on to the plane of the ecliptic.*

The increase in the brightness of the zodiacal light.—It seems significant that when the zodiacal light increases in brightness its position in space remains unchanged. The position of the zodiacal light cone, between the ecliptic and the invariable plane of the solar system, suggests that its source is a permanent feature of the solar system and is primarily gravitationally controlled, i.e. that free electrons are not an important contribution. This is supported by our spectroscopic measurements. If the light cone does not move when it brightens, following a solar disturbance, it seems unlikely that the extra light comes by electron scattering. We now examine the suggestion that this extra light is due to a fluorescence of the dust particles caused by collision between the high speed protons of the corpuscular stream and the dust particles of the zodiacal cloud.

To investigate the possibility that such a mechanism is of importance, we calculate the expected increase in brightness of the zodiacal light assuming that when a proton contained in the corpuscular stream collides with a dust particle a certain fraction of its kinetic energy is converted into energy of radiation in the visible spectrum. We neglect the electrons because of their small kinetic energy. Because of the various uncertainties, the calculations are necessarily very crude.

* This method of separation will be attempted during an Oxford–Cambridge expedition to Chacaltaya in 1961.

In the calculation we assume that the corpuscular emission has a density of 300 protons cm^{-3}, which is independent of distance from the Sun, corresponding to our estimate of an electron density of 300 cm^{-3}, and that the corpuscles are travelling at a speed of 4×10^8 cm sec^{-1}. Such a velocity as this has been suggested by Meinel (**17**) on the basis of studies of the broadened Hα line in the spectra of aurorae.

We also need the total cross section A, of all dust particles in unit volume of interplanetary space. In the calculation of this we anticipate a result from Paper IV of this series, where it is supposed that the distribution of particle size is given by the relation,

$$n(a)da = Ca^{-p}\,da$$

where $n(a)da$ is the number of dust particles having radius between a and $a + da$. We suppose also, that the space density of dust particles varies with distance from the Sun as $r^{-\alpha}$.

Following the methods of Paper IV, we find that proton impact on the dust cloud gives an increment in brightness at elongation ϵ equal to

$$1{\cdot}3 \times 10^3\,\pi Rf\,\mathrm{cosec}^{\alpha+1}\epsilon \int_{\theta_1}^{\theta_2} \sin^{\alpha-2}\theta\,d\theta \int_{a_1}^{a_2} Ca^{2-p}\,da \quad \text{erg sec}^{-1}\,\text{cm}^{-2}\,\text{sterad}^{-1}$$

where f is the fraction of the kinetic energy of the protons which is converted into radiation in the visible spectrum on collision with a dust particle. Evaluation of this expression, with $C = 4{\cdot}28 \times 10^{-30}$, $R = 1{\cdot}5 \times 10^{13}$ cm, $a = 4 \times 10^{-5}$ cm, $\alpha = 1$, $p = 5$, leads to an increment which is only $f/100$ of the brightness of the zodiacal light at elongation 35°. If $f < 1$ we conclude that this mechanism is not able to explain the observed increment.

We are faced here with an apparent contradiction. After a solar flare there is apparently a brightening of the zodiacal light which must surely be attributed to increased emission from the zodiacal dust cloud. If the increased emission is due to fluorescence, we require a proton density which is greater than the maximum electron density permitted by the changes in the night sky brightness. A way out of this difficulty could be to suppose that the corpuscular stream contains a high proportion of neutral hydrogen which does not scatter solar radiation, but which can excite fluorescence. The calculations of Kahn (**18**) of the ionization of hydrogen in a corpuscular stream do not support this view. Yet, as we have mentioned already, Biermann has suggested that the observed accelerations of ions in comet tails can be accounted for only by assuming a density of corpuscular radiation of between 10^3 and 10^5 cm^{-3}, the latter corresponding to an intense storm. We do not believe that such high densities of free electrons can exist in interplanetary space because unless they occur in very thin clouds the resulting increase in sky brightness could hardly escape detection. If Biermann's hypothesis is correct a corpuscular stream must contain a high proportion of neutral hydrogen. This is just the condition that we require to explain the increase in zodiacal light brightness through fluorescence without a large increase in sky background through electron scattering.

Conclusions.—We find that following a solar flare there is an increase in zodiacal light brightness and also an increase in the brightness of part of the sky. The increase in sky brightness is attributed to the temporary emission from the Sun

of a beam of corpuscular radiation of density 300 electrons cm^{-3}, and this view is supported by the colour of the increment in sky brightness and the place in the sky where the increase occurs. The increase can scarcely be due to an aurora because of its colour and because of the rarity of aurorae at the low geomagnetic latitude of 3°S.

The increase in brightness of the zodiacal light is not accompanied by a shift in its position, which suggests that the extra emission is from the interplanetary dust cloud. This extra emission cannot be due to interaction between the dust cloud and the protons of the corpuscular stream because these carry insufficient energy. While it is possible that the increase is due to fluorescence of the interplanetary dust under the action of short wavelength radiation, the scarcity of the data precludes adequate discussion of this hypothesis.

The Observatories,
Madingley Road,
Cambridge:
1960 *October* 5.

References

(1) G. Jones, *Japan Expedition* 1853/5, Vol. III, Washington, 1856.
(2) E. O. Hulburt, *Phys. Rev.*, **35**, 1098, 1930.
(3) E. G. Brenner, *Observatory*, **19**, 206, 1896.
(4) F. E. Roach, *et al.*, *Ap. J.*, **119**, 253, 1954.
(5) H. Huruhata, *Publ. Astr. Soc., Japan*, **2**, 156, 1951.
(6) C. T. Elvey and F. E. Roach, *Ap. J.*, **85**, 231, 1937.
(7) A. Thom, *Journ. B.A.A.*, **49**, 103, 1939.
(8) V. H. Regener, *Ap. J.*, **122**, 520, 1955.
(9) A. Searle, *Annals Harvard College Obs.*, **19**, 165, 1893.
(10) D. Barbier, *Les Particules Solides dans les Astres.* Sixth Liège Colloquium, p. 55, 1954.
(11) *Compilations of Solar-geophysical data.* Nat. Bur. Stands. Colorado, U.S.A.
(12) L. G. Jacchia, *Nature, Lond.*, **183**, 1662, 1959.
(13) L. Biermann, *Physics of comets.* Fifth Liège Colloquium, p. 251, 1953.
(14) J. W. Chamberlain, *Ap. J.*, **120**, 360, 566, 1954.
(15) V. C. A. Ferraro, *J. Geophys. Res.*, **57**, 15, 1952.
(16) V. C. A. Ferraro, *Ann. de Geophys.*, **11**, 284, 1955.
(17) A. B. Meinel, *Ap. J.*, **113**, 50, 1951.
(18) F. D. Kahn, *M.N.*, **110**, 483, 1950.

OBSERVATIONS OF THE ZODIACAL LIGHT FROM A VERY HIGH ALTITUDE STATION

IV. The Nature and Distribution of the Interplanetary Dust

M. F. Ingham

(Received 1960 October 11)

Summary

The problem of the separation of the *K*-(electron) and *F*-(dust) components of the corona is reconsidered in the light of the revised value of the interplanetary electron density at 1 A.U. derived in Paper II of this series. A method of separation is developed in which it is not necessary to assume that the polarization of the *F*-corona is zero, but instead a model of the electron density is assumed. A model of the surface brightness and polarization of the corona and the zodiacal light is constructed on the basis of existing observations and the method of separation applied to it. The results are compared with theoretical expressions for the surface brightness of the light scattered by solid particles by (*a*) diffraction and (*b*) reflection and refraction. Values of the albedo, mass density and number density of the particles composing the zodiacal cloud are derived. The theory does not, however, account for the observed reddening of the corona.

---

1. *Introduction.*—In Paper II of this series (**1**) it was shown that the density of free electrons in interplanetary space at 1 A.U. from the Sun is at most 120 cm^{-3} and probably considerably less than this. It is therefore certain that the interplanetary gas cannot account for the whole of the observed polarization of the zodiacal light and probably for not even a significant fraction of it. Hence the greater part, if not all, of the polarization must be due to scattering by interplanetary dust. Hitherto, computations of the electron density in the outer corona ($r > 2R_\odot$) have been made on the assumption that the polarization of the *F*-corona is negligibly small. Now, however, this assumption has been called into question since, although at elongations less than $5R_\odot$ the *F*-corona is probably due entirely to diffraction and has zero polarization, at larger elongations the strongly polarized component due to reflection and refraction becomes increasingly important. Furthermore, if the estimate of the electron density at 1 A.U. is to be greatly reduced, a revision of this quantity in the coronal regions near the Sun becomes necessary. The purpose of this paper is to develop and apply a method whereby the corona and the zodiacal light may be separated into their two components in the light of the revised values of the electron density at 1 A.U. and without making any assumptions about the polarization of the *F*-corona.

2. *Outline of the method.*—If we denote by K and F respectively the surface brightness of the *K*- and *F*-components of the corona, by p_K and p_F their polarizations and by p_0 the observed polarization of the total corona, then we have the simple relation

$$p_0 = \frac{K}{K+F}p_K + \frac{F}{K+F}p_F \qquad (1)$$

in which the quantities which are observed are p_0 and $K+F$. If we put $p_F = 0$ then

it is possible to deduce both K and p_K by a method of successive approximation due to van de Hulst (2). If, however, $p_F \neq 0$ this method is no longer available and we have therefore used a different means of separating the two components based on the following considerations.

Close to the Sun (at elongations $\leqslant 2R_\odot$) it is possible to perform the separation by spectroscopic means without appeal to assumptions concerning polarization. The same situation regarding the separation pertains, as was shown in Paper II of this series, at great distances from the Sun in the region of the zodiacal light, whose spectrum has now provided an upper bound to the electron density. Thus close to the Sun (i.e. for $1 \leqslant r \leqslant 4R_\odot$) it is in principle possible to obtain fairly reliable values of $n_e(r)$ and at great distances there is a useful upper bound.

We now construct a series of functions $n_e(r)$ which join on smoothly to the values in the range $1 \leqslant r \leqslant 4R_\odot$ and whose values at $r = 1$ A.U. are less than the upper bound. A given function $n_e(r)$ leads to values for K and p_K. Knowing $(K+F)$, F is obtained by subtraction and, from equation (1), $p_F F$. Division yields p_F and the separation is achieved. The mathematical details of this method and the criteria for deciding which of the functions $n_e(r)$ leads to the correct forms of K, F, p_K and p_F will be considered in the following sections.

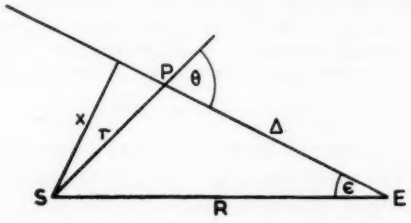

FIG. 1.—*Geometry of scattering in the corona and interplanetary space.*

3. *Basic equations for the scattering of sunlight by small particles in interplanetary space.*—The analysis presented here is based on the work of van de Hulst (3). We define the scattering function $I(\theta)$ of a spherical particle as the amount of radiation scattered per unit solid angle in a direction inclined at an angle θ to the direction of incidence, divided by the incident radiation that hits the geometrical cross section of the particle. Let $J_\lambda d\lambda$ denote the flux of the solar radiation in the wavelength range λ to $\lambda + d\lambda$ at a distance $R = 1$ A.U. from the Sun. Consider a column, lying in the line of sight, of height $d\Delta$, cross section σ, seen at elongation ϵ. Let its distance from the earth be Δ and from the Sun be r (Fig. 1).

Further, let there be $n(a)da$ particles per cubic centimetre at 1 A.U. whose radius lies between a and $a + da$. These particles receive solar energy at a rate of

$$J_\lambda d\lambda \left(\frac{R}{r}\right)^2 \sigma d\Delta n(a) da \left(\frac{R}{r}\right)^\alpha \pi a^2 \qquad \text{erg sec}^{-1}$$

where we have assumed that the space density of the particles varies with distance from the Sun as $r^{-\alpha}$. Of this energy a fraction $I(\theta)\Delta^{-2}$ is scattered to 1 cm^2 of the surface of the earth. This energy is seen coming from a solid angle $\sigma\Delta^{-2}$ so that the surface brightness of the column is

$$F_{\text{col}} = J_\lambda d\lambda \left(\frac{R}{r}\right)^{2+\alpha} n(a)\, da \pi a^2 I(\theta) d\Delta \quad \text{erg cm}^{-2} \text{ sec}^{-1} \text{ steradian}^{-1}.$$

Now from Fig. 1

$$r = R\frac{\sin\epsilon}{\sin\theta} \quad \text{and} \quad d\Delta = R\frac{\sin\epsilon}{\sin^2\theta}\,d\theta$$

and so for the surface brightness at elongation ϵ we have

$$F_\lambda(\epsilon) = J_\lambda d\lambda R \operatorname{cosec}^{1+\alpha}\epsilon \int_{a_1}^{a_2}\int_{\epsilon}^{\pi} n(a)\pi a^2 \sin^\alpha\theta I(\theta)\,d\theta\,da \tag{2}$$

where a_1, a_2 are the radii of the smallest and largest particles present. The expression on the right of equation (2) may be divided into two parts by writing

$$I(\theta) = I_d(\theta) + I_r(\theta)$$

where $I_d(\theta)$ is the scattering function due to diffraction and $I_r(\theta)$ is that due to reflection and refraction. The former predominates at small elongations and describes the *F*-corona, and the latter at large elongations and describes the zodiacal light. For the first, Fraunhofer diffraction theory leads to the result

$$\pi I_d(\theta) = \frac{J_1^2(x\sin\theta)}{\sin^2\theta} \tag{3}$$

where $x = ka = 2\pi a/\lambda$. On the other hand, the variation of the brightness of the zodiacal light with elongation does not depend strongly on the form of the function $I_r(\theta)$, and for convenience we write

$$\pi I_r(\theta) = \tfrac{1}{4}\gamma \tag{4}$$

which is the form for an isotropic scatterer with albedo γ. That there is some physical justification for this simplification is shown by Richter (**5**) who examined the scattering by particles of various sizes in the laboratory and found that for dielectric particles of diameter less than 10^{-2} cm the scattered intensity is approximately independent of θ for values of θ greater than about 40°.

We have considered two different functions $n(a)$. The first, which has been used by van de Hulst (**3**) and Beard (**6**) is

$$n(a)da = Ca^{-p}\,da \tag{5}$$

and the second has the form

$$n(a)da = Da\,e^{-a^2/a_0^2}\,da \tag{6}$$

where C, D, p and a are constants. In the first distribution the smallest particles are the commonest, whereas in the second the most numerous particles are distributed over a range of sizes rather than being concentrated at the small end of the distribution. The first function has the merit of simplicity and appears to describe the distribution of micrometeorites (see Section 7(ii)), whereas the second might describe more accurately a mixture of distributions, e.g. of particles of different materials, each with a different value of a_1.

Considering first the diffracted part of the scattered light and the first of the above functions, we have, from equations (2), (3) and (5), and since diffraction occurs in the forward direction only

$$F_{d_\lambda}(\epsilon;k) = J_\lambda d\lambda R \operatorname{cosec}^{1+\alpha}\epsilon \int_{a_1}^{a_2}\int_{\epsilon}^{\pi/2} Ca^{2-p}x^{2-\alpha}\frac{J_1^2(x\sin\theta)}{(x\sin\theta)^{2-\alpha}}\,d\theta\,da.$$

$$= J_\lambda d\lambda R \operatorname{cosec}^{1+\alpha}\epsilon \int_{\epsilon}^{\pi/2}\int_{a_1}^{a_2} k^{2-\alpha}a^{4-\alpha-p}\frac{J_1^2(ka\sin\theta)}{(ka\sin\theta)^{2-\alpha}}\,da\,d\theta.$$

Putting $ka\sin\theta = z$, $da = \dfrac{dz}{k\sin\theta}$, we have, after some reduction,

$$F_{d_\lambda}(\epsilon;k) = J_\lambda d\lambda RCk^{p-3}\operatorname{cosec}^{1+\alpha}\epsilon\int_\epsilon^{\pi/2}\sin^{\alpha+p-5}\theta\,.\,G_p(\theta;k)\,d\theta \tag{7}$$

where

$$G_p(\theta;k) = \int_{ka_1\sin\theta}^{ka_2\sin\theta}\frac{J_1^2(z)}{z^{p-2}}\,dz \tag{7a}$$

or

$$F_{d_\lambda}(\epsilon;k) = J_\lambda d\lambda RCk^{p-3}\operatorname{cosec}^{1+\alpha}\epsilon\,.\,H_{\alpha,p}(\epsilon;k) \tag{8}$$

where

$$H_{\alpha,p}(\epsilon;k) = \int_\epsilon^{\pi/2}\sin^{\alpha+p-5}\theta\,.\,Gp(\theta;k)\,d\theta. \tag{8a}$$

For the light scattered by reflection and refraction we have, using equation (4), and because $I_r(\theta)$ is independent of a,

$$F_{r_\lambda}(\epsilon) = J_\lambda\,d\lambda R\operatorname{cosec}^{1+\alpha}\epsilon\int_\epsilon^\pi \tfrac{1}{4}\gamma\sin^\alpha\theta\,d\theta\int_{a_1}^{a_2}Ca^{2-p}\,da \tag{9}$$

or, for $p \neq 3$,

$$F_{r_\lambda}(\epsilon) = J_\lambda d\lambda RC\gamma\operatorname{cosec}^{1+\alpha}\epsilon\,.\,H_{r_\alpha}(\epsilon)\left(\frac{a_2^{3-p}-a_1^{3-p}}{3-p}\right) \tag{10}$$

where

$$H_{r_\alpha}(\epsilon) = \int_\epsilon^\pi \tfrac{1}{4}\sin^\alpha\theta d\theta. \tag{10a}$$

Now $a_2 \gg a_1$ and (Section 7(ii)) on the basis of observations of small meteors, p will be given the values 4 and 5. In this case we may ignore a_2^{3-p} in comparison with a_1^{3-p} and in place of equation (10) write

$$F_{r_\lambda}(\epsilon) = J_\lambda d\lambda RC\gamma\operatorname{cosec}^{1+\alpha}\epsilon\,.\,H_{r_\alpha}(\epsilon)\left(\frac{a_1^{3-p}}{p-3}\right). \tag{11}$$

The mathematical details of the steps resulting from the use of equation (6) are similar to those just given and since what follows applies equally to both forms of $n(a)$ we shall consider only the first, giving the final results for both at the end.

In order to discuss the polarization of the light scattered by small particles it is necessary to know, or assume, something about their nature. The only certain samples of interplanetary material to hand are meteorites, and the work of Kloverstrom and Rense (**7**) on the polarization of light reflected from the plane ground surfaces of meteoritic samples, and also the work of Richter already referred to (**5**), indicates that the degree of polarization, $p(\theta)$, varies with the angle of scattering, θ, as a function of the form

$$p(\theta) = \frac{\sin^2\theta}{q-\sin^2\theta} \tag{12}$$

where q is a constant depending on the nature of the sample, for example whether it is stony or metallic.

If we adopt for $p(\theta)$ a function of the form given by equation (12) then we may use equation (9) to write the expression for the polarized component of the dust scattered light as

$$f_{r_\lambda}(\epsilon) = J_\lambda d\lambda R \operatorname{cosec}^{1+\alpha}\epsilon \int_\epsilon^\pi \tfrac{1}{4}\gamma p(\theta) \sin^\alpha\theta \, d\theta \int_{a_1}^{a_2} Ca^{2-p} da$$

$$= J_\lambda d\lambda R \operatorname{cosec}^{1+\alpha}\epsilon \int_\epsilon^\pi \tfrac{1}{4}\gamma \frac{\sin^{2+\alpha}\theta}{q-\sin^2\theta} d\theta \int_{a'}^{a_2} Ca^{2-p2}\, da.$$

Thus the observed polarization of this component is given by

$$p_{F_r}(\epsilon) = \frac{f_{r_\lambda}(\epsilon)}{F_{r_\lambda}(\epsilon)} = \frac{\int_\epsilon^\pi \dfrac{\sin^{2+\alpha}\theta}{q-\sin^2\theta} d\theta}{\int_\epsilon^\pi \sin^\alpha\theta \, d\theta}. \tag{13}$$

4. *Criteria for the choice of the electron density distribution.*—Once a model of the electron density has been chosen, K and p_K can be computed at all elongations from the equations given by van de Hulst (2) and, from the observed values of p_0 and $K+F$, values of F and p_F are derived. Lastly, F may be further separated into a component due to diffraction, F_d, and one due to reflection and refraction, F_r. By analogy with the total corona we have, in an obvious notation,

$$p_F F = p_F(F_d + F_r) = p_{F_d} F_d + p_{F_r} F_r.$$

Here, though, p_{F_d} is zero since we have used Fraunhofer diffraction theory in deriving an expression for F_d, and so

$$F_r = \frac{p_F F}{p_{F_r}}.$$

A theoretical expression for p_{F_r} was obtained in Section 3 (equation (13)) and was seen to depend both on the value of α and on the nature of the scattering particles. However, for the range of values of α and q with which we shall be concerned, p_{F_r} is constant for $\epsilon < 10^\circ$ and so an error in assigning a value to p_{F_r} does not affect the manner in which F_r varies with elongation. Finally by subtraction of F_r from F we obtain F_d.

Two criteria for the choice of $n_e(r)$ are available. The first concerns the variation of F_d and F_r with ϵ. From equations (8) and (10) we see that

$$F_d(\epsilon) \propto \operatorname{cosec}^{1+\alpha}\epsilon \, . \, H_{\alpha,p}(\epsilon) \tag{14}$$

and

$$F_r(\epsilon) \propto \operatorname{cosec}^{1+\alpha}\epsilon \, . \, H_{r_\alpha}(\epsilon). \tag{15}$$

Now $H_{\alpha,p}(\epsilon)$ and $H_{r_\alpha}(\epsilon)$ vary only little with ϵ as compared with $\operatorname{cosec}^{1+\alpha}\epsilon$. The slopes of the graphs of $\log F_d(\epsilon)$ and $\log F_r(\epsilon)$ as functions of $\log\epsilon$ are therefore a measure of the value of α in the regions from which come the major contributions to the functions $H_{\alpha,p}(\epsilon\,; k)$ and $H_{r_\alpha}(\epsilon)$, which, it will be remembered, are integrals evaluated along the line of sight.

Here it is necessary to anticipate the contents of Sections 6 and 7 and to say that two values of α will be considered, $\alpha = 1$ and $\alpha = 3/2$ and two values of p, $p = 4$ and $p = 5$. Consider for example the case $\alpha = 3/2$, $p = 5$ and $n(a)$ given by equation (5). For a wavelength of $\lambda = 6283\text{A}$ ($k = 2\pi/\lambda = 10^5$) the function $\sin^{\alpha+p-5}\theta \, . \, Gp(\theta\,; k)$,

whose integral between the limits ϵ and $\pi/2$ yields the function $H_{\alpha,p}(\epsilon;k)$, has such a form that for $\epsilon = 1^\circ$, say, half the integral comes from the region defined by $1^\circ \leqslant \theta \leqslant 14^\circ$ and half from the region $14^\circ < \theta \leqslant 90^\circ$. Furthermore, 10 per cent of the integral is contributed by the region $1^\circ \leqslant \theta < 4^\circ$ and 10 per cent by the region $30^\circ < \theta \leqslant 90^\circ$. In an acceptable sense, therefore, 80 per cent of the integral comes from the region defined by $4^\circ \leqslant \theta \leqslant 30^\circ$. Slightly different limits hold for other values of ϵ, and Table I shows the distances, in solar radii, which these limits are from the Sun. The function $\frac{1}{4}\sin^\alpha\theta$, whose integral from ϵ to π yields the function $H_{r_\alpha}(\epsilon)$ is symmetrical about $\theta = 90^\circ$ and 80 per cent of the integral comes from the region bounded by $\theta = 40^\circ$ and $\theta = 140^\circ$, whose limits are situated at distances from the Sun which are also given in Table I.

TABLE I

Elongation, scattering angle and distance from Sun. The values of θ define the range from which comes 80 per cent of the functions $H_{3/2,\,s}(\epsilon;k)$, $k = 10^s$ (a), and $H_{r_{3/2}}(\epsilon)$ (b).

	ϵ°	θ°	r in $R_\odot$
(a)	1	4	54
		30	7·5
	2	5	86
		30	15
	3	5	128
		30	22
	4	6	143
		30	30
	5	7	153
		30	37
(b)	1	40, 140	6
	2	40, 140	12
	3	40, 140	18
	4	40, 140	23
	5	40, 140	29

Thus the form of these functions is such that for any given elongation $< 5^\circ$ the major part of the component F_r arises from scattering by particles which lie nearer to the Sun than those which give rise to the component F_d. If therefore we find, for a given $n_e(r)$, that log F_d varies linearly with log ϵ as far as $\epsilon = 5^\circ$, then we can deduce that out to about 0·5 A.U. α has the constant value given by the gradient of the line, and hence that F_r, which arises closer to the Sun, must vary with ϵ in the same way as does F_d. If it does not, i.e. if the graph of log F_r against log ϵ either is not a straight line or has not the same slope as that of log F_d, then the model chosen for $n_e(r)$ is not satisfactory.

The second criterion concerns the function p_F. At elongations greater than 40° F_d is small in comparison with F_r and $p_F \simeq p_{F_r}$. With decreasing ϵ the rapidly increasing effect of the unpolarized component F_d results in a sharp decrease of p_F relative to p_{F_r}. At very small elongations ($\epsilon < 2^\circ$), where the functions $H_{\alpha,p}(\epsilon)$ and $H_{r_\alpha}(\epsilon)$ are approximately constant as compared to the behaviour of $\mathrm{cosec}^{1+\alpha}\epsilon$, equations (14) and (15) show that the ratio of F_d to F_r is very nearly independent of ϵ. It is therefore to be expected that, with decreasing ϵ, p_F will decrease rapidly at first and finally approach a constant value close to the Sun. At any rate, there

is no reason to suppose that p_F will increase with decreasing ϵ at any point, and hence a model for $n_e(r)$ which indicates that it does cannot be regarded as acceptable. Öhman (**8**), at the eclipse of 1945 July 9, measured the polarization of the *F*-corona and concluded that it was very small in comparison with that of the *K*-corona. In fact he found a small negative value at an elongation of $0{\cdot}19R_\odot$, but admitted that the material on which his analysis was based was "very meagre". The strong positive polarization of the zodiacal light makes it improbable that the *F*-corona should be negatively polarized.

In this argument we have ignored the fact that there must be a zone free of dust surrounding the Sun within which all particles are vaporized. Such a zone would produce a more or less sharp cut-off of F_r, while affecting F_d to a much lesser extent, and this in turn would cause a cut-off in p_{F_r}. Over (**9**) considers that a probable value for the radius of this zone is $4R_\odot$ and its presence in no way affects the argument that p_F must decrease with decreasing ϵ.

5. *Construction of an observational model of the corona and the zodiacal light.*—In order to apply this method of separation we require a set of measurements of $K+F$ and p_0 both for the corona and the zodiacal light, and here we are confronted by a difficulty for no one observer has made observations of the surface brightness and polarization of the corona from its innermost to its outermost parts.

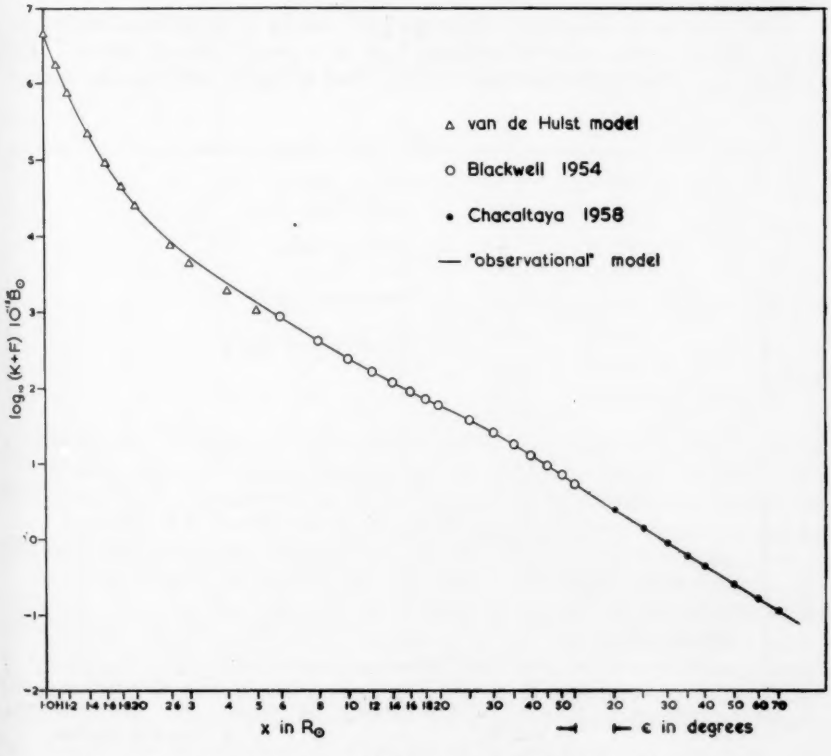

FIG. 2.—*The "observational" model of the corona and zodiacal light-surface brightness.*

Van de Hulst (**2**) has, on the basis of earlier observations and on the assumption that $p_F = 0$, constructed a model corona, both for sunspot maximum and for sunspot minimum, as far out as $x = 6R_\odot$. In the outer corona there are the observations of Blackwell (**10**) who measured $K+F$ in the range $6 \leqslant x \leqslant 55R_\odot$ and p_0 in the range $6 \leqslant x \leqslant 20R_\odot$. In region of the zodiacal light the most recent observations are those obtained at Chacaltaya which extend over the range of elongations $20^\circ \leqslant \epsilon \leqslant 70^\circ$.

The difficulty alluded to above arises from the fact that the van de Hulst models do not join on smoothly to Blackwell's observations, though these can reasonably be extrapolated to link up with the zodiacal light measurements (see Fig. 7 of Paper I in this series). In constructing an observational model of the corona and the zodiacal light we have therefore reconciled the inner two sets of observations by using the values of the brightness in the van de Hulst maximum model out to an elongation of $2R_\odot$ and then interpolating so as to join on smoothly to Blackwell's observations. It is true that Blackwell's observations were made at sunspot minimum (1954), but the van de Hulst minimum model is even less in agreement with them than is his maximum model. We have altered the outer values in the van de Hulst model rather than the inner values in Blackwell's range of observation because we consider the latter to be the more reliable since Blackwell observed from an aircraft flying at 30 000 feet and had vastly better sky conditions than are obtainable at a ground station.

Fig. 2 shows the resulting "observational" model of the surface brightness, $K+F$, of the corona and the zodiacal light at a wavelength of 6200A. The continuous curve represents the model. The triangles are van de Hulst's

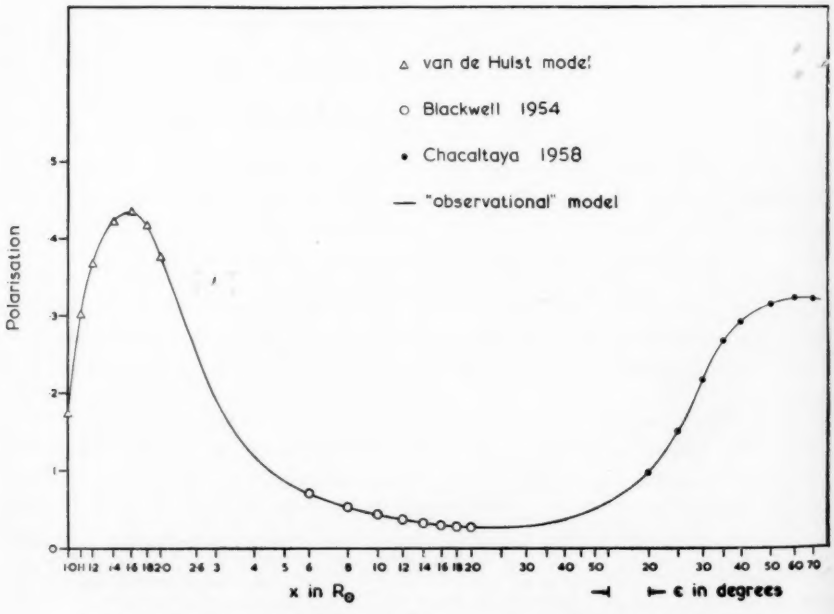

FIG. 3.—*The "observational" model of the corona and zodiacal light-polarization.*

maximum model, the open circles are Blackwell's coronal observations and the filled circles are an average of those for the zodiacal light.

Fig. 3 gives the values of the polarization, p_0, in the observational model. From $x = 1R_\odot$ to $x = 2R_\odot$, the range in which we are prepared to allow the assumption $p_F = 0$, these are deduced from the equation

$$p_0 = \frac{K}{K+F} p_K$$

and the values for the quantities given by van de Hulst. These points are marked by the triangles. The open circles are again Blackwell's coronal observations and the filled circles those for the zodiacal light. Interpolation bridges the gaps.

6. *Separation of the model.*—The choice of a function $n_e(r)$ which should satisfy both the conditions laid down in Section 3 proved to be a delicate matter since the variation of both F_r and p_F with ϵ depended strongly on the model chosen. The form of $n_e(r)$ selected was

$$n_e(r) = \frac{6{\cdot}75 \times 10^6}{r^3} \qquad (r \geqslant 6R_\odot)$$

and Table II gives the values of n_e, F_d, F_r and p_F for this model. The value of α indicated by the gradients of log F_d and log F_r is unity, or, if the values at smaller

TABLE II

Values of $n_e(x)$, F_d, F_r and p_F for the selected model of $n_e(r)$

x $R_\odot$	$n_e(x)$	F_d $10^{-13}\overline{B}_\odot$	F_r $10^{-13}\overline{B}_\odot$	p_F
6	31300	736	42·3	0·016
8	13200	362	22·0	0·017
10	6750	211	13·5	0·018
12	3910	144	9·83	0·019
14	2460	106	7·22	0·019
16	1650	80·1	5·64	0·019
18	1160	63·6	4·71	0·020
20	843	52·8	4·09	0·021

elongations are considered to be the more reliable, $\alpha = 3/2$ is admissible. Linking this function smoothly to the values of the van de Hulst maximum model in the range $1 \leqslant r \leqslant 4R_\odot$ completes the model of the electron density. Separation of $K+F$ into K and F can now be effected at all elongations and values of p_K and p_F derived. Columns 3 to 8 of Table III show the results of the first separation.

At elongations greater than 55° $H_{\alpha,p}(\epsilon; k)$ $(k = 10^5)$ vanishes for $\alpha = 1$ or $\alpha = 3/2$ and $p = 4$ or $p = 5$. We then have the situation in which K is negligible in comparison with F and F_d is negligible compared to F_r. This means that for $\epsilon < 55°$, $p_0 = p_F = p_{Fr}$. Thus observations of the zodiacal light at large elongations are observations of F_r and these measurements (Fig. 2) lie nearly on a straight line of gradient $-2{\cdot}4$. In the range $20° \leqslant \epsilon \leqslant 70°$ the graph of log $\{\text{cosec}^{5/2}\epsilon \,.\, H_{r_{3/2}}(\epsilon)\}$ as a function of log ϵ approximates to a straight line of gradient $-2{\cdot}4$ and so we can deduce that, for $r > 0{\cdot}5$ A.U., $\alpha = 3/2$, at least to 1 A.U.

TABLE

Separation of model

Elongation		$K+F$	K	F	p_0	p_K	p_F
$x/R_\odot$	ϵ°	$10^{-12}\overline{B}_\odot$	$10^{-12}\overline{B}_\odot$	$10^{-12}\overline{B}_\odot$			
1·0	16′	$5{\cdot}54\times10^6$	$5{\cdot}34\times10^6$	$1{\cdot}99\times10^5$	0·174	0·181	
1·1		$1{\cdot}74\times10^6$	$1{\cdot}62\times10^6$	$1{\cdot}16\times10^5$	·301	·323	
1·2		$7{\cdot}36\times10^5$	$6{\cdot}62\times10^5$	$7{\cdot}40\times10^4$	·367	·408	
1·4		$2{\cdot}20\times10^5$	$1{\cdot}84\times10^5$	$3{\cdot}56\times10^4$	·423	·505	
1·6		$9{\cdot}06\times10^4$	$6{\cdot}97\times10^4$	$2{\cdot}09\times10^4$	·435	·566	
1·8		$4{\cdot}47\times10^4$	$3{\cdot}09\times10^4$	$1{\cdot}38\times10^4$	·417	·604	
2·0	32′	$2{\cdot}52\times10^4$	$1{\cdot}52\times10^4$	$1{\cdot}00\times10^4$	·377	·625	0·000
2·6		$8{\cdot}61\times10^3$	$3{\cdot}31\times10^3$	$5{\cdot}30\times10^3$	·251	·650	·002
3·0		$5{\cdot}43\times10^3$	$1{\cdot}55\times10^3$	$3{\cdot}88\times10^3$	·192	·657	·005
4·0		$2{\cdot}40\times10^3$	392	$2{\cdot}01\times10^3$	·118	·665	·011
5·0	1° 20′	$1{\cdot}35\times10^3$	150	$1{\cdot}20\times10^3$	·087	·666	·014
6·0		851	72·5	778	·0712		·016
8·0		407	22·9	384	·0533		·017
10	2° 40′	234	9·38	225	·0435		·018
12		159	4·53	154	·0370		·019
14		115	2·44	113	·0324		·019
16		87·1	1·43	85·7	·0297		·019
18		69·2	0·89	68·3	·0283		·020
20	5° 20′	57·5	0·59	56·9	·0275		·021
25		37·2	0·24	37·0	·027		·022
30		25·1	0·12	25·0	·028		·025
35		17·8	0·062	17·7	·031	·666	·029
40	10° 43′	12·6	0·037	12·6	·036	·667	·034
45		9·33	0·023	9·31	·043		·042
50		6·92	0·015	6·90	·051	·667	·050
55	14° 50′	5·25	0·010	5·24	0·060	0·668	0·059
	20	2·35	0·003	2·35	0·100	0·669	0·099
	25	1·38	0·001	1·38	·152	0·673	·151
	30	0·884	0·001	0·884	·217	0·678	·216
	35	0·609	0·000	0·609	·268		·268
	40	0·442		0·442	·292		·292
	45	0·332		0·332	·306		·306
	50	0·258		0·258	·314		·314
	55	0·204		0·204	·320		·320
	60	0·166		0·166	·32		·324
	65	0·137		0·137	·32		·325
	70	0·115		0·115	0·32		0·324
1	2	3	4	5	6	7	8

We can now compute p_{F_r} from equation (13), choosing q so that $p_{F_r}=p_0$ at $\epsilon=60°$. Table IV shows the results of this calculation for $\alpha=1$, $q=3{\cdot}2$ and $\alpha=3/2$, $q=3{\cdot}3$. For $\epsilon>20°$ we require the values in the last column while for $x<20R_\odot$ we have seen that there is a case for either value of α. F_r may now be obtained by dividing $p_F F$ by p_{F_r}, F_d by subtraction of F_r from F and the separation is complete. The functions $p(\theta)$ which result from these choices of q are tabulated

III

corona and zodiacal light

p_{F_r}		F_r, $10^{-12}\bar{B}\odot$		F_d, $10^{-12}\bar{B}\odot$		n_e cm^{-3}
$\alpha=1$	$\alpha=3/2$	$\alpha=1$	$\alpha=3/2$	$\alpha=1$	$\alpha=3/2$	
0·279	0·290			$1·99\times10^{5}$	$1·99\times10^{5}$	$4·03\times10^{8}$
				$1·16\times10^{5}$	$1·16\times10^{5}$	$1·60\times10^{8}$
				$7·40\times10^{4}$	$7·40\times10^{4}$	$7·08\times10^{7}$
				$3·56\times10^{4}$	$3·56\times10^{4}$	$2·27\times10^{7}$
				$2·09\times10^{4}$	$2·09\times10^{4}$	$1·01\times10^{7}$
				$1·38\times10^{4}$	$1·38\times10^{4}$	$5·19\times10^{6}$
		0	0	$1·00\times10^{4}$	$1·00\times10^{4}$	$2·81\times10^{6}$
		35·8	34·5	$5·26\times10^{3}$	$5·27\times10^{3}$	$7·59\times10^{5}$
		71·6	69·0	$3·81\times10^{3}$	$3·81\times10^{3}$	$3·98\times10^{5}$
		78·8	75·9	$1·93\times10^{3}$	$1·93\times10^{3}$	$1·17\times10^{5}$
		60·9	58·6	$1·14\times10^{3}$	$1·14\times10^{3}$	$5·50\times10^{4}$
		44·4	42·8	734	735	$3·13\times10^{4}$
		23·4	22·5	361	361	$1·32\times10^{4}$
		14·5	14·0	210	211	$6·75\times10^{3}$
		10·5	10·1	143	144	$3·91\times10^{3}$
		7·71	7·41	105	106	$2·46\times10^{3}$
		5·84	5·62	79·9	80·1	$1·65\times10^{3}$
·279		4·91	4·72	63·4	63·6	$1·16\times10^{3}$
·280		4·25	4·10	52·6	52·8	843
		2·91	2·81	34·1	34·2	433
·280		2·23	2·16	22·8	22·8	250
·281		1·83	1·77	15·9	15·9	157
·281	·290	1·52	1·48	11·1	11·1	105
·282	·291	1·39	1·34	7·92	7·97	74
·283	·292	1·22	1·18	5·68	5·72	54
0·284	0·293	1·09	1·05	4·15	4·19	41
	0·295		0·790		1·56	
	0·297		0·700		0·680	
	0·300		0·637		0·247	
	0·304		0·536		0·073	
	0·309		0·417		0·025	
	0·313		0·326		0·006	
	0·317		0·256		0·002	
	0·321		0·203		0·001	
	0·324		0·166		0·000	
	0·325		0·137			
	0·324		0·115			
9	10	11	12	13	14	15

in Table V. Columns 11 to 14 of Table III exhibit the results of the second separation.

Fig. 4 shows p_0, p_K, p_F and p_{F_r}, the last for $\alpha=3/2$. The relations of the quantities may be understood as follows. At large elongations $K+F=F=F_r$ and $p_0=p_F=p_{F_r}$. As we approach the Sun we at first still have $K+F=F$ and $p_0=p_F$, but p_0 diminishes in relation to p_{F_r} because of increasing dilution by the unpolarized F_d.

TABLE IV

Values of p_{F_r}

ϵ°	p_{F_r}	
	$\alpha=1$	$\alpha=\frac{3}{2}$
0	0·279	0·290
10	·281	·290
20	·287	·295
30	·296	·300
40	·306	·309
50	·315	·317
60	·320	·324
70	·317	·324
80	·303	·312
90	·279	·290
100	·246	·255
110	·203	·213
120	·159	·169
130	·115	·123
140	·076	·082
150	·045	·051
160	·018	·029
170	·007	·003
180	0·000	0·000

Closer to the Sun at about $60R_\odot$, we begin to have $p_0 > p_F$ as the strongly polarized K-component becomes effective, and at about $x=25R_\odot$ p_0 begins to increase again and approaches p_K, though we never have $p_0=p_K$ because of dilution by F_d. Meanwhile p_F at first approaches a constant value, in sympathy with the behaviour of p_{F_r}, and then decreases sharply when the line of sight begins to pass through the dust-free zone.

TABLE V

Values of the function $p(\theta) = \dfrac{\sin^2\theta}{q-\sin^2\theta}$ (9.16)

θ°	$p(\theta)$		θ°
	$\alpha=1,\ q=3\cdot2$	$\alpha=3/2,\ q=3\cdot3$	
0	0·000	0·000	180
10	·009	·009	170
20	·038	·037	160
30	·085	·082	150
40	·148	·143	140
50	·225	·216	130
60	·306	·294	120
70	·381	·365	110
80	·435	·416	100
90	0·455	0·435	90

7. *Albedo, mass density and number density of the solid particles.*—Before we can evaluate the expressions in equations (8) and (11), developed in Section 3, we must consider what values to assign to the constants a_1, a_2, p and a_0; values of α have already been decided upon. We can then use the "observed" values of F_d and F_r to deduce C and γ.

(i) *The value of* a_1. The lower limit to the size of particle present in interplanetary space is set by the point at which the repulsive force of radiation pressure balances the gravitational attraction of the Sun. This limit depends on the density of the particles and if it be allowed that the material composing the zodiacal cloud is similar to that of which meteorites are made we may estimate this quantity. The majority (> 90 per cent) of meteorites seen falling are stones (**11**) with a density of about 3 gm cm^{-3}. On the other hand, Whipple (**12**) suggests $\rho = 2$ for an aggregate of stony-iron particles. Moreover, the finest dust may possibly originate from porous friable material of low density. We shall therefore consider the two cases $\rho = 2$ and $\rho = 3$ as being representative figures for the density of the smallest particles composing the zodiacal cloud.

For black spheres the lower limits are $a_1 = 0{\cdot}3\mu$ and $a_1 = 0{\cdot}2\mu$ in the two cases. The problem of the pressure of radiation on small, totally reflecting spheres has been discussed by Proudman (**13**) and use of his results leads to the values $a_1 = 0{\cdot}4\mu$ if $\rho = 2$ and $a_1 = 0{\cdot}3\mu$ if $\rho = 3$ at a wavelength given by $k = 2\pi/\lambda = 10^5$, i.e. $\lambda = 6283$ A.

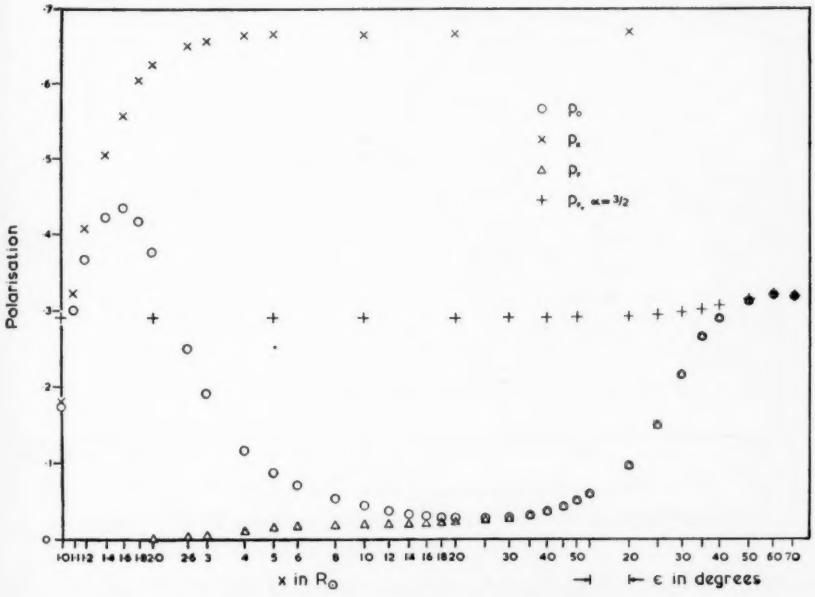

FIG. 4.—*Polarization of the components of the "observational" model.*

(ii) *The value of* p.—The observations of both Watson (**14**) and of Lovell (**15**) on micrometeorites yield a value for p of about 5, though these results refer to particles whose radii lie in the range $100\mu < a < 1000\mu$, whereas the present investigation considers particles whose radii are 1μ and less. Since other authors (**3**, **6**) have found smaller values for p, we have considered the two cases $p = 5$ and $p = 4$.

(iii) *The value of* a_2. This is very uncertain but must be several orders of magnitude larger than a_1 if the distribution defined by (**5**) or (**6**) holds for values of a up to 1 mm (1000μ). In Section 3 we saw that we may treat the upper limits involving a_2 as infinite for the values of p selected above.

The integrals in equations (7*a*) and (8*a*) were evaluated graphically at a wavelength of 6283A so that the expressions for F_d and F_r could be compared directly with the observations of the outer corona and the zodiacal light made at an effective wavelength of 6200A. The functions

$$\log\{\operatorname{cosec}^{1+\alpha}\epsilon \,.\, H_{\alpha,p}(\epsilon\,;\,k)\} \text{ and } \log\{\operatorname{cosec}^{1+\alpha}\epsilon \,.\, H_{r_\alpha}(\epsilon)\}$$

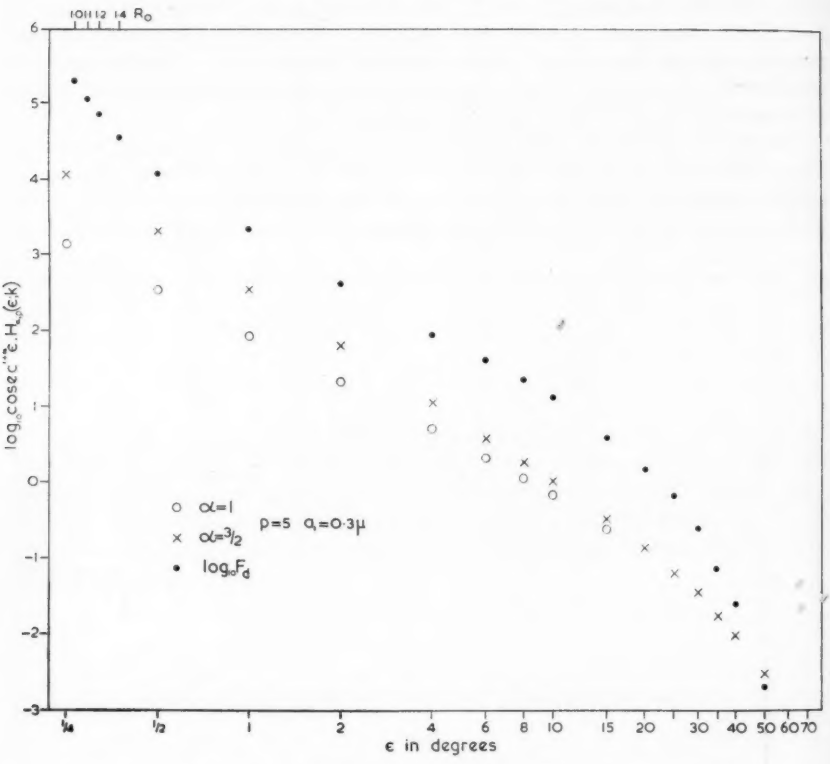

FIG. 5.—*The function* $\operatorname{cosec}^{1+\alpha}\epsilon$. $H_{\alpha,p}(\epsilon;k)$ *for* $p=5$, $a_1=0{\cdot}3\mu$, $k=10^5$ *and* $\alpha=1$ *and* $\alpha=3/2$.

were then plotted against log ϵ on the same diagrams respectively as log F_d and log F_r (Figs. 5 and 6) and the values of

$$(J_\lambda\, d\lambda RCk^{p-3}) \text{ and } \left(J_\lambda\, d\lambda RC\gamma\,\frac{{a_1}^{3-p}}{p-3}\right)$$

deduced by securing the best agreement between the computed functions and the observations. Values of C and γ were then obtained.

The mass density and number density of particles in interplanetary space near the plane of the ecliptic may now be derived. Using equation (5), the total mass in grams, M, of the dust particles in 1 cm³ at 1 A.U. from the Sun is given by

$$M=\tfrac{4}{3}\pi\rho\int_{a_1}^{a_2} a^3\, n(a)\, da$$

and the total number N, of particles of all sizes in 1 cm^3 at 1 A.U. is given by

$$N = \int_{a_1}^{a_2} n(a)\, da.$$

Since C is known the evaluation of these expressions is elementary.

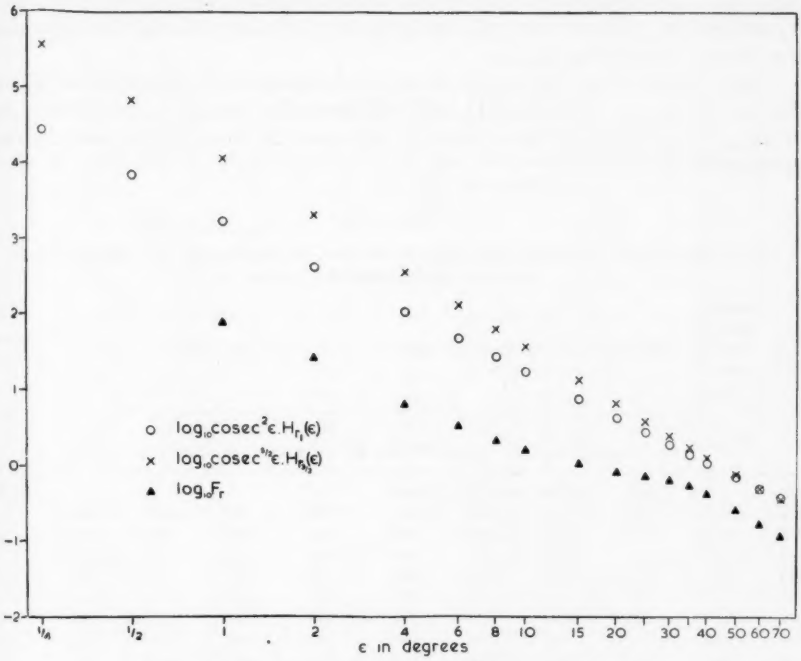

FIG. 6.—*The function* cosec $^{1+\alpha}\epsilon$. $H_{r_\alpha}(\epsilon)$ *for* $\alpha = 1$ *and* $\alpha = 3/2$.

TABLE VI

Albedo, mass density and number density of interplanetary dust particles. M and N refer to the plane of the ecliptic at 1 A.U. from the Sun

First distribution: $n(a)\, da = Ca^{-p}\, da$

p	a_1 10^{-4} cm	γ		C		M 10^{-24} gm cm^{-3}		N km^{-3}	
		$\alpha=1$	$\alpha=3/2$	$\alpha=1$	$\alpha=3/2$	$\alpha=1$	$\alpha=3/2$	$\alpha=1$	$\alpha=3/2$
4	0·3	0·19	0·48	$3{\cdot}9\times10^{-28}$	$1{\cdot}6\times10^{-28}$	5·1	2·0	500	190
5	0·3	0·23	0·56	$2{\cdot}0\times10^{-30}$	$7{\cdot}8\times10^{-31}$	0·82	0·33	600	240
4	0·4	0·16	0·39	$6{\cdot}2\times10^{-28}$	$2{\cdot}5\times10^{-28}$	5·3	2·1	300	130
5	0·4	0·18	0·51	$4{\cdot}3\times10^{-30}$	$1{\cdot}6\times10^{-30}$	0·90	0·33	400	140

Second distribution: $n(a)\, da = Dae^{-a^2/a_0^2}\, da$

a_0 10^{-4} cm	a_1 10^{-4} cm	γ		D		M 10^{-24} gm cm^{-3}		N km^{-3}	
		$\alpha=1$	$\alpha=3/2$	$\alpha=1$	$\alpha=3/2$	$\alpha=1$	$\alpha=3/2$	$\alpha=1$	$\alpha=3/2$
1	0·3	0·16	0·51	$3{\cdot}1\times10^{-5}$	$9{\cdot}8\times10^{-6}$	2·3	0·71	130	40
2	0·3	0·16	0·35	$1{\cdot}9\times10^{-6}$	$8{\cdot}7\times10^{-7}$	4·8	2·2	40	17

The results of these calculations in the various cases considered are shown in Table VI.

No account has so far been taken of the effects of the finite size of the Sun or of the dust-free zone surrounding it. The former will cause an increase in the values of F_d over those calculated assuming a point source. The latter will cause F_r to decrease sharply as soon as the line of sight begins to pass through the zone; F_d will be less affected since it arises from particles more distant from the Sun than those responsible for F_r.

The first effect was treated by the method described by van de Hulst (**3**) and the second column of Tables VII and VIII shows the amount by which the value of $\log_{10} F_d(x)$ calculated from equation (8) must be increased in order to take account of it.

TABLE VII

Change in $\log_{10} F_d$ due to the finite size of the Sun and the presence of a dust-free zone of radius $4R_\odot$—first distribution

x $R_\odot$	Increase due to finite size of Sun	Decrease due to dust-free zone				Total change				"Observed" increase
$\alpha=1$	all p, a_1	$p=4$ $a_1=0{\cdot}3\mu$	$p=4$ $a_1=0{\cdot}4\mu$	$p=5$ $a_1=0{\cdot}3\mu$	$p=5$ $a_1=0{\cdot}4\mu$	$p=4$ $a_1=0{\cdot}3\mu$	$p=4$ $a_1=0{\cdot}4\mu$	$p=5$ $a_1=0{\cdot}3\mu$	$p=5$ $a_1=0{\cdot}4\mu$	
1·0		0·287	0·184	0·460	0·286					+0·80
1·1	0·326	·246	·158	·404	·243	+0·080	+0·168	−0·078	+0·083	·63
1·2	·232	·219	·136	·359	·208	+ ·013	+ ·096	− ·127	+ ·024	·49
1·4	·146	·174	·097	·284	·144	− ·028	+ ·049	− ·138	+ ·002	·30
1·6	·103	·139	·070	·227	·101	− ·036	+ ·033	− ·124	+ ·002	·20
1·8	·078	·111	·050	·178	·068	− ·033	+ ·028	− ·100	+ ·010	·12
2·0	·061	·087	·035	·138	·045	− ·026	+ ·026	− ·077	+ ·016	·07
2·6	·034	·037	·009	·064	·009	− ·003	+ ·025	− ·030	+ ·025	·00
3·0	·025	·018	·000	·035	·000	+ ·007	+ ·025	− ·010	+ ·025	
4·0	·015	·000		·000		+ ·015	+ ·015	+ ·015	+ ·015	
5·0	·009					+ ·009	+ ·009	+ ·009	+ ·009	
6·0	·006					+ ·006	+ ·006	+ ·006	+ ·006	
8·0	·003					+ ·003	+ ·003	+ ·003	+ ·003	
10	·000					+ ·000	+ ·000	+ ·000	+ ·000	
$\alpha=3/2$										
1·0		0·452	0·310	0·646	0·422					+0·53
1·1	0·551	·406	·266	·587	·362	+0·145	+0·285	−0·036	+0·189	·39
1·2	·395	·362	·230	·525	·308	+ ·033	+ ·165	− ·130	+ ·087	·29
1·4	·240	·290	·170	·398	·219	− ·050	+ ·070	− ·158	+ ·021	·14
1·6	·171	·230	·123	·331	·153	− ·059	+ ·048	− ·160	+ ·018	·05
1·8	·125	·191	·089	·261	·104	− ·066	+ ·036	− ·136	+ ·021	·00
2·0	·096	·154	·062	·209	·071	− ·058	+ ·034	− ·113	+ ·025	
2·6	·047	·075	·015	·101	·015	− ·028	+ ·032	− ·054	+ ·032	
3·0	·028	·040	·002	·054	·002	− ·012	+ ·026	− ·026	+ ·026	
4·0	·000	·000	·000	·000	·000	− ·000	+ ·000	− ·000	+ ·000	

Recently Over (**9**) has considered theoretically the vaporization of solid particles of SiO_2 near the Sun and concludes that half the particles would have evaporated at 4 solar radii from the Sun's centre. Here we shall consider a crude model in which there is a sharp cut-off in the density of solid particles at $4R_\odot$.

There will thus be a cut off in the integral which yields $H_{\alpha,p}(\epsilon; k)$ and instead of equation (8*a*) we must, in the range $1 \leqslant x < 4R_\odot$ write

$$H_{\alpha,p}'(\epsilon; k) = \int_{\epsilon}^{\theta_0} \sin^{\alpha+p-5}\theta \,.\, Gp(\theta; \kappa) d\theta$$

where θ_0 is the scattering angle at the point where the line of sight enters the dust-free zone. Tables VII and VIII show the amounts by which $\log_{10} F_d(x)$ must be

TABLE VIII

Change in $\log_{10} F_d$ due to the finite size of the Sun and the presence of a dust-free zone of radius $4R_\odot$—second distribution

x $R_\odot$	Increase due to finite size of Sun	Decrease due to dust-free zone		Total change		"Observed" increase
$\alpha = 1$	all a_0	$a_0 = 1\,\mu$	$a_0 = 2\,\mu$	$a_0 = 1\,\mu$	$a_0 = 2\,\mu$	
1·0		0·082	0·022			+0·80
1·1	0·326	·070	·017	+0·256	+0·309	·63
1·2	·232	·064	·012	+ ·168	+ ·220	·49
1·4	·146	·048	·006	+ ·098	+ ·140	·30
1·6	·103	·037	·003	+ ·066	+ ·100	·20
1·8	·078	·029	·001	+ ·049	+ ·077	·12
2·0	·061	·022	·000	+ ·039	+ ·061	·07
2·6	·034	·010		+ ·024	+ ·034	·00
3·0	·025	·004		+ ·021	+ ·025	
4·0	·015	·000		+ ·015	+ ·015	
5·0	·009			+ ·009	+ ·009	
6·0	·006			+ ·006	+ ·006	
8·0	·003			+ ·003	+ ·003	
10	·000			+ ·000	+ ·000	
$\alpha = 3/2$						
1·0		0·157	0·049			+0·53
1·1	0·551	·137	·039	+0·414	+0·512	·39
1·2	·395	·120	·030	+ ·275	+ ·365	·29
1·4	·240	·094	·017	+ ·146	+ ·223	·14
1·6	·171	·076	·007	+ ·095	+ ·164	·05
1·8	·125	·061	·003	+ ·064	+ ·122	·00
2·0	·096	·049	·000	+ ·047	+ ·096	
2·6	·047	·023		+ ·024	+ ·047	
3·0	·028	·011		+ ·017	+ ·028	
4·0	·000	·000		+ ·000	+ ·000	

decreased in consequence in the various cases and also gives the total change in $\log_{10} F_d(x)$, while the last columns show the increase in the "observed" values of $\log F_d$ over a straight line of slope $-(1+\alpha)$ passing through the point which represents $\log F\,(1^\circ)$ (Fig. 5).

8. *Discussion of results.*—Although the results of the preceding section are based on a smoothed mean of a large number of different observations it is worth while discussing the results obtained from the model. There we will consider under five headings.

(i) *The values of* γ, M *and* N.—The values of the albedo γ in Table VI are consistently higher for $\alpha = 3/2$ and for $\alpha = 1$. Kloverstrom and Rense (**7**) obtained values of 0·27, 0·62 and 0·38 for three stony meteorites and 0·58 for a metallic sample. For either value of α it is clearly not possible to select either the distribution of particle sizes, or a value for p, a_1 or a_0 on the basis of the value of γ.

The mass densities are of the same order of magnitude as those deduced by Behr and Siedentopf (**16**). Recently attempts have been made to measure the density of solid particles near the Earth with satellites and space probes, but although the results appear to agree with ours to within one or two orders of magnitude, they differ widely among themselves. Since no other independent measurements of this quantity exist the differences between the values of M in Table VI afford no criterion for selecting values of p, a_1 or a_0.

The values of N are from one to three orders of magnitude greater than previous estimates, the reason being that we have accounted for the zodiacal light and the F-corona in terms of many small particles rather than fewer larger ones. Behr and Siedentopf (**16**), Blackwell (**17**) and Allen (**18**) considered models involving particles of one size only and those sizes were one to three orders of magnitude greater than the values of a considered here.

The values of both M and N may be compared with the figures for the interstellar grains near the galactic plane (**19**) which are $M = 1{\cdot}4 \times 10^{-26}\,\mathrm{gm\,cm^{-3}}$ and $N = 200\,\mathrm{km^{-3}}$. These values are, however, derived on the assumption that $\rho = 1{\cdot}1\,\mathrm{gm\,cm^{-3}}$ and $a = 3 \times 10^{-5}\,\mathrm{cm}$.

(ii) *Surface brightness of F-corona close to the Sun.*—Tables VII and VIII show that only the first distribution with $\alpha = 3/2$, $p = 4$ and $a = 0{\cdot}4\mu$ and the second distribution with $\alpha = 3/2$ and both values of a_0 account at all satisfactorily for the rise in log F_d close to the Sun; the results for $\alpha = 1$ are in all cases bad. The figures for the "observed" increase given in the last columns are, however, somewhat arbitrary.

(iii) *Number of particles in the range of sizes* $10^{-2} < a < 10^{-1}$ *cm.*—Van de Hulst (**3**), who considered the distribution of particle sizes given by equation (5), arrived at the values $C = 10^{-20}$, $p = 2{\cdot}6$ and comparison with Watson's analysis of meteor frequencies (**14**) led to the conclusion that "*the number of particles with sizes between* 1 *mm and* 0·1 *mm in interplanetary space is about* 10 000 *times larger than can be inferred from the number of telescopic meteors*". Using the values $C = 10^{-20}$, $p = 2{\cdot}6$, $a_1 = 10^{-2}\,\mathrm{cm}$ and $a_2 = 10^{-1}\,\mathrm{cm}$ the expression

$$\int_{a_1}^{a_2} Ca^{-p}\,da$$

has the value 10^{-17}, whereas our values of $C \simeq 10^{-30}$, $p = 5$ and $C \simeq 10^{-26}$, $p = 4$ lead to values for the integral of the order 10^{-22} and 10^{-20} respectively. The discrepancy between the predicted number of telescopic meteors and those actually observed is thus to a large extent removed.

(iv) *The polarization function* $p(\theta)$.—Table V shows that in order to account for the observed polarization of the zodiacal light in terms of scattering by dust particles alone we have had to assume a function for the degree of polarization due to a single particle which has a maximum value of about 45 per cent when the angle of scattering is 90°. Such a large value has never been obtained in laboratory measurements. Kloverstrom and Rense (**7**) obtained maxima of about 30 per cent

for stony and 20 per cent for iron meteorites, though this work dealt with large plane surfaces and not with a cloud of tiny particles. Richter (**5**) worked with an aerosol of iron particles prepared from iron carbonyl and also with a suspension of small particles of quartz in a sealed room and recorded maximum polarizations of 15 per cent and 30 per cent for dielectric and metallic particles respectively. It is, however, doubtful just how far the materials and physical conditions in these experiments are representative of interplanetary space.

It is possible that independent evidence may be obtained from the study of noctilucent clouds. These are observed mainly in high northern latitudes and are formed at an altitude of between 80 and 90 km, but the nature and origin of the particles of which they are composed is uncertain. Witt (**20**) has measured the polarization of the sunlight scattered by such clouds. The measurements were made in red and blue light and at scattering angles of up to 60°. The degree of polarization exceeds 40 per cent at $\theta = 60°$ in both colours and appears to reach even higher values at larger angles of scattering. He interprets these measurements according to the Mie theory in terms of scattering by dielectric spheres, and shows that the curves indicate a particle radius of $0{\cdot}1$–$0{\cdot}2\,\mu$, depending on the refractive index. Without asserting any connection between these particles and the interplanetary dust we nevertheless have here a mechanism capable of producing an even greater degree of polarization than appears to be required to account for the observed polarization of the zodiacal light.

(v) *The reddening of the corona.*—We consider finally the variation of F_d with $k(=2\pi/\lambda)$. It was predicted by van de Hulst (**3**), observed by Allen (**18**) and confirmed by Blackwell (**17**) that the F-corona is redder than the Sun. Van de Hulst predicted that F_d should vary with k as $k^{-0{\cdot}4}$ and Blackwell showed that the reddening of the total corona increases with elongation as the reddened F-corona increases relative to the almost colourless K-corona.

TABLE IX

The reddening of the corona

	1st distribution		2nd distribution	
	$p=4$	$p=5$	$a_0=10^{-4}$ cm	$a_0=2\times10^{-4}$ cm
$\alpha=1$	1·02	1·00	0·99	1·02
$\alpha=3/2$	1·13	1·13	1·09	1·12

This reddening may be described by the ratio

$$R=\frac{I(\lambda_2, x_2)}{I(\lambda_1, x_2)} \Big/ \frac{I(\lambda_2, x_1)}{I(\lambda_1, x_1)}$$

where $I(\lambda, x)$ is the surface brightness of the total corona at wavelength λ and elongation x. Blackwell, using the values $\lambda_1 = 4300$ A, $\lambda_2 = 19\,000$ A; $x_1 = 1{\cdot}5R_\odot$, $x_2 = 2{\cdot}5R_\odot$ obtained $R = 2{\cdot}17$. It would not be correct, though to use the analysis developed here to calculate a theoretical value for this ratio since $\lambda = 2{\cdot}9\times10^{-4}$ cm and $a_1 = 03\times10^{-4}$ cm leads to $x_1 = 2\pi a_1/\lambda \simeq 1$, for which Fraunhofer diffraction theory is certainly inapplicable. Allen, however, measured this ratio at wavelengths 4000 A and 6500 A and at elongations $1{\cdot}2R_\odot$ and $2{\cdot}4R_\odot$ and obtained

the value 1·48, though Blackwell considers this to be too high. On the other hand Ney, in a private communication, states that at the eclipse of 1959 October 2 he obtained the value $R = 1{\cdot}08$ in the equatorial region for $\lambda_1 = 4750$ A, $\lambda_2 = 8300$ A; $x_1 = 1{\cdot}2R_\odot$, $x_2 = 2{\cdot}1R_\odot$. Table IX shows the values for $a_1 = 0{\cdot}4 \times 10^{-4}$ cm; $\lambda_1 = 4189$ A $(k_1 = 1{\cdot}5 \times 10^{-5})$, $\lambda_2 = 6283$ A $(k_2 = 10^5)$; $x_1 = 1{\cdot}2R_\odot$, $x_2 = 2{\cdot}4R_\odot$. There is a clear distinction between the values for $\alpha = 1$ and those for $\alpha = 3/2$ and the latter are in reasonable agreement with Ney's result, though considerably lower than Allen's. Further observations of this quantity are required.

Our treatment thus appears able to account for the observed trends in the *F*-corona and the zodiacal light and the figures given in Table VI are plausible.

9. *Acknowledgments.*—My thanks are due to Professor D. E. Blackwell and Professor R. O. Redman for much advice and many fruitful discussions of this problem. I am particularly grateful to Professor E. P. Ney for permission to refer to a result of his work prior to its publication in the *Astrophysical Journal.* I am indebted to the Electors to the Isaac Newton Studentship for support during the period in which this work was done.

The Observatories,
Madingley Road,
Cambridge:
1960 *October* 10.

References

(1) D. E. Blackwell and M. F. Ingham, *M.N.*, **122,** 129, 1961.
(2) H. C. van de Hulst, *B.A.N.*, **11,** 135, 1950.
(3) H. C. van de Hulst, *Ap. J.*, **105,** 471, 1947.
(4) H. C. van de Hulst, *Light Scattering by Small Particles*, Chapter 8, Wiley, 1957.
(5) N. Richter, *Mon. Deut. Akad. Wiss. Berlin*, **1,** 727, 1959.
(6) D. B. Beard, *Ap. J.*, **129,** 496, 1959.
(7) F. A. Kloverstrom and W. A. Rense, *Ap. J.*, **115,** 495, 1952.
(8) Y. Öhman, *Stockholm Obs. Ann.*, **15,** No. 2, 1947.
(9) J. Over, *Proc. Kon. Ned. Akad. van Wetenschappen*, **51B,** 74, 1958
(10) D. E. Blackwell, *M.N.*, **115,** 629, 1955.
(11) F. Watson, *Between the Planets*, Harvard Books on Astronomy, 1941.
(12) F. L. Whipple, *Ap. J.*, **111,** 375, 1950.
(13) J. Proudman, *M.N.*, **73,** 535, 1913.
(14) F. Watson, *Harvard Annals*, **105,** 623, 1937.
(15) A. C. B. Lovell, *Meteor Astronomy*, p. 139, Oxford, 1954.
(16) A. Behr and H. Siedentopf, *Zeits. f. Astrophys.*, **32,** 19, 1953.
(17) D. E. Blackwell, *M.N.*, **112,** 652, 1952.
(18) C. W. Allen, *M.N.*, **106,** 137, 1946.
(19) C. W. Allen, p. 226, *Astrophysical Quantities*, London, Athlone Press, 1955.
(20) G. Witt, *J. Geophys. Res.*, **65,** 925, 1960.

THE *K*-CORRECTION AND "STEBBINS-WHITFORD" CORRECTION IN RELATIVISTIC COSMOLOGY

R. Van der Borght

(Communicated by G. C. McVittie)

(Received 1960 November 2)*

Summary

In the present paper we derive an expression for the *K*-correction and the "Stebbins-Whitford" correction in relativistic cosmology, correct to the second order in the redshift δ, and with coefficients calculated for the present epoch. The results are then compared with those derived by McVittie and Davidson and it is shown that, if one works to this order of approximation, the two corrections cannot be completely separated and that a "mixed" correction has to be introduced.

In the study of a uniform model universe, one is led to the following formula (McVittie 1956, p. 156, Davidson 1959, p. 60) connecting the luminosity distance D and the apparent magnitude m of a given galaxy

$$\log_{10} D = 0{\cdot}2\,(m - M_0) + 1 + F \tag{1}$$

where

(*a*)
$$F = \tfrac{1}{2}\log_{10}\left\{\frac{1}{(1+\delta)\,I_0}\int_0^\infty \sigma(\lambda) B\left(h_1\tau, \frac{\lambda}{1+\delta}\right) d\lambda\right\} \tag{2}$$

(*b*) M_0 is the absolute magnitude of a typical galaxy

(*c*) h_1 is the "Hubble constant"

(*d*) $\tau = t_0 - t$ is the time of travel of light emitted at the time t and observed at the time t_0.

(*e*) $B(h_1\tau, \lambda)\,d\lambda$ is the energy emitted by a galaxy at the time t in the range $d\lambda$ in ergs/sec cm^2.

(*f*) $\sigma(\lambda)$ is an empirical function depending on the atmospheric extinction and the response of the apparatus.

(*g*)
$$I_0 = \int_0^\infty \sigma(\lambda)\, B(0, \lambda)\, d\lambda. \tag{3}$$

Writing

$$B\left(x, \frac{\lambda}{1+\delta}\right) = B\{x, \lambda - \lambda\,(\delta - \delta^2)\}$$

where

$$x = h_1\tau$$

we have, using a Taylor expansion,

$$B\left(x, \frac{\lambda}{1+\delta}\right) = B - x\,B_x - \lambda(\delta - \delta^2)\,B_\lambda + \tfrac{1}{2}x^2\,B_{xx} + x\lambda(\delta - \delta^2)B_{x\lambda} + \tfrac{1}{2}\lambda^2(\delta - \delta^2)^2\,B_{\lambda\lambda}$$

* Received in original form 1960 September 5.

or, to the second order in x and δ

$$B\left(x, \frac{\lambda}{1+\delta}\right) = B - x B_x - \delta\lambda B_\lambda + \tfrac{1}{2}x^2 B_{xx} + x\delta\lambda B_{x\lambda} + (\lambda B_\lambda + \tfrac{1}{2}\lambda^2 B_{\lambda\lambda})\delta^2, \quad (4)$$

where we have denoted $B(0, \lambda)$ by B and defined

$$B_x = \left(\frac{\partial B}{\partial x}\right)_{0,\lambda}, \qquad B_\lambda = \left(\frac{\partial B}{\partial \lambda}\right)_{0,\lambda}$$

with a corresponding notation for the second derivatives.

Then it follows from (4) that

$$\int_0^\infty \sigma(\lambda) B\left(x, \frac{\lambda}{1+\delta}\right) d\lambda = \overline{B} - \overline{B}_x . x - \overline{\lambda B_\lambda} . \delta + \tfrac{1}{2}x^2 \overline{B_{xx}} + \overline{\lambda B_{x\lambda}} x\delta + (\overline{\lambda B_\lambda} + \tfrac{1}{2}\overline{\lambda^2 B_{\lambda\lambda}})\delta^2 \quad (5)$$

where

$$\left.\begin{aligned} \overline{B} &= \int_0^\infty \sigma(\lambda) B(0,\lambda)\, d\lambda \\ \overline{B_x} &= \int_0^\infty \sigma(\lambda) B_x(0,\lambda)\, d\lambda \\ \overline{\lambda B_\lambda} &= \int_0^\infty \sigma(\lambda) \lambda B_\lambda(0,\lambda)\, d\lambda \\ \overline{B_{xx}} &= \int_0^\infty \sigma(\lambda) B_{xx}(0,\lambda)\, d\lambda \\ \overline{\lambda B_{x\lambda}} &= \int_0^\infty \sigma(\lambda) \lambda B_{x\lambda}(0,\lambda)\, d\lambda \\ \overline{\lambda^2 B_{\lambda\lambda}} &= \int_0^\infty \sigma(\lambda) \lambda^2 B_{\lambda\lambda}(0,\lambda)\, d\lambda \end{aligned}\right\} . \quad (6)$$

The expression (2) for F can be written

$$F = \frac{1}{2E}\left\{\ln \int_0^\infty \sigma(\lambda) B\left(x, \frac{\lambda}{1+\delta}\right) d\lambda - \ln \int_0^\infty \sigma(\lambda) B(0,\lambda)\, d\lambda - \ln(1+\delta)\right\} \quad (7)$$

where $E = \ln 10 = 2{\cdot}303$.

Substituting (5) in this expression we obtain, after some calculations,

$$F = \frac{1}{2E}\left\{ -\frac{\overline{B}_x}{\overline{B}} x - \left(1 + \frac{\overline{\lambda B_\lambda}}{\overline{B}}\right)\delta + \tfrac{1}{2}x^2 \left[\frac{\overline{B_{xx}}}{\overline{B}} - \left(\frac{\overline{B}_x}{\overline{B}}\right)^2\right] + \left[\tfrac{1}{2} + \frac{\overline{\lambda B_\lambda}}{\overline{B}} + \tfrac{1}{2}\frac{\overline{\lambda^2 B_{\lambda\lambda}}}{\overline{B}} - \tfrac{1}{2}\left(\frac{\overline{\lambda B_\lambda}}{\overline{B}}\right)^2\right]\delta^2 + \left[\frac{\overline{\lambda B_{x\lambda}}}{\overline{B}} - \frac{\overline{B_x}\,\overline{\lambda B_\lambda}}{(\overline{B})^2}\right] x\delta \right\} . \quad (8)$$

Substituting this value of F into (1) we have

$$\log_{10} D = 0{\cdot}2\{m - K - M_0 - \Delta M - C\} + 1 \quad . \quad . \quad . \quad . \quad . \quad (9)$$

where

$$\left.\begin{aligned} K &= K_1\delta + K_2\delta^2 \\ \Delta M &= W_1 x + W_2 x^2 \\ C &= C_1 x\delta \end{aligned}\right\} \quad (10)$$

and

$$K_1 = \frac{2{\cdot}5}{E}\left(1 + \frac{\overline{\lambda B_\lambda}}{\overline{B}}\right) \tag{11}$$

$$K_2 = \frac{2{\cdot}5}{E}\left[-\tfrac{1}{2} + \tfrac{1}{2}\left(\frac{\overline{\lambda B_\lambda}}{\overline{B}}\right)^2 - \frac{\overline{\lambda B_\lambda} + \tfrac{1}{2}\overline{\lambda^2 B_{\lambda\lambda}}}{\overline{B}}\right] \tag{12}$$

$$W_1 = \frac{2{\cdot}5}{E}\frac{\overline{B_x}}{\overline{B}} \tag{13}$$

$$W_2 = \frac{2{\cdot}5}{dE}\left[\left(\frac{\overline{B_x}}{\overline{B}}\right)^2 - \frac{\overline{B_{xx}}}{\overline{B}}\right] \tag{14}$$

$$C_1 = \left[\frac{\overline{B_x}.\overline{\lambda B_\lambda}}{(\overline{B})^2} - \frac{\overline{\lambda B_{x\lambda}}}{\overline{B}}\right]\frac{2{\cdot}5}{E}. \tag{15}$$

The coefficients K_1 and K_2 are similar to those given by McVittie (1956, p. 157, formula 8.616) but now evaluated at the present epoch.

K_1 is in fact Davidson's κ^* (1959, p. 62, formula 5.7).

Using the formula

$$x = \delta\left[1 - \frac{2h_1^2 - h_2}{2h_1^2}\delta \ldots\right] \tag{16}$$

it is possible to write ΔM as a power series in δ. It is then easily seen that W_1 is in fact Davidson's λ^* (1959, p. 61, formula 5.4) and can also be derived from McVittie's expression for ΔM (1956, p. 157, formula 8.617).

McVittie's and Davidson's treatment of the K-correction and the "Stebbins-Whitford" effect, which really means any kind of secular variation in the intrinsic luminosity of the light source, differ mainly through the way in which the expression for F has been split up in an attempt to account separately for the two effects.

(*a*) McVittie separates the expression for F into the factors:

$$\frac{\int_0^\infty \sigma(\lambda)\, B(x,\lambda)\, d\lambda}{\int_0^\infty \sigma(\lambda)\, B(0,\lambda)\, d\lambda} \tag{17}$$

which only depends on the time variable τ, from which the Stebbins-Whitford correction is derived, and

$$\frac{\frac{1}{1+\delta}\int_0^\infty \sigma(\lambda)\, B\left(x, \frac{\lambda}{1+\delta}\right) d\lambda}{\int_0^\infty \sigma(\lambda)\, B(x,\lambda)\, d\lambda} \tag{18}$$

which reduces to 1 if $\delta = 0$ and is used to derive the K-correction.

(*b*) Davidson separates the expression for F into the factors:

$$\frac{\frac{1}{1+\delta}\int_0^\infty \sigma(\lambda)\, B\left(t_0, \frac{\lambda}{1+\delta}\right) d\lambda}{\int_0^\infty \sigma(\lambda)\, B(t_0,\lambda)\, d\lambda} \tag{19}$$

which depends only on δ and has the advantage of yielding the K-correction directly with coefficients evaluated at the present epoch t_0,

and
$$\frac{\int_0^\infty \sigma(\lambda) B\left(t, \frac{\lambda}{1+\delta}\right) d\lambda}{\int_0^\infty \sigma(\lambda) B\left(t_0, \frac{\lambda}{1+\delta}\right) d\lambda} \tag{20}$$

which is only a function of the time if $\delta = 0$, and from which the Stebbins-Whitford correction is derived.

But (18) and (20) are, in fact, functions of both δ and x, and if the corrections are pushed to a higher order of approximation, one gets also a "mixed" correction of the form

$$C = C_1 x\delta \tag{21}$$

where the coefficient C_1 is given by formula (15).

It appears from the above analysis that it might be dangerous to split the expression for F from the beginning, since it is impossible, except to the first order approximation, to separate completely the corrections due to x and δ.

So far, only the first order approximations have been used but, if it were decided to extend the "apparent magnitude-redshift" relation to a higher order in δ, a "mixed" correction (21) should also be included.

University of Natal,
Durban,
South Africa:
1960 *October* 18.

References

Davidson, W., *M.N.*, **119**, 54, 1959.
McVittie, G. C., *General Relativity and Cosmology*, Chapman and Hall, London, 1956.